Functional characterization of αMβ2-uPar interaction

Tang, Manli

2009

Tang, M. L. (2009). Functional characterization of αMβ2-uPar interaction. Doctoral thesis, Nanyang Technological University, Singapore.

https://hdl.handle.net/10356/42240

https://doi.org/10.32657/10356/42240

FUNCTIONAL CHARACTERIZATION OF αMβ2-uPAR INTERACTION

TANG MANLI

School of Biological Sciences

A thesis submitted to the Nanyang Technological University
in fulfillment of the requirement for the degree of
Doctor of Philosophy

2009

Acknowledgements

I would like to express special gratitude to my supervisor Dr. Tan Suet Mien for his direction, encouragement and help during the process of the project. His forthrightness and serious attitude about science gave me deep impression and had a huge effect on me.

I would like to acknowledge the financial support of scholarship from Nanyang Technological University, without which I could not have undertaken this study.

I would like to extent my thanks to my colleagues for their support during my study, particularly: Ardcharaporn Vararattanavech, Chua Geok Lin, Foo Shen Yun, Li Yanfeng, Lim Kok Guan, Liu Ying, Manisha Cooray, Soon Gaik Hong, Tang Xiaoyan, Ye Zhanrui, for their friendship, assistance and helpful discussions. I would also like to express my sincere thanks to my good friend Ji Zhe for his generous help though my rough time financially and emotionally.

I would like to thank my family for their selfless love and support. I am grateful to my father for his understanding towards my lack of accompany over the past years. My husband, Lei Shuo, deserves a special mention for his decision to stay and take care of me for my last year of study. I also dedicate this thesis of work to my late mother whom I miss dearly.

Contents

Abstract i

Abbreviations iii

Chapter One: Introduction 1

1.1 Overview 1

1.2 The domain organization of the integrins 3

1.2.1 Extracellular domains 8

1.2.1.1 The α subunit 8

1.2.1.2 The β subunit 14

1.2.2 Transmembrane (TM) domains 17

1.2.3 Cytoplasmic tails 18

1.3 Regulation of integrin function 21

1.3.1 Affinity regulation 21

1.3.2 Valency regulation 26

1.4 The β2 integrins 27

1.5 αMβ2 associated proteins 33

1.6 uPAR (Urokinase Plasminogen Activator Receptor) 34

1.7 Aims of Study 41

Chapter Two: Materials and Methods 42

2.1 General reagents 42

2.1.1 Enzymes 42

2.1.2 Commercially available kits 42

2.1.3 cDNA clones provided by others 43

2.1.4 Cells 43

2.1.5 Antibodies 43

2.1.6 Ligands for cell binding analysis 46

2.1.7 Expression Vectors 46

2.2 Solutions, buffers, and media 46

2.2.1 Laboratory stocks 46

2.2.2 Media 47

2.2.3 Solutions 48

2.3 Methods 49

2.3.1 General methods for DNA manipulation 49

2.3.1.1 Quantitation of DNA 49

2.3.1.2 Restriction endonuclease digestion 49
2.3.1.3 DNA separation by agarose gel electrophoresis 50
2.3.1.4 Purification of DNA fragments by agarose gel electrophoresis 50
2.3.1.5 DNA ligation 51
2.3.1.6 Preparation of E.coli competent cells 51
2.3.1.7 Transformation of plasmid DNA 52
2.3.1.8 Purification of plasmid DNA 52
2.3.1.9 Polymerase chain reaction (PCR) 53
2.3.1.10 Standard PCR protocol 53
2.3.1.11 Identification of colonies that contain recombinant plasmids of interest 54
2.3.1.12 Site-directed mutagenesis 54
2.3.2 General methods for cell culture 55
2.3.2.1 Cell storage in liquid nitrogen 55
2.3.2.2 Cell recovery from liquid nitrogen 55
2.3.2.3 Culture of HEK-293 and 293T cells 55
2.3.2.4 Culture of K562 cells 56
2.3.3 Transfection of cells 56
2.3.3.1 Transfection of HEK-293 and 293T cells by the calcium phosphate method (for 10 cm dish) 56
2.3.3.2 Transfection of K562 cells by the electroporation method 57
2.3.3.3 Harvesting transfected cells (adherent) 57
2.3.3.4 FACS analysis 58
2.3.3.5 Surface biotinylation and preparation of whole cell lysates 58
2.3.3.6 Preparation of protein A sepharose beads 59
2.3.3.7 Immunoprecipitation of cell lysates 59
2.3.3.8 Sodium dodecyl sulphate polyacrylamide gel electrophoresis (SDS-PAGE) 61
2.3.3.9 Western blotting 61
2.3.3.10 ECL detection of proteins blotted onto PVDF membrane 61
2.3.3.11 Coating microtitre wells with ICAM-1 for cell adhesion assay 62
2.3.3.12 Coating microtitre plates with BSA or fibrinogen for cell adhesion assay 63
2.3.3.13 Cell adhesion assay 63
2.3.3.14 Cell migration assay 64
2.3.3.15 Fluorescence Resonance Energy Transfer (FRET) analyses 64
2.3.3.16 Model of integrin αMβ2 65
2.4 Plasmid construction details 66
2.4.1 Integrin plasmids 66
2.4.2 uPAR plasmids 73

Chapter Three: Down regulation of integrin αMβ2 ligand-binding function by uPAR 76

3.1 Background 76

3.2 Results 78

3.2.1 Analyses of integrin αMβ2 and uPAR interaction interface by immunoprecipitation 78

3.2.2 The ligand-binding property of integrin αMβ2 was attenuated by uPAR expression 86

3.2.3 uPAR expression reduced the ligand-binding capacity of a constitutively active integrin αMβ2 mutant 91

3.3 Conclusion and discussion 94

Chapter Four: uPAR induces conformational changes in the integrin headpiece and re-orientation of its transmembrane domains 99

4.1 Background 99

4.2 Results 101

4.2.1 Interaction with uPAR induces the movement of the αMβ2 hybrid domain 101

4.2.2 Interaction with uPAR induces the separation of the αMβ2 TMs. 107

4.2.3 Disulphide clasp in the αMβ2 TMs prevent their separation induced by uPAR. 118

4.3 Discussion 126

Chapter Five: Discussion 132

References 139

Publications from this study

1. Tang ML, Vararattanavech A, Tan SM. (2008)
uPAR induces conformational changes in the integrin αMβ2 headpiece and re-orientation of its transmembrane domains. ***J Biol Chem***. 2008 Jul 21. [Epub ahead of print]

2. Tang ML, Kong LS, Law SK, Tan SM. (2006)
Down-regulation of integrin αMβ2 ligand-binding function by the urokinase-type plasminogen activator receptor. ***Biochem Biophys Res Commun***. 2006 348(3):1184-93.

Publication from other study

1. Vararattanavech A, **Tang ML**, Li HY, Wong CH, Law SK, Torres J, Tan SM. (2008)
Permissive transmembrane helix heterodimerization is required for the expression of a functional integrin. ***Biochem J.*** 2008 410(3):495-502.

Abstract

The cell adhesion molecule integrin αMβ2, one of the β2 integrins, associates with the urokinase-type plasminogen activator receptor (uPAR) on monocytes and neutrophils. The GPI-linked uPAR also associates with members of the β1 and β3 integrins, and it modulates the ligand-binding and migration functions of these integrins. In the first part of this study, we show that co-expressing uPAR with αMβ2 in HEK-293 transfectants down-regulates the ligand-binding capacity of αMβ2 to denatured proteins, fibrinogen, and the intercellular adhesion molecule 1 (ICAM-1). Migration of transfectants on fibrinogen mediated by αMβ2 was reduced in the presence of uPAR. In addition, the constitutive ligand-binding property of an αMβ2 mutant was attenuated by its association with uPAR. Co-immunoprecipitation analyses using a panel of αMβ2-specific mAbs suggest shielding of the ligand-recognition site of αMβ2 by uPAR.

Although devoid of a cytoplasmic domain, uPAR triggers intracellular signaling via its associated molecules that contain cytoplasmic domains. Interestingly, uPAR changes the ectodomain conformation of one of its partner molecules integrin α5β1, and elicits cytoplasmic signaling. The separation or re-orientation of integrin transmembrane domains (TMs) and cytoplasmic tails are required for integrin outside-in signaling. However, there is a lack of direct evidence showing these conformational changes of an integrin that interacts with uPAR. In the second part of this study, we used reporter mAbs and FRET analyses to show conformational

changes in the αMβ2 headpiece and re-orientation of its TMs when αMβ2 interacts with uPAR.

Abbreviations

ADMIDAS	adjacent to metal ion-dependent adhesion site
ATP	adenosine triphosphate
bp	base pair(s)
BSA	bovine serum albumin
CD	cluster of differentiation
cDNA	complementary DNA
CR3	complement receptor type 3
C-terminal	carboxy terminal
DMSO	dimethyl sulphoxide
dNTP	deoxynucleotide triphosphate
dATP	deoxyadenosine triphosphate
dCTP	deoxycytidine triphosphate
dGTP	deoxyguanidine triphosphate
dTTP	deoxythymidine triphosphate
DTT	dithiothreitol
DNA	deoxyribonucleic acid
ECL	enhanced chemiluminescence
ECM	extracellular matrix
EDTA	ethylene-diamine-tetra acetic acid
EM	electron microscopy
Fab	antibody binding fraction (of Ig)
FACS	fluorescent activated cell sorter
FBS	fetal bovine serum
Fc	fragment crystallizable (of Ig)
FITC	fluorescein isothiocyanate
FRET	fluorescence resonance energy transfer
GPI	glycosylphosphatidylinositol
GT	Glanzmann's Thrombasthenia
h	hour(s)
HA	hemagglutinin
HEPES	N-[2-hydroxyethy] piperazine-N'-[2-ethanesulfonic acid]
HRP	horseradish peroxidase
JAM-1	junctional adhesion molecule 1
JEB	junctional epidermolysis bullosa
kbp	kilobase pairs
kDa	kilodaltons
I domain	inserted domain
ICAMs	intercellular adhesion molecules
I-EGF	integrin epidermal growth factor-like
Ig	immunoglobulin
IgSF	Immunoglobulin superfamily

I-like domain	I domain-like structure
IP	immunoprecipitation
LAD I	leukocyte adhesion deficiency type I
LDL	low density lipoprotein
LIMBS	ligand-induced metal ion-binding site
LPG	lipophosphoglycan
LPS	lipopolysaccharide
mAb	monoclonal antibody
MCS	multi-cloning site
MIDAS	metal ion-dependent adhesion site
min	minute(s)
mRNA	messenger ribonucleic acid
MW	molecular weight
NMR	nuclear magnetic resonance
NK cell	natural killer cell
N-terminal	amino terminal
O.D.	optical density
PAGE	polyacrylamide gel electrophoresis
PBS	phosphate buffered saline
PCR	polymerase chain reaction
PIPES	piperazine-N', N'-bis-[2-ethanesulfonic acid]
PiPLC	phosphatidylinositol-specific phospholipase C
PMA	phorbol myristate acetate
PMSF	phenylmethylsulphonylfluoride
PSI	plexins, semaphorins, and integrins
PTB domain	phosphor-tyrosine binding domain
PVP10	polyvinylpyrrolidone (average molecular weight 10000)
RNA	ribonucleic acid
rpm	revolutions per minute
RT	room temperature
s	second(s)
SD	standard deviation
SDS	sodium dodecyl sulphate
SDS-PAGE	sodium dodecyl sulphate polyacrylamide gel electrophoresis
TEMED	N, N, N', N'-tetramethylethylenediamine
Tm	melting point
TM	transmembrane
Tris	Tris (hydroxymethyl)-aminoethane
Tween 20	Polyoxyethylene sorbitan monolaurate
uPA	urokinase plasminogen activator
uPAR	urokinase plasminogen activator receptor
UV	ultraviolet
VLA	very late antigens
vWF	von Willebrand factor

v/v	volume per volume
w/v	weight per volume
βTD	β tail domain

The single-letter and triplet codes for amino acid residues are used. Restriction enzymes are referred to by their three-letter names derived from that of the source microorganism. Other abbreviations are defined in the text where first encountered.

Chapter One: Introduction

1.1 Overview

Leukocytes are bone marrow-derived cells and they are principal components of the immune system. Most leukocytes are normally non-adherent, and circulate in the bloodstream as round and non-polarized cells (Blois et al. 2005). During inflammation leukocytes accumulate in affected tissues, resulting in characteristic inflammatory symptoms including pain, elevated temperature, and reddish and swollen tissues (Gahmberg et al. 1998). The targeting of leukocytes to the sites of infection involves a sequence of activation and adhesion events which are mediated by several members of different molecular cell adhesion families, including integrins, selectins, immunoglobin-like molecules and cadherins (Mazzone et al. 1995). Adhesion molecules coordinate the various phases of leukocyte adherence to resting or inflamed endothelium in a stepwise fashion through a regulated mechanism of ligand binding (Springer 1994). Leukocytes attach loosely to endothelium by the interaction of selectins with carbohydrate ligands on the endothelium. When this interaction occurs, leukocytes can be activated by, for example, immobilized chemokine on the surface of endothelium. This will trigger integrin activation that promotes firm adhesion of the leukocytes to the endothelium (Campbell 1998). This is followed by the polarization of the leukocyte with membrane protrusion (lamellipodium) forming a leading edge guiding the cell body containing the nucleus, and an elongated uropod at the rear end of the cell (Sanchez-Madrid et al. 1999).

Leukocytes migrate on the endothelium and invade between neighboring endothelial cells. The migration process includes (1) pseudopod extension and attachment to the surface, (2) cell polarization, (3) contraction of the cell body, (4) release of rear attachment sites, and (5) uropod retraction (Springer 1994). Among these adhesion molecules, the leukocyte integrins, notably the leukocyte-specific β2 integrins (CD11/CD18), play a pivotal role (Hogg 1989). The β2 integrins bind to the intercellular adhesion molecules (ICAMs) and to several soluble proteins, many of which are involved in inflammation (Gahmberg et al. 1998).

Integrins are expressed in all nucleated cells and mediate adhesion to many different types of ligand, including: members of the immunoglobulin superfamily (IgSF), components of the extracellular matrix (ECM), components of micro-organisms and plasma proteins (Humphries 2000a; Hynes 1992; Loftus et al. 1994; Springer 1990). Integrins play a critical role in many cellular processes: cell growth, differentiation, tissue organization, cell migration, fertilization, blood clotting and leukocyte recognition (Clark et al. 1995). In addition to providing a structural link, integrins act as a bi-directional signalling device between the extracellular environment and the intracellular machinery (Springer 1990). The significance of integrins in this wide range of processes is underscored by the existence of several heritable diseases of integrins. For example, Leukocyte adhesion deficiency type I (LAD I) is caused by defects in integrin β2 subunit (Arnaout 1990a; Hogg et al. 2000). Defects in both αIIb and β3 have been associated with Glanzmann's Thrombasthenia (GT) (Morel-Kopp et

al. 1997; Nurden 2006). Defects of the β4 subunit have also been described in association with Junctional Epidermolysis Bullosa (JEB) (Vidal et al. 1995).

Each integrin is a heterodimer composed of an α and a β subunit via non-covalent association (Hynes 2002). Both the α and the β subunits are type I membrane glycoproteins. They have a large extracellular domain and a single transmembrane domain, followed by a relatively short cytoplasmic tail (Tuckwell et al. 1993). In humans, 18 α subunits and 8 β subunits associate to form 24 different receptors identified to date (Fig. 1.1), and the rules which regulate specific heterodimer formation are not clear. The integrin family may be divided into four major subgroups: β1 (CD29) integrins (or very late antigens (VLA)), β2 (CD18) integrins, β3 (CD61) integrins (or cytoadhesins), and β7 integrins (Gahmberg 1997; Harris et al. 2000; Springer 1990). For example, β1 integrins are expressed on almost all cell types (Zutter et al. 1990), whereas β2 integrins expression is restricted to leukocytes (Springer 1990). A hallmark of integrins is the ability of individual family members to recognize multiple ligands (Plow et al. 2000) (Table 1.1).

1.2 The domain organization of the integrins

Integrins are type I membrane glycoproteins that contain two non-covalently associated α and β subunits. Each subunit is composed of a large extracellular domain, a single transmembrane domain and a short cytoplasmic tail. An exception to this is

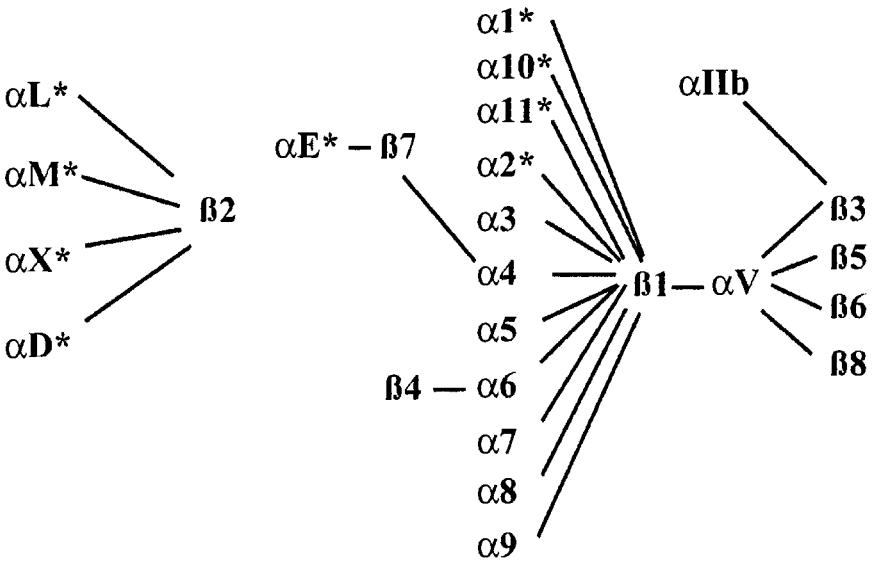

FIG 1.1 Integrin superfamily. In humans, 24 different integrin heterodimers are reported. The α subunits containing inserted (I) domains are asterisked.

Adenovirus penton base protein	$\alpha_v\beta_3$, $\alpha_v\beta_5$
Bone sialoprotein	$\alpha_v\beta_3$, $\alpha_v\beta_5$
Borrelia burgdorferi	$\alpha_{IIb}\beta_3$
Candida albicans	$\alpha_M\beta_2$
Collagens	$\alpha_1\beta_1$, $\alpha_2\beta_1$, $\alpha_{11}\beta_1$, $\alpha_{1b}\beta_3$
Denatured collagen	$\alpha_5\beta_1$, $\alpha_v\beta_3$, $\alpha_{IIb}\beta_3$
Cytotactin/tenascin-C	$\alpha_8\beta_1$, $\alpha_9\beta_1$, $\alpha_v\beta_3$, $\alpha_v\beta_6$
Decorsin	$\alpha_{IIb}\beta_3$
Disintegrins	$\alpha_v\beta_3$, $\alpha_{IIb}\beta_3$
E cadherin	$\alpha_E\beta_7$
Echovirus 1	$\alpha_2\beta_1$
Epiligrin	$\alpha_3\beta_1$
Factor X	$\alpha_M\beta_2$
Fibronectin	$\alpha_2\beta_1$, $\alpha_3\beta_1$, $\alpha_4\beta_1$, $\alpha_4\beta_7$, $\alpha_5\beta_1$, $\alpha_8\beta_1$, $\alpha_v\beta_1$, $\alpha_v\beta_3$, $\alpha_v\beta_5$, $\alpha_v\beta_6$, $\alpha_v\beta_8$, $\alpha_{IIb}\beta_3$
Fibrinogen	$\alpha_5\beta_1$, $\alpha_M\beta_2$, $\alpha_v\beta_3$, $\alpha_x\beta_2$, $\alpha_{IIb}\beta_3$
HIV Tat protein	$\alpha_v\beta_3$, $\alpha_v\beta_5$
iC3b	$\alpha_M\beta_2$, $\alpha_x\beta_2$
ICAM-1	$\alpha_L\beta_2$, $\alpha_M\beta_2$
ICAM-2,3,4,5	$\alpha_L\beta_2$
Invasin	$\alpha_3\beta_1$, $\alpha_4\beta_1$, $\alpha_5\beta_1$, $\alpha_6\beta_1$
Laminin	$\alpha_1\beta_1$, $\alpha_2\beta_1$, $\alpha_6\beta_1$, $\alpha_7\beta_1$, $\alpha_6\beta_4$, $\alpha_v\beta_3$
MAdCAM-1	$\alpha_4\beta_7$
Matrix metalloproteinase-2	$\alpha_v\beta_3$
Neutrophil inhibitory factor	$\alpha_M\beta_2$
Osteopontin	$\alpha_v\beta_3$
Plasminogen	$\alpha_{IIb}\beta_3$
Prothrombin	$\alpha_v\beta_3$, $\alpha_{IIb}\beta_3$
Sperm fertilin	$\alpha_6\beta_1$
Thrombospondin	$\alpha_3\beta_1$, $\alpha_v\beta_3$, $\alpha_{IIb}\beta_3$
VCAM-1	$\alpha_4\beta_1$, $\alpha_4\beta_7$
Vitronectin	$\alpha_v\beta_1$, $\alpha_v\beta_3$, $\alpha_v\beta_5$, $\alpha_{IIb}\beta_3$
von Willebrand factor	$\alpha_v\beta_3$, $\alpha_{IIb}\beta_3$

Table 1.1 Integrin extracellular ligands. (From Plow *et al.*, 2000)

the β4 subunit which has an extended cytoplasmic tail of over 1000 amino acids (Suzuki et al. 1990). The extracellular region of the integrin α subunit is linearly organized to contain from the N-terminus a β-propeller, thigh, calf-1 and calf-2 domains. Nine of the human α subunits contain an additional inserted (I)-domain in the β-propeller. The β subunits contain from the N-terminus a PSI (for Plexins, Semaphorins, and Integrins) domain, hybrid domain, I-like domain, four I-EGF (Integrin Epidermal Growth Factor-like) repeats and a β tail domain (βTD) (Takagi et al. 2002a) (Fig. 1.2). The properties and functions of these domains will be discussed in later sections. Association of the α and β subunit precursors occurs in the Golgi apparatus, and the assembled receptors are then transported to the cell surface or to intracellular stores (Fearon 1980).

Early electron microscopy (EM) images of two integrins, αIIbβ3 (Rivas et al. 1991; Weisel et al. 1992) and α5β1 (Nermut et al. 1988), suggest an integrin with a globular (~10 nm diameter) head and two stalks corresponding to the C termini of the subunits. A major breakthrough in the understanding of integrin structure and function came from the resolution of the integrin αVβ3 crystal structure (Xiong et al. 2001; Xiong et al. 2002). EM images of αIIbβ3 complexed to its ligand fibrinogen indicate the globular head is the ligand-binding site (Weisel et al. 1992) (Fig. 1.2C). From the structure of αVβ3, the globular head is formed by the N-terminal portions of the integrin (Xiong et al. 2003) in line with the EM data. A surprising finding from the αVβ3 structure is that the legs are severely bent, thus generating an overall V –

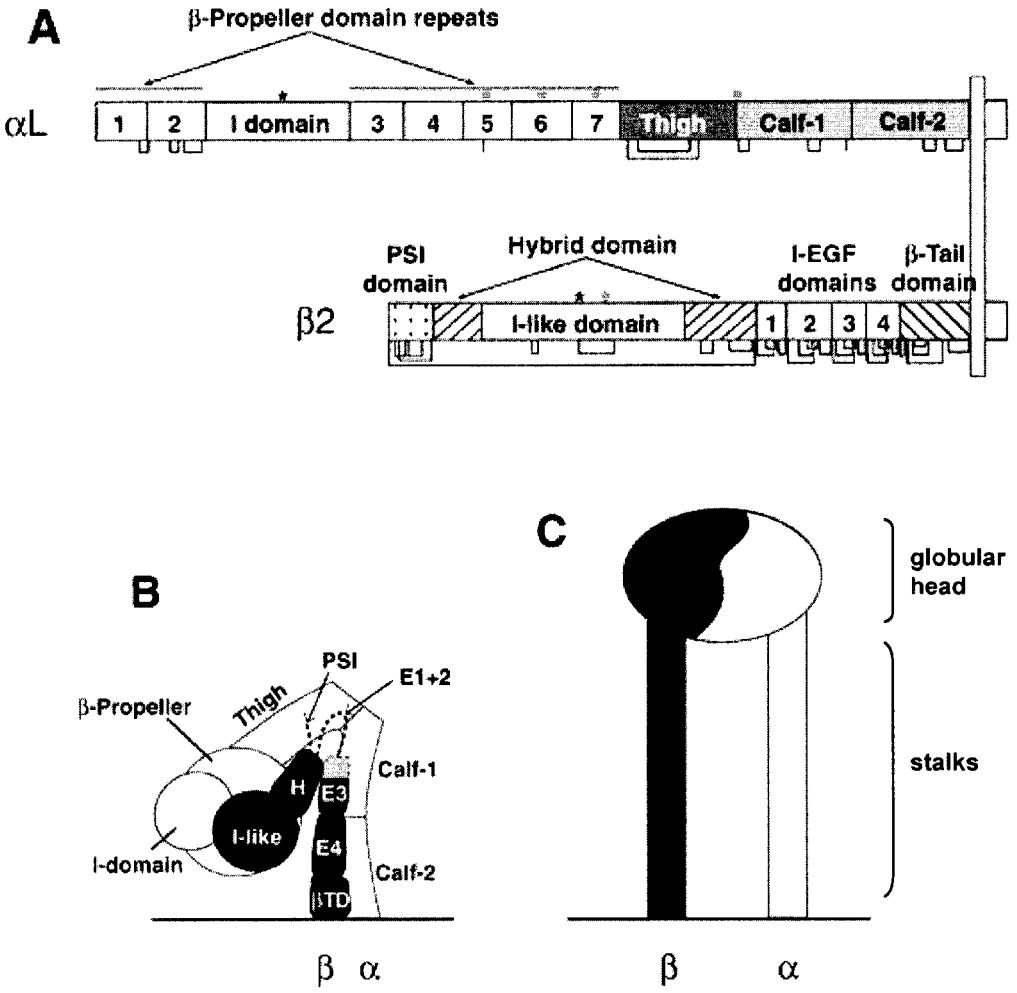

FIG 1.2 Integrin domain organization. (A) Organization of domains within the primary structure of αLβ2. In the integrins that do not contain I domain, the β-propeller repeats 2 and 3 are connected to each other. (B) Illustration of the domain arrangement of I domain-containing integrins. (C) Illustration of the general shape of an integrin based on previous EM studies. (Adapted from Shimaoka *et al.*, 2002)

shaped topology in which the head is closely juxtaposed to the membrane-proximal portions of the legs (Xiong et al. 2003) (Fig. 1.3). An increasing number of studies have together established that the bent conformation seen in the crystal structure is inactive and that the extended conformation commonly seen in electron micrographs represents the active conformation (Fig. 1.3). The overall concept is that integrin activation results in a switchblade-like upward movement of the head, which is coupled to other conformational movements within the ligand-binding sites. This eventually leads to an increase in the ligand-binding affinity of the integrin (Luo et al. 2007). Although integrin extension is one of the hallmarks of integrin activation, there are also reports of activated bent integrins (Adair et al. 2005; Arnaout et al. 2007; Chigaev et al. 2001; Larson et al. 2005; Luo et al. 2007; Nishida et al. 2006).

1.2.1 Extracellular domains

1.2.1.1 The α subunit

The α subunit is linearly organized from the N to the C terminus into a β-propeller with seven repeats (the I domain of ~200 amino acids is inserted between repeat II and III in all I domain-containing integrins), thigh, calf-1 and calf-2 domains. This is followed by a transmembrane domain and a cytoplasmic tail (Takagi et al. 2002a) (Fig. 1.2).

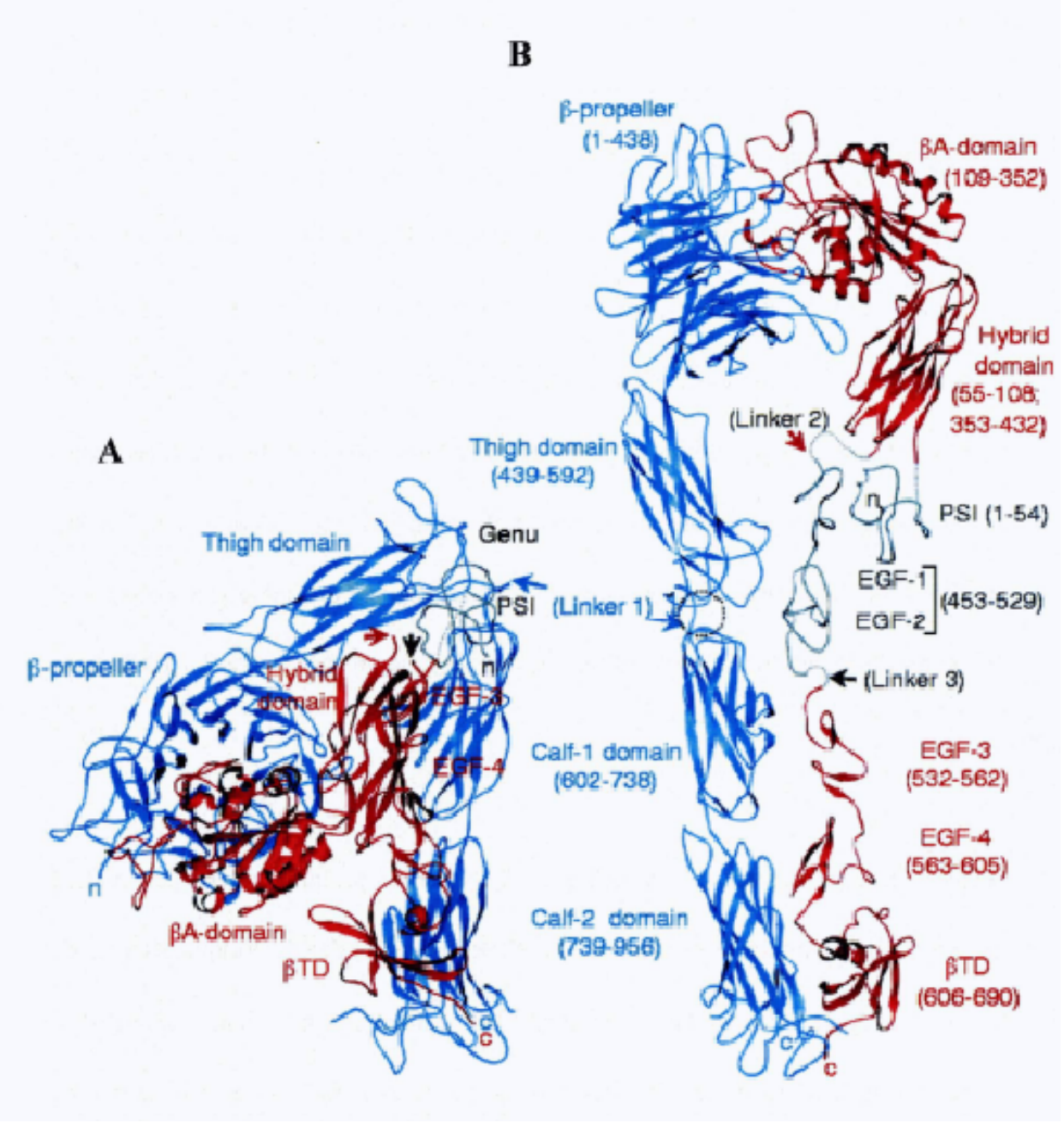

FIG 1.3 Structure of the extracellular segment of αVβ3. (A) Ribbon drawing of αVβ3 crystal structure [shown in blue (αV) and red (β3)]. (B) Model of a straightened extracellular segment of αVβ3. (Adapted from Xiong *et al.*, 2001)

The N-terminal of the α subunits contains seven weakly homologous tandem repeats each of approximately 60 amino acids. These are named as W1-W7. Extensive analyses have led to the prediction that these repeats fold into a β-propeller with seven β-sheets (blades) (Springer 1997). This is verified by the αVβ3 crystal structure (Xiong et al. 2001). In the αVβ3 crystal structure, each blade of the β-propeller is formed by a four-stranded β-sheet (Fig. 1.4). The inner strand (strand A) of each blade lines the channel at the center of the propeller, with strands B and C of the same repeat radiating outward, and strand D of the next repeat forming the outer edge of the blade. Strands within the repeating units are connected by hairpin turns and the β-propeller is circularized by juxtaposition of the C7 and D1 strands (Fig. 1.4) (Xiong et al. 2001). Further, Ca^{2+} binding sites in β hairpin loops are observed (Xiong et al. 2001).

In the integrins without the I domain, the β-propeller directly participates in ligand binding (Humphries 2000a; Xiong et al. 2002). In integrins that contain I domains, the β-propeller domain can cooperate in binding to some but not other ligands, as in αM (Yalamanchili et al. 2000), or it plays no direct role as in αL (Lu et al. 2001b; Shimaoka et al. 2001).

Nine of the 18 human integrin α subunits contain the I domain (Fig. 1.2). The I domain is homologous to a plasma glycoprotein von Willebrand factor (vWF) A (A1-A3) domain (Colombatti et al. 1991) and it was predicted that the I domain lies

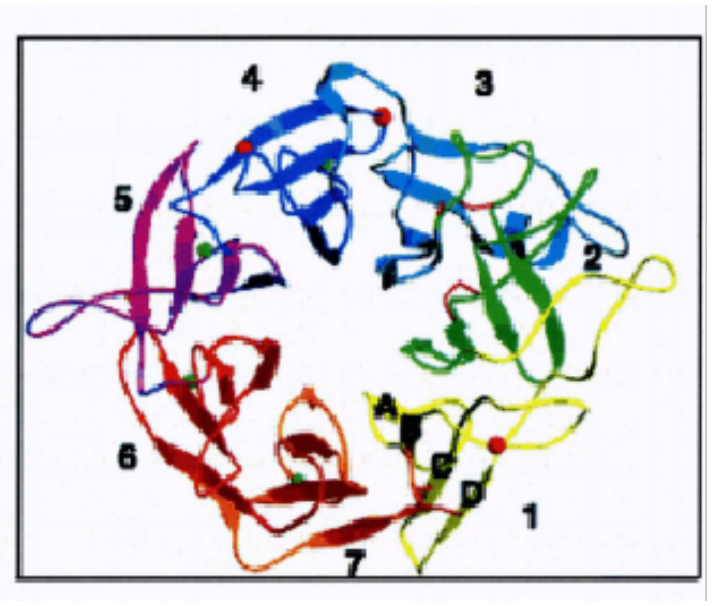

FIG 1.4 Structure of the integrin β-propeller. The β-propeller domain of αV is composed of the seven blades (numbered). Bottom view is shown. Glycans (spheres) are in red and Ca^{2+} ions are in green. (Adapted from Xiong *et al*., 2001)

on top of the β-propeller (Springer 1997). In the I domain-containing integrins, the I domain plays an essential role in ligand binding, which is strongly supported by monoclonal antibody (mAb)-mapping, mutation, and I domain deletion studies (Diamond et al. 1993; Leitinger et al. 2000; Randi et al. 1994).

Crystal structures have been determined for isolated I domains of integrins αM, αL, α2, α1, and αX (Emsley et al. 1997; Lee et al. 1995b; Nolte et al. 1999; Qu et al. 1995; Vorup-Jensen et al. 2003). The I domain adopts a Rossmann fold in which six central β strands are surrounded by either six or seven α helices. The top face of the I domain contains a divalent cation-binding site, referred to as the Metal Ion-Dependent Adhesion Site (MIDAS) (Fig. 1.5). This site is critical for ligand binding. Mutations of the MIDAS amino acids are reported to disrupt integrin ligand binding (Bajt et al. 1995). The cation in the I domain is coordinated by six residues. Five of these residues are from the MIDAS pocket. These are the conserved DXSXS sequence (single letter code; X is any amino acid) and two distal residues in the I domain. The sixth coordinating residue is provided by the integrin's ligand (Shimaoka et al. 2003).

The β-propeller of the α subunit is attached to an elongated leg formed by three β-sandwich domains termed thigh, calf1 and calf2 (Xiong et al. 2001). Much of this C-terminal region appears to correspond to the stalk region visualized in electron micrographs (Lu et al. 1998). Between the thigh and calf-1 is the "genu", which is capped by a divalent cation, and rearrangement of the genu/calf-1 interface together

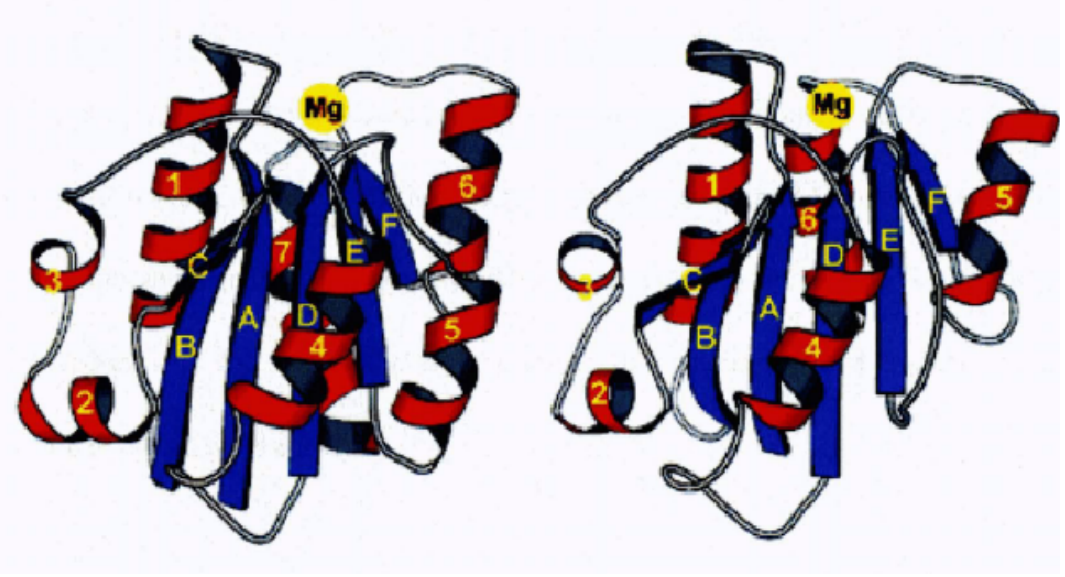

FIG 1.5 Crystal structures of I domains from two integrins. The I domain of the αM (left) and αL (right) subunits are shown. The position of the Mg^{2+} ion at the MIDAS motif is indicated at the top of the structure. Structures are derived from the studies by Lee *et al.*, 1995a (αM) and Qu and Leahy, 1995 (αL). The figure is from Plow *et al.*, 2000.

with the thigh/genu interface will occur upon the activation of the integrin (Xie et al. 2004).

1.2.1.2 The β subunit

The extracellular part of the β subunit is linearly organized into: a PSI domain; hybrid domain; an I domain like structure (also known as the I-like domain or β A domain); four I-EGF repeats, which share homology with the Epidermal Growth Factor fold and a membrane proximal tail domain (βTD) (Fig. 1.2). An interesting feature of all the β subunits is the unusually large number of cysteines found mainly in the C-terminal half of the β subunits.

The first 50-80 residues of the β subunit N-terminal region have a high content of cysteines and it shares sequence homology with the plexins and semaphorins. Thus, it is known as the PSI domain for Plexins, Semaphorins, and Integrins (Bork et al. 1999). The PSI domain is in position to make contacts with the β subunit hybrid domain and stalk (Xiao et al. 2004). Thus, it may transmit structural changes from the β subunit head to the stalk and then to the cytoplasmic tails (Xiao et al. 2004). The epitopes of some activating anti-β3 mAbs map to the PSI (Honda et al. 1995). Previous studies indicated that mutations in integrin αXβ2 (Zang et al. 2001) and αIIbβ3 (Sun et al. 2002) PSI domains can increase integrin activity.

All integrin β subunits contain a highly conserved domain of about 240 residues. This domain has similar tertiary structure to the I domain found in some α subunits. Thus, it is referred to as the "I-like domain". Like the α I domain, the β I-like domain contains a MIDAS with the DXSXS sequence motif for binding negatively charged residues that provide the sixth coordinating residue for the cation in the MIDAS (Xiao et al. 2004). In addition to the MIDAS, two other cation binding sites are found in the I-like domain. They are known as the LIMBS (ligand-induced metal ion-binding site) and ADMIDAS (adjacent to metal ion-dependant adhesion site). Interestingly, they share a few of the MIDAS coordinating residues for cation coordination (Xiong et al. 2001; Xiong et al. 2002). Ca^{2+}, Mg^{2+} and Mn^{2+} were reported to bind to these cation-binding sites and regulate the ligand-binding property of integrins (Dransfield et al. 1992; Shimizu et al. 1993).

The I-like domain is critical for integrin function because many mutations identified in LAD I and GT patients are located in this domain (Hogg & Bates 2000). These mutations disrupt integrin function and/or impair integrin heterodimer formation (Hogg & Bates 2000). The I-like domain participates directly to bind ligand in integrins that lack I domains and indirectly regulates ligand binding in I domain-containing integrins (Takagi 2007). Based on mutational studies and crystallography studies of αVβ3, there is a large interface between the β-propeller domain and the I-like domain (Xiong et al. 2001; Zang et al. 2000) and these contacts are essential for the proper folding of the integrin subunits (Huang et al. 1997).

The next domain after the I-like domain in the β subunit tertiary structure is the hybrid domain. The hybrid domain is formed by two separate sequences flanking the N- and C- termini of the I-like domain. It adopts an immunoglobulin-like fold (Takagi et al. 2002b). The hybrid domain is also known to be critical for the propagation of integrin activation signals (Luo et al. 2007), which will be discussed in later section.

The C-terminal portion of the β subunit extracellular domain is composed of four I-EGF repeats: I-EGF1, 2, 3 and 4. This is followed by βTD. As mentioned before, this region is cysteine-rich. Collective data from the crystal structure of αVβ3 (Xiong et al. 2001), NMR structure of the β2 I-EGF2 and I-EGF3 (Beglova et al. 2002), and the crystal structures of the β2 PSI, hybrid, and I-EGF1~3 domains (Shi et al. 2007; Shi et al. 2005), suggest that the bend in the β subunit is located between I-EGF1 and I-EGF2. Many activating antibodies and antibodies that bind only to activated integrins recognize the β I-EGF repeats (Humphries 2000b), which suggest the importance of this region in integrin signal transmission.

The four I-EGF repeats are followed by the βTD. In the crystal structure of αVβ3, βTD consists of a four-stranded β sheet that faces an NH2-terminal α helix (Xiong et al. 2001). From the same study, it also suggests that the linkage between βTD and I-EGF4 may be flexible, because only weak hydrophobic contacts are found between them. The βTD also contains epitopes of activating mAbs (Wilkins et al. 1996), and

this region is proposed to be involved in locking the β I-like domain in the low-affinity state (Arnaout et al. 2005).

1.2.2 Transmembrane (TM) domains

All integrin α and β subunits contain a single pass transmembrane (TM) domain. The α and β TMs are shown to interact with each other. Electron cryomicroscopy and single particle analysis showed a parallel crossed α-helical structure of the two TM helices within the membrane (Adair et al. 2005; Adair et al. 2002). Cysteine scanning mutagenesis of αIIbβ3 TMs also revealed a specific interface between the TMs (Luo et al. 2004). Recently, we also showed that specific pair of α and β TMs is required for the expression of a functional integrin (Vararattanavech et al. 2008). Integrin activation was observed after disruption of the TM interface (Gottschalk et al. 2002; Li et al. 2005). Therefore, the TMs not only connect the integrin cytoplasmic tail and its ectodomain, they also contribute to integrin bi-directional signaling across the plasma membrane. Several models have been proposed to explain the importance of TM domain in integrin signaling. In these models, the TM domains are proposed to undergo different orientation/movements such as rotation, tilting, hinging and piston movement or lateral separation in the plane of the plasma membrane (Adair & Yeager 2002; Armulik et al. 1999; Gottschalk et al. 2002; Luo et al. 2004; O'Toole et al. 1994; Williams et al. 1994).

1.2.3 Cytoplasmic tails

The integrin cytoplasmic tails are relatively short (except for the β4 subunit which has an extended cytoplasmic tail of over 1000 amino acids), and they lack intrinsic enzymatic activities. Nonetheless, they are functionally important. The α and β cytoplasmic tails contain conserved motifs shared amongst the subunits. A membrane-proximal 'KXGFFKR' sequence is found in all α cytoplasmic tails. Proximal to the membrane of the β cytoplasmic tails, a conserved positively charged residue (K/R) is followed by a 'LLVXIHDRRE' morif (Hynes 1992; Vinogradova et al. 2002). The 'D' in the β tail conserved motif has been identified as a residue to form a salt-bridge with the 'R' residue from the conserved sequence in the α cytoplasmic tail (Hughes et al. 1996; Vinogradova et al. 2002). Charge reversal mutation of either the 'D' to 'R' or 'R' to 'D' yields a constitutively active integrin (Hughes et al. 1996). Deletion of the entire cytoplasmic tail or of just the highly conserved 'GFFKR' sequence produces a constitutively active integrin (O'Toole et al. 1994; van Kooyk et al. 1999). Disruption of the interaction between the α and β tail results in an increased ligand binding affinity suggesting that this interaction may serve to constrain the integrin heterodimer in a low affinity state (Chen et al. 1994). Fluorescent resonance energy transfer (FRET) studies using αLβ2 with FRET pair fluorophores fused to its cytoplasmic tails in cells suggest that in the resting state the integrin α and β cytoplasmic tails are close to one another (Kim et al. 2003). Intracellular activation of integrin by cytoplasmic proteins such as talin is shown to

trigger the separation of the cytoplasmic tails (Kim et al. 2003). Similarly, extracellular activation by Mn^{2+} and soluble ligand of the integrin induces the separation of the α and β cytoplasmic tails (Kim et al. 2003).

The cytoplasmic tails connect the integrins to the cytoskeleton and allow the recruitment of signalling molecules (Hynes 2002). Many proteins have been reported to interact with the α or β cytoplasmic tails (Table 1.2). These proteins have a variety of functions. They include cytoskeletal, adaptor, signaling proteins and transcription factor, which are well described in many reviews (Calderwood et al. 2003; Lad et al. 2007; Liu et al. 2000).

There are two NPXY/F motifs in the β cytoplasmic tail. The first NPXY motif in some β cytoplasmic tails is a potential phosphorylation site, which serves as a docking site for the PTB (Phospho-Tyrosine Binding domain) -containing proteins (Calderwood et al. 2001). In the β3 subunit, this motif is found to be critical for the docking of talin, a well established activator of integrins (Tadokoro et al. 2003). This motif can also serve as an internalization signal because in the low density lipoprotein (LDL) receptor, it promotes internalization of the receptor via clathrin coated pits (Chen et al. 1990). Similarly, mutation of this motif in αMβ2 decreases its internalization (Rabb et al. 1993).

Protein	Integrin chain	Binding site	Reference
calreticulin	α-tails	KXGFFKR	Coppolino et al, 1997
filamin	β1, β2,β7	724-747	Sharma et al, 1995 Pavalko et al, 1998
α-actinin ,	β1, β2	736-746(β2) 762-774(β1)	Pavalko and LaRoche 1993 Sampath et al, 1998
Rack -1	β1,β2,β3	724-743(β2)	Lilienthal and Chang, 1998
14-3-3	β1	776-790	Han et al, 2001
talin	β1A,β1D,β2,β3,β7	membrane distal, several areas	Knezevic et al, 1996 Sampath et al, 1998, Pfaff et al, 1998, Calderwood et al, 2001
ILK	β1,β2,β3	N.D.	Hannigan et al, 1996
JAB-1	β2	N.D.	Bianchi et al, 2000
FAK	β1,β2,β3	membrane proximal	Schaller et al, 1995
paxillin	β1,β3,α4,α9	β subunit membrane proximal, α subunit 983-991	Schaller et al, 1995, Tanaka et al, 1996 Liu et al, 1999, Young et al, 2001
Phospholipase Cψ	β1	conserved membrane proximal region, α-chain GFFKR	Vossmeyer et al, 2002
myosin	β3	TyrP β3	Jenkins et al, 1998
Shc	β3	TyrP β3	Cowan et al, 2000
DRAL/FHL2	α3A,α3B,α7A,β	β:C-tennina1 NXXY α:12 aa next to membrane proximal	Wixler et al, 2000
cytohesin 1 and 3	β2	723-725	Kolanus et al, 1996, Geier et al, 2000
β3 endonexin	β3	membrane distal	Shattil et al, 1995
ICAP-I	β1	785-799	Chang et al, 1997 Zhang and Hemler, 1999, Degani et al,2002
PI 3-kinase	β1	pTyr-peptide	Johansson et al, 1994
CIB	αIIb	N.D.	Naik et al, 1997, Tsuboi, 2002
IRS-1	αVβ3	N.D.	Vuori and Ruoslahti,1994
melusin	β1A,β1D	membrane proximal	Brancaccio et al, 1999
MIBP	β1A,β1B,β1D	membrane proximal	Li et al, 1999
c-src	β3	C-terminal RGT	Arias-Salgado et al, 2005
Fyn	β3	N.D.	Arias-Salgado et al, 2003
Hck	β1,β2,β3	N.D.	Arias-Salgado et al, 2003
Lyn	β1,β2,β3	N.D.	Arias-Salgado et al, 2003
c-Yes	β1,β2,β3	N.D.	Arias-Salgado et al, 2003
radixin	β2	membrane proximal	Tang et al., 2007
Def-6	α7A	GTVGWDSSSGRST	Samson et al., 2007
Rab25	β1	N.D	Caswell et al., 2007
Kindlin-1	β1	N.D	Herz et al., 2006
Kindlin-2	β3	C terminal region	Ma et al., 2008
Kindlin-3	β1, β3	membrane distal	Moser et al., 2008

Table 1.2 Proteins interacting with integrin cytoplasmic tails. The list of proteins interacting with the integrin cytoplasmic tail is from Liu *et al.*, 2000, and additional interact proteins identified are also included.

1.3 Regulation of integrin function

The overall strength of integrin mediated cell adhesion, referred to as avidity, can be altered by changing either the intrinsic affinity of the individual receptor-ligand bonds or, the total number of these bonds formed (valency). Integrin affinity changes are regulated by conformational changes triggered by extracellular and/or intracellular activation signals. Integrin valency changes are modulated by the density of receptors on the adhesive surface. Integrin affinity and valency regulation are distinct processes, but they need not be mutually exclusive at the site of adhesion (Constantin et al. 2000; Giagulli et al. 2004). The relative contributions of each regulatory mechanism are integrin- and cell-type specific (Carman et al. 2003).

1.3.1 Affinity regulation

Integrins undergo global conformational changes when activated. These conformational changes are relayed from one end of the integrin to the other. Integrins are therefore bi-directional signaling receptors. In "inside-out" signaling or priming, stimuli received by other cell-surface receptors for chemokines, cytokines, and foreign antigens initiate intracellular signals that impinge on integrin cytoplasmic tails and alter the adhesiveness for extracellular ligand (Hynes 1992). In the reverse process known as "outside-in" signaling, the ligand-binding of integrins will influence the morphology, growth, and differentiation of cells (Hynes 1992).

Three key conformational changes are reported during integrin activation. These are namely: (i) the separation of the integrin cytoplasmic tails, (ii) the unbending of the integrin from a bent to an extended conformation, and (iii) the opening of the integrin headpiece.

The separation of the integrin α and β subunit transmembrane and cytoplasmic tails has emerged as the critical trigger for the initiation of an inside-out activation signal. As mentioned in previous section, in the resting integrin, its α and β cytoplasmic tails are in close proximity, and perturbation of this interaction will trigger integrin activation. This is well demonstrated in a FRET-based study in which the activation of integrin αLβ2 by the cytosolic protein talin involves the physical separation of the integrin cytoplasmic tails (Kim et al. 2003). The separation of the cytoplasmic tails most probably involves the disruption of the salt-bridge that links these tails as reported previously (Hughes et al. 1996). Thus, the interaction of the α and β cytoplasmic tails play important regulatory roles in the transmission of inside-out and outside-in activation signals (Kinashi 2007)

The unbending or switch-blade motion of an integrin from a bent to an extended conformation is widely accepted as the hallmark of integrin activation (Takagi et al. 2002a). This involves the projection of the integrin headpiece at least 16 nm from the membrane. The headpiece is composed of the I domain, β-propeller, thigh domain of the α subunit, and the I-like domain, PSI, hybrid, IEGF1-2 of the β subunit. This

projection serves to allow accessibility of the ligand-binding site of an integrin to macromolecular ligands, which is not favorable due to steric constraints in a bent integrin (Shimaoka et al. 2002).

From the recent EM study of integrin αLβ2 and αXβ2, two distinct conformations of the integrin headpiece have been observed (Nishida et al. 2006), which are reminiscence of the integrin conformations under transitions proposed previously (Xiao et al. 2004) (Fig. 1.6). These are the closed and the open conformations. The major difference between the two conformations is the orientation of the hybrid domain with respect to the I-like domain and the α subunit. In the closed headpiece, the hybrid is juxtaposed to the α subunit. In the open headpiece conformation, the hybrid undergoes a marked displacement away from the α subunit commonly referred to as the hybrid "swing-out" (Humphries 2000b). The open headpiece conformation is generally accepted as the high-affinity and ligand-bound conformation. This is supported by crystal structure data of αIIbβ3 and αVβ3 headpiece in the presence of a ligand-mimetic, which revealed a ~62Å displacement of the hybrid (Xiao et al. 2004).

In integrins that do not contain an I domain, the opening of the headpiece by hybrid swing-out leads to conformational changes in the β I-like domain and thus the affinity of the integrin to bind its ligands. However, in I domain-containing integrins, further structural changes are required for ligand binding. This involves the activation of the α I domain in a ratchet-like mechanism. The swing-out of the hybrid domain will lead

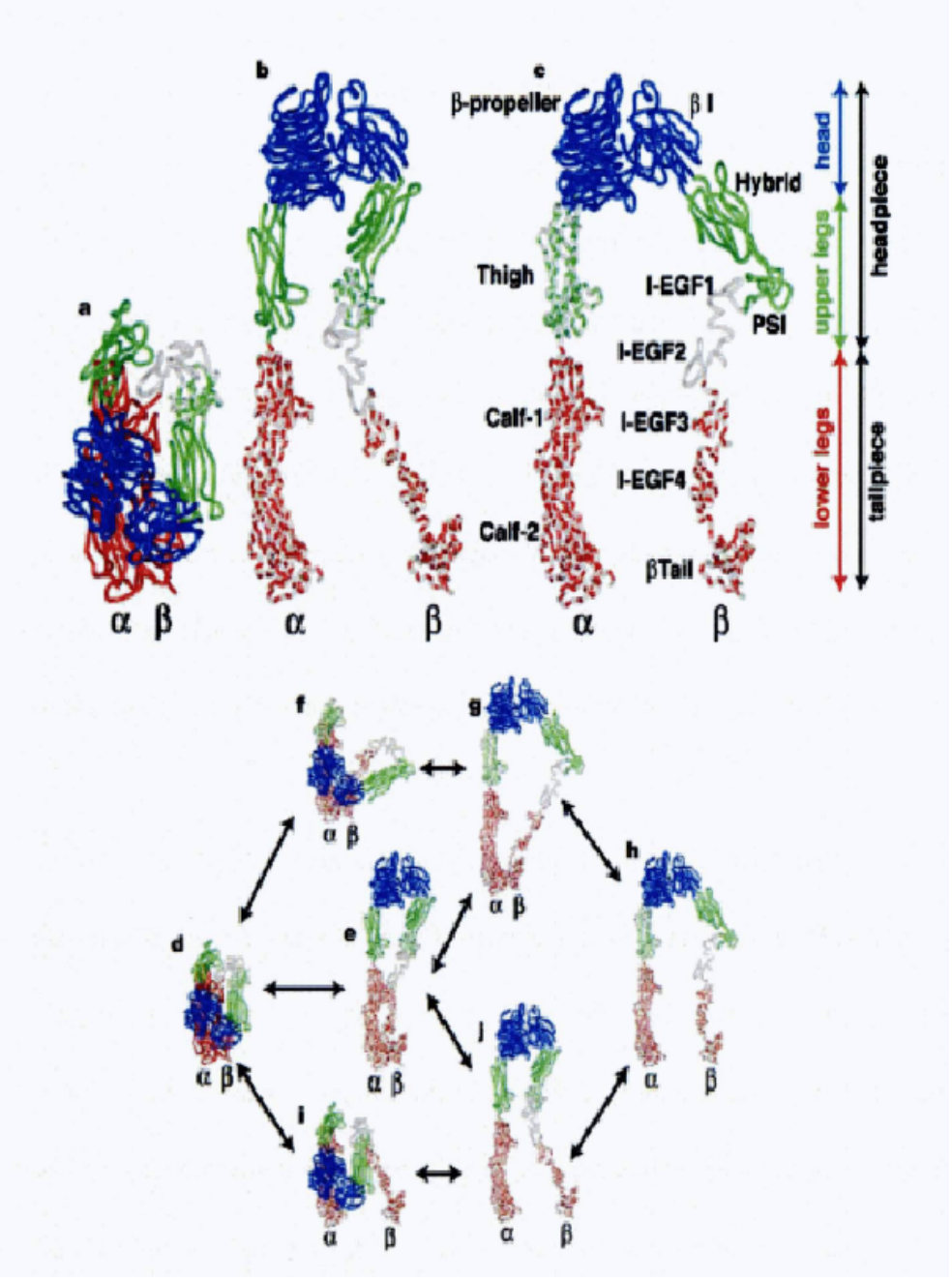

FIG 1.6 Quaternary rearrangements in integrin ectodomain. a-c, three conformational states visualized in electron microscopy and crystal structure. d-j, proposed intermediate integrins between known conformational states. The upper pathways may be stimulated by ligand binding outside the cell and the lower pathways by signal within the cell that separate the α and β transmembrane domains. In a-j, solid color represents the domains which are known directly from crystal structures; dashed with grey represents the domains which are placed from crystal structures into electron microscopy image averages; and solid grey represents for I-EGF1 and I-EGF2, which are modeled on I-EGF3 and I-EGF4. (From Xiao *et al.*, 2004)

to the activation of the β I-like domain, which triggers the binding of the β I-like domain MIDAS to a conserved glutamate residue (Glu310 in αL) in the last helix of the α I domain (Luo et al. 2007). In this case, the conserved Glu serves as an intrinsic ligand for the β I-like domain. Linking the β I-like domain ligand-binding site to the last helix of the α I domain by an engineered disulphide bond activates the αLβ2 integrin (Luo et al. 2007). Thus, it is proposed that the binding of the β I-like domain to the α I domain induces the downward motion of the last helix in the I domain, which leads to further structural changes at the ligand-binding site and the ligand-binding affinity of the I domain. It is also evident from these studies that the β I-like domain act as an allosteric regulator of the α I domain (Luo et al. 2007).

Other than the closed and open conformations of the integrin headpiece, two major conformations of the I domain have also been reported (Lee et al. 1995a). The close conformation represents the low affinity state whereas the open conformation represents the high-affinity or ligand-bound state. The primary difference between the two I domain conformations is the position of the last helices in these structures (Lee et al. 1995a). Indeed, mutations that stabilize the closed or open conformation by the introduction of disulphide bonds linking the last helix and its preceding linker exhibit constitutively low or high affinity for ligand, respectively (Lu et al. 2001c; Shimaoka et al. 2001; Shimaoka et al. 2000).

1.3.2 Valency regulation

The strength of integrin-mediated adhesion is also dependent on the valency or number of integrins at the adhesion site. This is modulated by (i) the total number of receptors expressed, (ii) the density of the integrins at the contact site, and (iii) the surface area of the contact site (Stewart et al. 1996).

The total number of integrins can be up-regulated by translocation of integrins from intracellular stores to the plasma membrane upon cellular stimulation (Bainton et al. 1987; Gogstad et al. 1981). For example, while αLβ2 appears very early in neutrophil maturation, it is becoming clear that the surface expressions of αMβ2 and αXβ2 are upregulated by translocation from an intracellular storage pool of peroxidase-negative granules that appear during the myelocyte stage of differentiation (Bainton et al. 1987). The density of integrins at the site of adhesion can be modulated by the micro- and/or macro-clustering of integrins via the reorganization of the cytoskeletal networks that connect the integins (Carman & Springer 2003). Release of the integrins from the cytoskeletal connection is also reported to facilitate integrin membrane diffusion required for clustering (Carman & Springer 2003). The clustering of the integrins can also occur post-ligand binding when multivalent ligands of integrins are considered (Shimaoka et al. 2002). During cell spreading, the area of cell contact with the substratum is also increased, allowing the interaction of a larger number of receptor-ligand complexes (Singer 1992). Further, the importance of cell

spreading is obvious in venules where cell flattening would provide a means of streamlining leukocytes onto endothelial cells, thus reducing the shear imposed on them by vascular flow (Springer 1994).

1.4 The β2 integrins

The focus of this thesis is the integrin αMβ2, which belongs to the β2 integrin subfamily. The β2 integrin subfamily is composed of four members that share a common β2 subunit but different α subunits, namely: αLβ2 (lymphocyte function-associated antigen-1, CD11a/CD18), αMβ2 (Mac-1, CD11b/CD18, CR3), αXβ2 (p150/95, CD11c/CD18, CR4) and αDβ2 (CD11d/CD18). The β2 integrins mediate the stable adhesion of leukocytes to endothelium and subsequent leukocytes transendothelial migration into inflamed organs (Arnaout 1990b; Springer 1990). They are also critical to the aggregation of phagocytes, ingestion of opsonized particles and macrophage oxidative burst (Arnaout et al. 1983; Hogg 1989). Their importance is well exemplified in LAD I patients that lack functional β2 due to mutations in the β2 subunit. As a consequence, LAD I patients suffer from repeated microbial infections and impaired wound healing due to the inability of circulating phagocytes to extravasate into infected tissues (Hogg & Bates 2000).

The αLβ2 integrin is expressed exclusively on leukocyte (Barclay et al. 1997). It was first described on murine and human lymphocytes by using monoclonal antibodies

that could inhibit both cytotoxic T cell-mediated killing and T cell proliferation (Davignon et al. 1981; Sanchez-Madrid et al. 1982). To date, six ligands for αLβ2 have been identified (Table 1.3). All are single chain type I membrane glycoproteins and are members of the Immunoglobulin-superfamily (IgSF) that contain variable numbers of tandem immunoglobin-folds (Ig domains) (Fig. 1.7). These are the intercellular adhesion molecules (ICAMs): ICAM-1 (Marlin et al. 1987), ICAM-2 (Staunton et al. 1989), ICAM-3 (de Fougerolles et al. 1993; de Fougerolles et al. 1992; Fawcett et al. 1992), LW (ICAM-4) (Bailly et al. 1995) and telencephalin (ICAM-5) (Tian et al. 1997), and the newly-identified IgSF member JAM-1 (Junctional Adhesion Molecule 1) (Ostermann et al. 2002).

αXβ2 (complement receptor type 4, CR4) was initially identified as an iC3b receptor. It is mainly expressed on myeloid cells with high levels expressed on tissue macrophages, and it is a marker for hairy cell leukemia (Larson et al. 1990). It is also expressed, at lower levels, on dendritic cells, granulocytes, natural killer (NK) cells, lymphoid cell lines and populations of activated T and B cells (Barclay & Brown 1997). Its role is poorly defined compared to αLβ2 and αMβ2, but it shares overlapping ligands with that of αMβ2 (Table 1.3), which will be discussed in later section. A good example is the binding of αXβ2 to iC3b-opsonized particles (Myones et al. 1988) and its role in the adhesion of monocytes and granulocytes to endothelium (Keizer et al. 1987).

Integrin	Other names	Expression	Ligands
αLβ2	CD11a/CD18; LFA-1	All leulocytes	ICAM-1; ICAM-2; ICAM-3; ICAM-4; ICAM-5; JAM-1
αMβ2	CD11b/CD18; Mac-1 CR3, Mo1	Monocytes, macrophages; neutrophils; NK cells; γδ T cells	iC3b; fibrinogen, ICAM-1; ICAM-2; ICAM-4; JAM-3; Factor X; NIF; denature proteins; β-glucan; lipopolysaccharide; and others
αXβ2	CD11c/CD18; P150,95; CR4; Leu-M5	Monocytes; macrophages; NK cells; dendritic cells; neutrophils	iC3b; fibrinogen; ICAM-1; denatured proteins; lipopolysaccharide; and others
αDβ2	CD11d/CD18	Monocytes; macrophages; eosinophils; neutrophils	ICAM-3; VCAM-1

Table 1.3 A summary of the expressions and ligand binding properties of the β2 integrins. (Adapted from Luo *et al.*, 2007; Berton *et al.*, 1999)

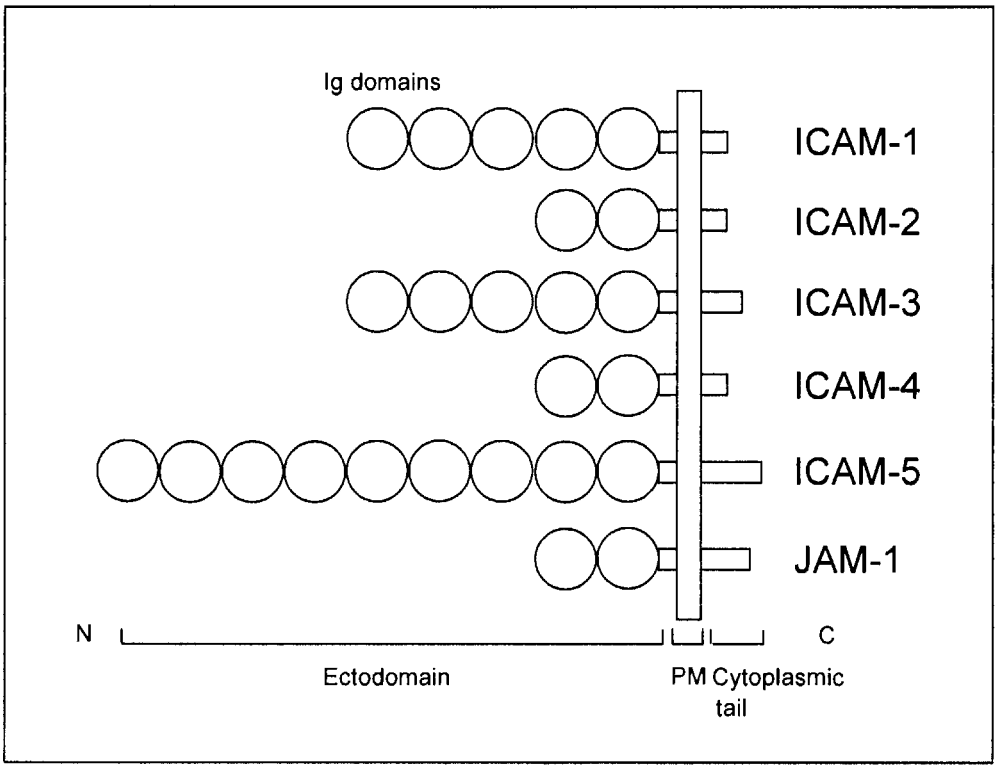

FIG 1.7 Schematic structures of the ICAMs and JAM-1. ICAM-1 and ICAM-3 have five Ig-domains while ICAM-2, ICAM-4 and JAM-1 have only two. ICAM-5 is the largest ICAM, with nine Ig-domains.

Being the latest member of the β2 integrins to be identified, the function of αDβ2 remains to be fully characterized. αDβ2 is expressed at moderate levels on myelomonocytic cell lines and subset of peripheral blood leukocytes, and more strongly on tissue-compartmentalised cells such as foam cells, specialized macrophages found in aortic fatty streaks that may develop into atherosclerotic lesions (Van der Vieren et al. 1995). It may have a role in the processing of blood components of effete erythrocytes by αDβ2-mediated phagocytosis in splenic red pulp macrophages (Van der Vieren et al. 1995). αDβ2 was reported to bind to ICAM-3 (Van der Vieren et al. 1995) and VCAM-1 (Vascular Cell Adhesion Molecule-1, CD106) (Van der Vieren et al. 1999). This interaction may contribute to the trafficking of the αDβ2-expressing leukocytes.

The αMβ2 integrin is expressed mainly on cells of the myeloid lineage, such as granulocytes, monocytes, and macrophages, and it is also found on natural killer cells and γδ T cells (Graff et al. 2007; Larson & Springer 1990). It was first shown to bind to iC3b-coated erythrocytes and found to be equivalent to the complement receptor type 3 (CR3) (Beller et al. 1982). Numerous physiological functions have been attributed to αMβ2, including adhesion and transmigration of leukocytes through endothelium (Springer 1994), the phagocytosis of infectious agents (Graham et al. 1989), and the activation of neutrophils and monocytes (Shappell et al. 1990). Excessive activation of αMβ2 can lead to inflammation and pathogenic tissue damage

(von Asmuth et al. 1991). A role for αMβ2 has been established in reperfusion injury (Horgan et al. 1990).

Other than serving as the receptor of iC3b, αMβ2 binds to a broad spectrum of ligands, such as ICAM-1, ICAM-2 and ICAM-4, but not to the ICAM-3 (de Fougerolles et al. 1995). The αMβ2-binding sites on these ICAMs are apparently different (Diamond et al. 1990; Diamond et al. 1991; Hermand et al. 2000; Xie et al. 1995). αMβ2 has also been reported to bind to extracellular matrix proteins such as: fibronectin, laminin, and collagen (Bohnsack et al. 1990). Binding of the zymogen factor X to αMβ2 results in the acceleration of its conversion to activated factor Xa and constitutes an alternative pathway for the initiation of the coagulation serine protease cascade (Altieri et al. 1988b; Altieri et al. 1988c; Plescia et al. 1996). The capacity of αMβ2 to bind to proteins of the blood clotting system such as zymogen factor X and fibrinogen (Altieri et al. 1988a; Ugarova et al. 2001), together with its reported ICAM-4 (LW) binding capacity may allow αMβ2 to be involved in the regulation of the blood clotting process and the tureover of erythrocytes. αMβ2 is also known to bind to denatured proteins such as denatured BSA (Davis 1992). αMβ2 can also bind to non-proteinaceous moieties of a number of bacterial components including: β-glucan (Ross et al. 1987), lipopolysaccharide (LPS) (Van Strijp et al. 1993; Wright et al. 1986) or lipophosphoglycan (LPG) (Talamas-Rohana et al. 1990). Thus, αMβ2 serves an important role in the clearance of opsonized or non-opsonized microbes.

Unlike certain integrins in the β1 and β3 subfamilies, where a single receptor interacts with many different proteins through the common RGD sequence (D'Souza et al. 1991), the αMβ2 ligands share few, if any, similarities or conserved sequences. It was found by phage display that the leukocyte-specific β2 integrins bind sequences containing a leucine-leucine-glycine (LLG) tripeptide motif, which is present on ICAM-1 and several matrix proteins. A bicyclic peptide, CPCFLLGCC (LLG-C4), was isolated as the most active binder to the purified αMβ2 integrin (Koivunen et al. 2001). Thereafter, another negatively charged peptide motif, (D/E) (D/E) (G/L) W, was obtained by screening phage display libraries to isolate peptides that bind to the αM I domain (Stefanidakis et al. 2003). This peptide was the only peptide obtained by this approach despite the known ligand binding promiscuity of αMβ2. Such negatively charged sequences are present in many known β2 integrin ligands, which suggest these sequences and LLG sequences play a role in the binding of leukocytes, and that peptidomimetics derived from these two motifs could provide a therapeutic approach to αMβ2-mediated inflammatory reactions (Koivunen et al. 2001).

1.5 αMβ2 associated proteins

Integrins interact with cytosolic proteins via their cytoplasmic tails. Integrins can also interact with proteins on the membrane of the same cell via lateral association (Porter et al. 1998). Many of these interactions are important to the function of the integrins and their partner molecules. αMβ2 is known to interact with membrane molecules

such as FcγRIIIB (Zhou et al. 1993), FcγRIIA (Annenkov et al. 1996), CD14 (Todd et al. 1997), LDL-receptor (Spijkers et al. 2005), and uPAR (Urokinase Plasminogen Activator Receptor, CD87) (Bohuslav et al. 1995). Of particular interest in this study is the association of αMβ2 with the uPAR.

1.6 uPAR (Urokinase Plasminogen Activator Receptor)

uPAR is a highly glycosylated 50~65-kD protein linked to the plasma membrane by glycosylphosphatidylinositol (GPI) anchor (Ploug et al. 1994). It is expressed on mononuclear phagocytes, neutrophils, activated T cells, endothelial cells, and several types of tumor cells (Blasi 1999; Mazar et al. 1999). uPAR has a high content of cysteine residues that are arranged in a triplicate pattern that defines three homologous domains, referred to as D1, D2 and D3 (Fig. 1.8A). This motif is shared with three other GPI-anchored membrane proteins (murine Ly-6, CD59, and squid glycoprotein Sgp-2) and with a variety of elapid snake venom toxins (the erabutoxinn-bungarotoxin series), suggesting that these proteins comprise a superfamily of proteins (Ploug & Ellis 1994). The crystal structure reveals that the three domains of uPAR are assembled in a right-handed orientation generating an almost globular receptor with a breach between D1 and D3 (Fig. 1.8B) (Barinka et al. 2006; Llinas et al. 2005). Expression of uPAR has been shown to correlate with the prognosis of many human cancers (Blasi 1999; Mazar et al. 1999). In murine tumor models, expression or administration of uPAR antagonists has a marked inhibitory

A

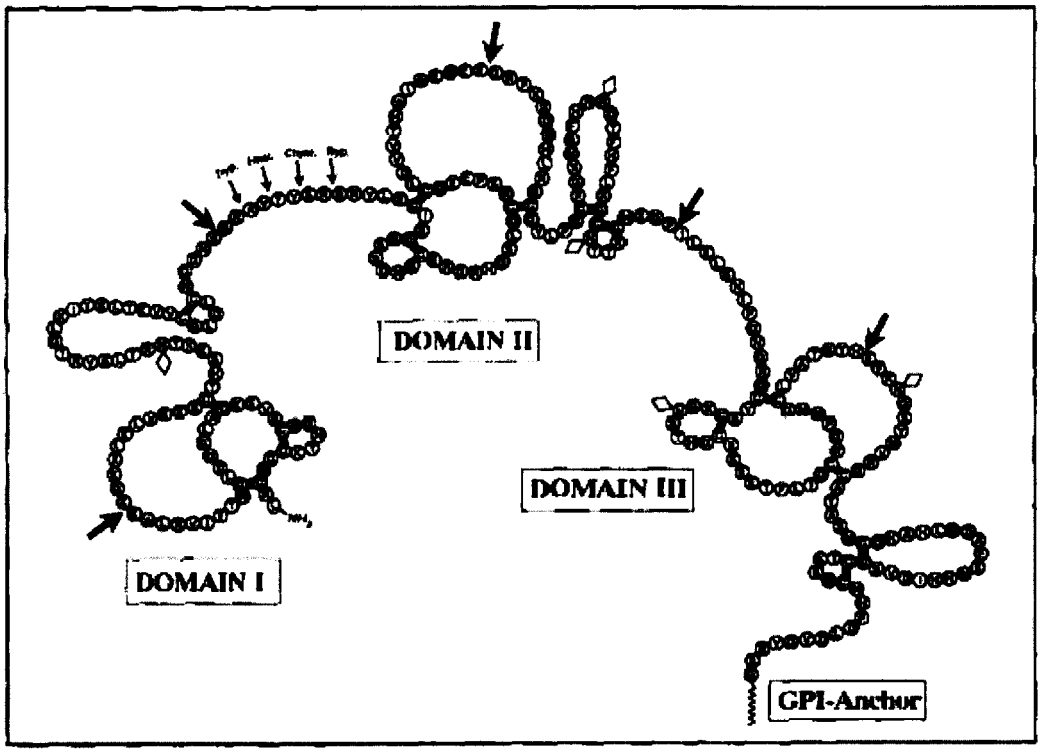

B

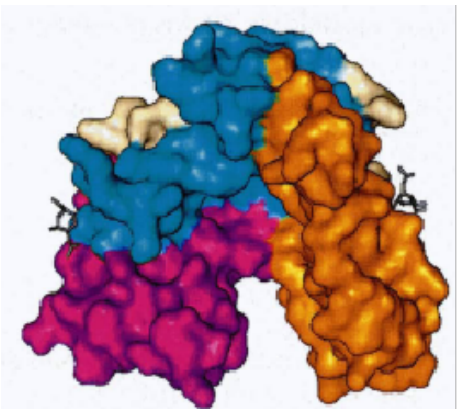

C-terminal region; GPI-linked

N-terminal region

FIG 1.8 Structure of uPAR. (A) The primary sequence of human uPAR is shown as encircled amino acids in the single letter code. Circles joined by a black bar represent disulfide bonded cysteine residues. Diamonds represent potential attachment sites for N-linked carbohydrate. The large arrows indicate positions corresponding to the presence of introns in the uPAR gene. The smaller arrows identify peptide bonds that are extremely susceptible to proteolysis in the native non-denatured protein. (From Ploug *et al.*, 1994) (B) Overall structure of human uPAR. The individual uPAR domains are assembled in a right-handed orientation and are colored in yellow (D1), blue (D2) and red (D3). (Adapted from Llinas *et al.*, 2005)

effect on the metastatic ability of cancer cells (Crowley et al. 1993) and on the growth of the primary tumor (Hong et al. 1996), and the down-regulation of uPAR leads to dormancy of carcinoma cells *in vivo* (Kook et al. 1994; Yu et al. 1997). Thus, uPAR expression has been implicated in cancer progression. Growth factors such as vascular endothelial growth factor, fibroblast growth factor, platelet-derived growth factor, and the interleukins can up-regulate uPAR in endothelial cells, smooth muscle cells, and leukocytes *in vitro*, whereas unstimulated cells have low or undetectable expression of uPAR. uPAR is the cellular receptor for urokinase (uPA), a serine protease that is constitutively or inducibly secreted by most uPAR-expressing cells. Receptor-bound uPA can convert plasminogen to plasmin, which mediates pericellular proteolysis of extracellular matrix proteins in the path of cellular invasion (Bohuslav et al. 1995). This is exemplified in macrophage invasion, ovulation, angiogenesis, wound healing, and in pathological conditions of neoplasia and metastasis (Blasi 1999; Mazar et al. 1999).

uPA/uPAR is considered as one of the earliest mediators of fibrinolysis by activating plasminogen into plasmin, which in turn degrades fibrin and prevents its extracellular deposition. In animal models of septic shock (Yamamoto et al. 1996), lung injury (Barazzone et al. 1996), impaired wound healing (Romer et al. 1996) and glomerulonephritis (Kitching et al. 1997), reduced uPA-mediated proteolysis correlated with excessive fibrin deposition. Moreover, in the absence of uPA, the local generation of plasmin is reduced, and this was shown to hamper the recovery of

damaged muscle (Lluis et al. 2001). In addition to fibrinolysis, the uPA/uPAR system might modulate several steps of the inflammatory cascade (Fig. 1.9). uPA/uPAR participates in the innate immune system by regulating the adhesion and migration of the neutrophils and macrophages. In uPAR-deficient mice, macrophages and neutrophils failed to infiltrate the lungs of mice infected with *Streptococcus pneumonia* (Rijneveld et al. 2002) or *Pseudomonas aeruginosa* (Gyetko et al. 2000), or to migrate into inflamed peritoneal cavity of thioglycollate-induced mice (May et al. 1998). In the absence of uPAR, the migration of lymphocytes was also reduced (Gyetko et al. 2001). In addition to the contribution of uPA/uPAR to the innate immune system, it has a role in the adaptive immune response. Native T cells express low level of uPA and uPAR, but their expression is rapidly upregulated when T cells are activated (Bianchi et al. 1996; Nykjaer et al. 1994). It was observed that splenocytes derived from uPA-deficient mice elicit only suboptimal T-cell activation and proliferations in vitro (Gyetko et al. 1999). It has also been suggested that uPA-dependent fibrinolysis and tissue remodeling might favor antigen presentation and T-cell re-activation *in situ* by eliciting the degradation of tissue components (Mondino et al. 2004). The binding of uPA to uPAR also initiates signaling cascades that require receptor occupancy but not uPA catalytic activity. Signaling pathways which are lined to uPA/uPAR include cytosolic kinase pathways (tyrosine kinases, serine/threonine kinases and protein kinase C) (Bohuslav et al. 1995; Degryse et al. 2001; Resnati et al. 1996), focal adhesion kinase (FAK) pahway (Blasi et al. 2002), extracellular signal-regulated kinase/mitogen-activated protein kinase (ERK/MAPK)

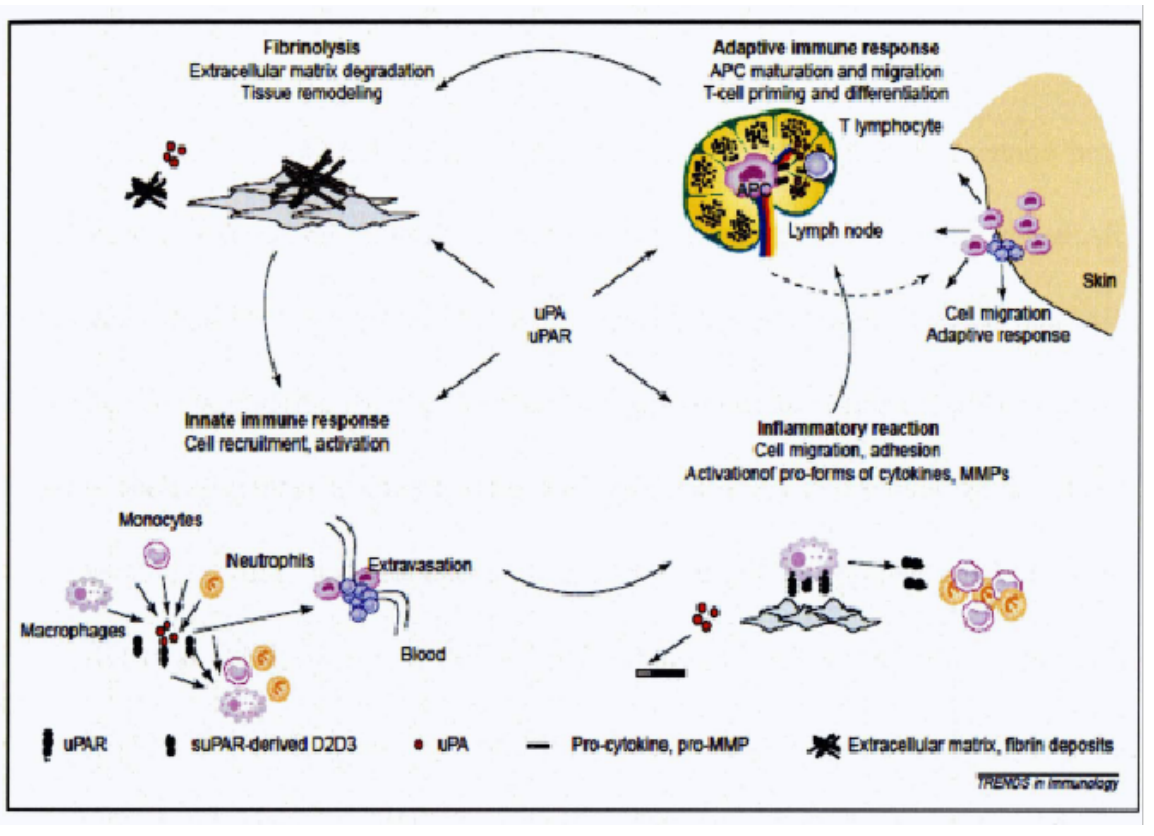

FIG 1.9 uPA and uPAR contribute to fibrinolysis, inflammation, and innate and adaptive immune responses. Abbreviations: APC, antigen-presenting cell; MMP, matrix metalloprotease; uPA, urokinase plasminogen activator; uPAR, uPA receptor; suPAR, soluble uPAR. (Taken from Mondino *et al*., 2004)

pathway (Aguirre Ghiso et al. 1999; Webb et al. 2000), and intracellular calcium mobilization (Sitrin et al. 1999). These signaling pathways regulate cell adhesion, migration, proliferation and differentiation as a consequence of uPA binding to uPAR (Aguirre Ghiso et al. 1999; Degryse et al. 2001; Nusrat et al. 1991; Wei et al. 1996).

uPAR is devoid of a cytoplasmic domain, thus it is interesting to understand how uPAR acts as a signaling molecule in these functions. It is well reported that uPAR associates with other molecules including the integrins. Such interaction allows uPAR signaling via its integrin partner. uPAR has been shown to associate with multiple integrins including those of the β1, β2 and β3 subfamilies by co-immunoprecipitation, immunocolocalization, and resonance energy transfer (RET) approaches (Wei et al. 1996; Xue et al. 1994; Xue et al. 1997). The formation of uPAR complexes with αLβ2 was demonstrated on monocytes by co-immunoprecipitation and receptor co-capping (Bohuslav et al. 1995). It was shown by fluorescence resonance energy transfer (FRET) microscopy that αXβ2 and uPAR were in close physical proximity on migrating neutrophils (Kindzelskii et al. 1997). uPAR is well reported to interact with the αMβ2 (Bohuslav et al. 1995; Simon et al. 2000; Sitrin et al. 1996; Xue et al. 1994), and is known to exert different effects on the function of αMβ2. Interestingly, αMβ2 is also required for plasminogen activation and fibrinolysis by neutrophils (Pluskota et al. 2004). This also suggests a ternary complex comprising of uPA/uPAR/αMβ2 in the process of fibrinolysis. uPAR was found to co-cap with αMβ2 in resting neutrophils, but it dissociate from αMβ2 during neutrophil polarization (Kindzelskii et al. 1997;

Kindzelskii et al. 1996). Several studies reveal that uPAR has a positive regulatory role on αMβ2 function. Recent *in vitro* studies have shown that the presence of uPAR is needed for αMβ2 binding to fibrinogen, and it also regulates fibrinogen degradation by forming a functional unit with the β2 integrins (Zhang et al. 2003). Indeed, mAbs having different epitopes in uPAR can affect αMβ2-dependent adhesion, and removal of uPAR with phosphatidylinositol-specific phospholipase C (PiPLC) (May et al. 1998) or inhibition of uPAR synthesis with an antisense oligonucleotide (Gyetko et al. 1994; Sitrin et al. 1996) diminishes αMβ2-dependent adhesion. In cells lacking uPAR by PiPLC treatment, the αMβ2-dependent adhesion is recovered by reconstituting with soluble recombinant uPAR (sr-uPAR) (May et al. 1998). Neutrophils from uPAR-deficient mice also exhibit defective diapedesis into certain inflammatory sites (Gyetko et al. 2000; May et al. 1998).

It was also reported that uPAR exert a negative effect on the ligand-binding function of αMβ2 (Simon et al. 2000; Wei et al. 1996). This may be explained by the close proximity of the uPAR interaction site on αMβ2 with the I domain. It was shown that uPAR binds to a stretch of sequence in the W4 (blade 4) of the αM β-propeller, which is in the proximity of the αM I domain (Simon et al. 2000).

1.7 Aims of Study

Although the importance of uPAR on αMβ2 function is widely reported, the molecular association and the signaling mechanism of the uPAR-αMβ2 complex remain unclear. The structure of uPAR-αMβ2 complex remains unknown. Further, whether other sites of the integrin are involved in uPAR interaction are not well characterized. Thus, the first part of my study aims to define the other sites in αMβ2 that are involved in uPAR interaction. The second part of this study investigates whether uPAR induces shape changes in αMβ2, and the possible molecular mechanism by which uPAR signal via its integrin partner. In this study, we report that uPAR domain 1 (D1) is the primary binding site of αMβ2, and its association with αMβ2 attenuates αMβ2 binding to its ligands BSA, fibrinogen, and ICAM-1. Analyses of the interacting interface between αMβ2 and uPAR by co-immunoprecipitation studies suggest that a substantial surface area of the αMβ2 is shielded by its association with uPAR and uPAR might modulate the function of αMβ2 by steric occlusion of the ligand-binding site on the αM I domain. Further, we show that uPAR induces the opening of αMβ2 headpiece and the re-orientation of αMβ2 TMs, which could provide the trigger for downstream signaling.

Chapter Two: Materials and Methods

2.1 General reagents

General reagents and solvents were of analytical grade, and were obtained from Sigma Aldrich Chemical Company Ltd., BDH Chemicals Ltd., Becton-Dickenson Ltd., GIBCO-BRL Ltd., Pierce Ltd., unless otherwise stated. Solutions were sterilized where required, by autoclaving or by passing through a 0.22μm filter (Millipore, Billerica, MA).

2.1.1 *Enzymes*

All restriction endonucleases and other enzymes were obtained from New England Biolabs, Promega Ltd., Fermentus Ltd, Roche diagnostics unless otherwise stated and were used according to the manufacturers' instructions.

2.1.2 *Commercially available kits*

ECL Detection Kit	GE Healthcare, Buckinghamshire, UK
Plasmid Maxi Kit	QIAGEN Ltd., Valencia, CA
QIAprep Spin MINIprep Kit	QIAGEN Ltd. , Valencia, CA
QIAquik PCR purification Kit	QIAGEN Ltd. , Valencia, CA

QIAquik Gel Extraction Kit	QIAGEN Ltd. , Valencia, CA

2.1.3 *cDNA clones provided by others*

CD11a (integrin αL)	From Prof. LAW SK (School of Biological Sciences, NTU)
CD11b (integrin αM)	From Prof. LAW SK (School of Biological Sciences, NTU)
CD18 (integrin β2)	From Prof. LAW SK (School of Biological Sciences, NTU)
ICAM-1-(D1-D5)-Fc	From Dr DL, Simmons, IMM, Oxford

2.1.4 *Cells*

293T (human embryonic kidney cell with SV40 large T antigen)	Purchased from ATCC, Manassas, VA
HEK-293 (human embryonic kidney cell)	Purchased from ATCC, Manassas, VA
K562 (human leukemia cells)	Purchased from ATCC, Manassas, VA

2.1.5 *Antibodies*

MHM24	anti-αL	Hybridoma from Prof. A.J. McMichael,

		John (John Radcliffe Hospital, Oxford, UK) (Hildreth et al. 1983)
LPM19c	anti-αM	Hybridoma from Dr. K. Pulford (LRF Diagnostic Unit, Oxford, UK) (Shaw et al. 2001)
OKM1	anti-αM	From Prof. T.A. Springer (Harvard Medical School, Boston, MA) (Diamond et al. 1993)
CBRM1/10	anti-αM	From Prof. T.A. Springer (Harvard Medical School, Boston, MA) (Diamond et al. 1993)
CBRM1/23	anti-αM	From Prof. T.A. Springer (Harvard Medical School, Boston, MA) (Diamond et al. 1993)
MHM23	anti-β2 heterodimer dependent	Hybridoma from Prof. A.J. McMichael (John Radcliffe Hospital, Oxford, UK) (Hildreth et al. 1985)
IB4	anti-β2 heterodimer dependent	Hybridoma purchased from ATCC, Manassas, VA (Wright et al. 1983)
7E4	anti-β2	Purchased from Beckman Coulter, Fullerton, CA (Tan et al. 2001)
KIM185	anti-β2 activating mAb	Hybridoma purchased from ATCC,

		Manassas, VA (Robinson et al. 1992)
MEM148	anti-β2	Purchased from AbD Serotec, Oxford, UK (Tang et al. 2005)
KIM127	anti-β2	Hybridoma purchased from ATCC, Manassas, VA (Beglova et al. 2002)
VIM5	anti-uPAR domain 1	Purchased from BD Biosciences, San Jose, CA
anti-D2	anti uPAR domain 2	Purchased from American Diagnostica Inc., Stamford, CT
anti-D3	anti uPAR domain 3	Purchased from American Diagnostica Inc., Stamford, CT
399	Rabbit anti-human uPAR polyclonal antibody	Purchased from American Diagnostica Inc., Stamford, CT
Ab-1	anti-uPA	Purchased from Calbiochem, San Diego, CA
Ab-5	Anti-actin	Purchased from BD Biosciences, San Jose, CA
HA(I9)	Anti-HA	Purchased from Delta Biolabs, Gilroy, CA

2.1.6 *Ligands for cell binding analysis*

ICAM-1-(D1-D5)-Fc	Prepared by Miss Manisha Cooray (SBS, NTU) (Tan et al. 2001)
BSA	Purchased from Sigma, St. Louis, MO
Fibrinogen (human)	Purchased from Sigma, St. Louis, MO
uPA (HMW-tc) (human)	Purchased from American Diagnostica Inc., Stamford, CT

2.1.7 *Expression Vectors*

pcDNA3.0	Invitrogen, Carlsbad, CA
pDisplay	Invitrogen, Carlsbad, CA

2.2 Solutions, buffers, and media

2.2.1 *Laboratory stocks*

10 mg/ml BSA in ddH_2O	Stored at -20°C
0.1 M DTT in ddH_2O	Stored at -20°C
0.5 M EDTA in ddH_2O, pH 8.0	Stored at RT
10 mg/ml ethidium bromide	Stored at 4°C

1 M HEPES, pH 7.4	Stored at 4°C
3 M NaAc in ddH_2O, pH 4.8	Stored at RT
5 M NaCl in ddH_2O	Stored at RT
0.1 M Sodium Bicarbonate Buffer	Stored at RT
2x protein solubilisation buffer	0.16 M Tris pH 8.0, 8 M Urea, 1.6% (w/v) SDS, 0.08% (w/v)bromophenol blue
10%(w/v) SDS in ddH_2O	Stored at RT
10x TAE	0.4 M Tris pH 8.0, 1.14% (v/v) glacial acetic acid, 10 mM EDTA
1M Tris-HCl in ddH_2O, pH 8.0	Stored at RT

2.2.2 *Media*

All media were sterilized by autoclaving followed by addition of relevant antibiotics unless otherwise stated.

LB medium	1% (w/v) Bacto-tryptone (BD), 0.5% (w/v) yeast extract (BD), 1% (w/v) NaCl, supplemented with 60 μg/ml ampicillin or 30 μg/ml kanamycin
LB agar	LB medium plus 2% (w/v) Bacto-agar (BD), supplemented with 60 μg/ml ampicillin or 30 μg/ml kanamycin

HEK-293 and 293T cell culture media	DMEM (JRH) containing 10% (v/v) heat-inactivated FBS, 100 IU/ml penicillin, 100 µg/ml streptomycin
K562 cell culture media	RPMI (JRH) containing 10% (v/v) heat-inactivated FBS, 100 IU/ml penicillin, 100 µg/ml streptomycin

2.2.3 *Solutions*

blocking buffer (Western)	PBS containing 1% (w/v) non-fat milk, 0.1% (v/v) Tween20
blotting buffer (Western)	12.5 mM Tris pH 8.0, 96 mM glycine, 10% (v/v) ethanol
cell freezing media	10% DMSO in heat-inactivated FBS
100 mM iodoacetamide	prepared fresh in ddH_2O
lysis buffer	150 mM NaCl, 50 mM Tris-HCl pH 7.5, 1% (v/v) deoxycholate, 0.1% (w/v) SDS, and 1% (v/v) Trixon-100, 2.5 mM iodoacetamide
100 mM PMSF	prepared in ethanol, stored at -20 °C
10x SDS-PAGE running buffer	0.25 M Tris, 1.9 M glycine, 1% (w/v) SDS
4x resolution gel buffer	0.25 Tris, 0.4% (w/v) SDS, pH 8.8

4x stacking gel buffer	0.5M Tris, 0.4% (w/v) SDS, pH 6.8
sodium bicarbonate buffer	1.36 g sodium carbonate, 7.35 g sodium bicarbonate, pH 9.2

2.3 Methods

2.3.1 *General methods for DNA manipulation*

2.3.1.1 Quantitation of DNA

The concentration of DNA was determined by its absorbance at wavelength 260nm based on the calculation; 50 mg/ml double-stranded DNA gives an OD_{260} of 1. The OD_{280} was also read and the ratio of OD_{260}/OD_{280} was calculated to estimate the purity of the DNA solutions. An OD_{260}/OD_{280} ratio about 1.6-2.0 was considered satisfactory.

2.3.1.2 Restriction endonuclease digestion

Restriction endonuclease digestions were usually carried out in a 20-100 µl reaction volume, with 2-5 U of enzyme used for up to 500 ng DNA, for 1-18 h at an appropriate temperature. Commercially available 10x buffers were used according to the manufacturers' instructions. Digests with more than one enzyme were carried out simultaneously in a suitable buffer. When the buffer requirements were incompatible,

restriction digestions were performed sequentially with individual buffer for each enzyme.

2.3.1.3 DNA separation by agarose gel electrophoresis

A 50 ml 1% (w/v) agarose gel was routinely used for the analysis of 0.1-8 kb DNA fragments. Agarose was melted in 1x TAE, cooled to 55°C, before adding ethidium bromide to a final concentration of 0.3 mg/ml followed by casting in a mini-gel apparatus. The gel was left to set at RT for at least 30 min. Electrophoresis was carried out in a horizontal electrophoresis apparatus with the gel submerged in 1x TAE. DNA samples were loaded with one-fifth volume glycerol loading dye. A standard DNA ladder was also run to allow estimation of the sizes of the sample DNA fragments. DNA fragments were visualized by fluorescence over a UV light (302 nm, UV Transilluminator TM-20, UVP), and the image was recorded with Molecular Imager Gel Doc XR System (Biorad, Hercules, CA) and Mitsubishi video copy processor.

2.3.1.4 Purification of DNA fragments by agarose gel electrophoresis

When a particular fragment of DNA in a mixture of fragments was required e.g. in ligations or as a PCR template, it was routinely separated from other fragments by agarose gel electrophoresis. Gel slice containing the DNA fragments to be purified was cut from the gel using a razor blade, carefully avoiding their exposure to the UV light. DNA was extracted using a QIAquik Gel Extraction Kit.

2.3.1.5 DNA ligation

DNA vectors with complementary ends to be used for ligation were prepared by restriction enzyme digestion and where necessary treated with alkaline phosphatase and purified using agarose gel electrophoresis. Vector DNA (~10 ng) and insert DNA (20-40 ng) were ligated by incubation at RT for 2-3 h, using 1U of T4 DNA ligase with ligase buffer provided together with the enzyme in a 20 µl reaction volume. A reaction without insert DNA was included in the experiments as controls.

2.3.1.6 Preparation of *E.coli* competent cells

The *E.coli* strain DH5α was used to prepare competent cells in advance which were stored at -70°C. A fresh plate of cells was prepared by streaking out cells from frozen stocks and growing overnight at 37°C. On the second day, an individual colony was picked and grown in 10 ml LB broth culture overnight. On the third day, 5 ml of overnight culture was transferred into each of the two flasks containing 500 ml LB broth and incubate at 37°C with aeration ~2 h until the culture reaches OD_{550} of 0.5. The cells were transferred to centrifuge bottles and spin at 4°C for 8 min at 8000 rpm. Pellets were gently resuspended in 250 ml ice cold 0.1 M $CaCl_2$ and combined into a single bottle. Cells were resuspended again in 250 ml ice cold 0.1 M $CaCl_2$ and centrifuged at 8000 rpm for 8 min at 4°C. Finally the pellet was resuspended in 43 ml ice cold 0.1 M $CaCl_2$ in ddH_2O with 7 ml sterile glycerol. Competent cells were distributed into convenient aliquots (0.2 ml) in cold microfuge tubes. Cells were stored at -80°C. A portion of the cells was used to assay for viability and competence.

2.3.1.7 Transformation of plasmid DNA

For each transformation, only 50-100 µl of competent cells are necessary. Competent cells were defrozed on ice. DNA was added to cells (the volume of DNA should not exceed 40% of the cell volume). The mixture was incubated on ice for 20-30 min followed by a heat shock in a 42°C water bath for 2 min. 1 ml LB broth was added to the tube. The tube was incubated at 37°C with constant shaking for 30 min to 1h. 50-500 µl of the mixture was streaked out onto plates containing the appropriate antibiotics.

2.3.1.8 Purification of plasmid DNA

For small scale purification of plasmid DNA, 5 ml LB with appropriate antibiotics was inoculated with a single colony that contains recombinant plasmid from an agar plate and incubated at 37°C with constant shaking overnight. A QIAprep Spin Miniprep Kit (QIAGEN) was used to extract DNA according to the manufacturer's instructions.

For large scale purification of plasmid DNA, a Plasmid Maxi Kit (QIAGEN) was used according to the manufacturer's instructions. This kit routinely yielded between 200-750 µg DNA from 100 ml of overnight bacterial cultures.

2.3.1.9 Polymerase chain reaction (PCR)

DNA fragment between two oligonucleotide primers were amplified by PCR through repeated cycles of three incubation steps where the DNA template is denatured, allowed to anneal with the primers and a new strand synthesized using a thermo-stable DNA polymerase. A typical cycle included denaturation at 94°C for 1 min, annealing for 1 min at a temperature ~5°C below the lower Tm of the two primers, and finally an extension at 72°C for an appropriate time (normally 1 min per kb). Tm refers to the melting temperature for each oligonucleotide was calculated using the free internet software Oligocalculator.

2.3.1.10 Standard PCR protocol

PCR was routinely performed in a 50 µl reaction volume containing less than 1 µg template DNA, 1 µM of each oligonucleotide primer, 200 µM of each dNTP, and 1 U DNA polymerase. *Taq* polymerase (Fermentas, Glen Burnie, MD) was used for PCR colony screening. Pfu DNA polymerase (Fermentas), which possesses a 3'-5' proofreading activity resulting in a twelve fold increase in fidelity of DNA synthesis over *Taq* DNA polymerase, was used for high fidelity DNA synthesis. Each polymerase has its own reaction buffer, normally supplied by the manufacturer. The reaction mixtures were subjected to a varying number of cycles of amplification using the DNA Thermal Cycler (MJ research, Waltham, MA).

2.3.1.11 Identification of colonies that contain recombinant plasmids of interest

After transformation of competent cells, colonies of interest were identified using either PCR screening or restriction digestion, depending on the availability of suitable PCR primers for screening and the degree of background indicated by the control plates. Each colony to be tested was used to inoculate 15 µl LB. 1 µl of this inoculated LB broth was added to a 25 µl PCR reaction containing 0.5 U *Taq* polymerase. A negative control and, where possible, a positive control were included in the experiment. Colonies containing the recombinant plasmid of interest were identified by the size of their PCR products using agarose gel electrophoresis. Positives from PCR screening were confirmed using restriction digestion.

2.3.1.12 Site-directed mutagenesis

Point mutations were made using QuikChange Site-Directed Mutagenesis Kit (Stratagene, La Jolla, CA), and following the manufacturer's protocols. Complementary primers with the desired mutations were used in the long PCR cycle. The restriction enzyme Dpn I was used to digest the original template. The Dpn I treated PCR product was transformed in competent *E.coli* and plated onto LB agar plates with appropriate antibiotics. All constructs were verified by sequencing (Research Biolabs, Singapore).

2.3.2 *General methods for cell culture*

All cell lines were maintained in 5% CO_2 at 37°C in a humidified tissue culture incubator using Nunc tissue culture flasks or dishes.

2.3.2.1 Cell storage in liquid nitrogen

Cells were sedimented at 400 g for 5 min, resuspended in cell freezing media at a concentration of 5 x 10^6 cells/ml and dispensed into Cryo Vials (Greiner, Kremsmünster, Austria). Cells were frozen in a NALGENE™ Cryo 1°C Freezing Container (Nalgene, Rochester, NY) for 24 h at -70°C to achieve a 1°C/min cooling rate. Thereby the vials were transferred into liquid nitrogen for long term storage.

2.3.2.2 Cell recovery from liquid nitrogen

Cells were removed from the liquid nitrogen storage and quickly brought to 37°C in a water bath. Cells were washed in 10 ml warmed media to remove DMSO. Each cell pellet was resuspended in complete media and cultured in 75 cm^2 flask.

2.3.2.3 Culture of HEK-293 and 293T cells

HEK-293 and 293T cells were maintained in DMEM with 10% (v/v) heat-inactivated FBS, 100 IU/ml penicillin and 100 µg/ml streptomycin in a 5% CO_2 and humidified tissue culture incubator at 37°C. Cells were passaged when they were subconfluent. Cells were washed twice in PBS, incubated in 0.25% (w/v) trypsin (GIBCO) for 5 min at RT, followed by tapping of each flask to dislodge the adherent cells. Trypsin

was inactivated by adding full media and cells were directly seeded into fresh culture media in new flasks at desired cell density.

2.3.2.4 Culture of K562 cells

K562 cells were grown in RPMI1640 with 10% (v/v) heat- inactivated FBS, 100 IU/ml penicillin and 100 µg/ml streptomycin. Cells were passaged by diluting cells with fresh media.

2.3.3 *Transfection of cells*

2.3.3.1 Transfection of HEK-293 and 293T cells by the calcium phosphate method (for 10 cm dish)

Cells were seeded into 10 cm dishes the night before to give 60-70% confluence at the day of transfection. On the next day, 10 ml of fresh medium containing 25 µM chloroquine was added to replace the old medium one hour prior to the transfection. 10µg DNA was added to ddH_2O (1095 µl total) in a 15 ml sterile tube, followed by adding in 155 µl 2M $CaCl_2$. 1250 µl of 2xHBS (270 mM NaCl, 10 mM KCl, 1.5 mM $Na_2HPO_4 \cdot 7H_2O$, 0.2% (w/v) glucose, 1% (w/v) HEPES, pH 7.05 and filter sterilized, store at 4°C) was added to that tube drop by drop with gentle mixing. Finally, this mixture was added directly to the cells within 1-2 min after adding 2xHBS. The cells were then incubated for 7-11 h. After incubation, 10 ml of fresh medium was added to

replace the old media which contain chloroquine. Cells, or culture supernatant, was used 48-72 h after transfection.

2.3.3.2 Transfection of K562 cells by the electroporation method

K562 cells were transfected by electroporation using the Amaxa nucleofector device and reagents (Amaxa Gmbh, Germany) as per manufacturer's instruction. Two days before transfection, cells were passaged to give a density of 1 x 10^5 cells/ml and to achieve the density of 2-5 x 10^5 cells/ml at the time of transfection. On the day of transfection, 1 x 10^6 cells/sample were counted and centrifuged for 10 min at 200 x g. Cell pellet was resuspended in Nucleofector™ solution V (with supplement added following manufacturer), which had been pre-warmed to room temperature, to a final concentration of 1 x 10^6 cells/100 µl. For each sample, 100 µl cell suspension was mixed with 5 µg DNA and transferred the sample into an Amaxa certified cuvette followed by inserting the cuvette into the cuvette holder. The program T-16 was selected and used for the K562 cells transfection. After the program was finished, cells were immediately transferred into 12 well plate with culture media inside, which had been pre-warmed to 37°C. Cells were used for subsequent analyses 24 h after transfection.

2.3.3.3 Harvesting transfected cells (adherent)

24-48 h after transfection, the cells in each plate were washed in PBS and detached in 5 ml of 0.5 mM EDTA in PBS by incubation at RT for 10 min with gentle rocking.

Cells were collected and mixed with 10 ml full media and transferred to centrifuge tubes. Cells were spun down (400g, 5 min, 4 °C) for subsequent analysis.

2.3.3.4 FACS analysis

Cells were incubated with 20 µg/ml primary mAb in RPMI1640 for 1 h at 4°C. The cells were then washed twice and incubated with FITC-conjugated sheep anti-mouse F (ab') $_2$ secondary antibodies (1:400 dilution; Sigma) for 45 min at 4°C. Stained cells were washed once in RPMI1640 and fixed in 1% (v/v) formaldehyde in PBS. Cells were analyzed on a FACSCalibur flow cytometer (BD). Data were analyzed using CellQuest pro software (BD).

2.3.3.5 Surface biotinylation and preparation of whole cell lysates

Harvested cells were pelleted by centrifugation (400 g, 5 min, 4 °C), washed twice in ice cold PBS and resuspended in ice cold PBS at ~ 2.5 x 10^6 cells/ml in microfuge tubes. 200 µl cells were mixed with 200 µl of 1 mg/ml sulpho-NHS-biotin (Pierce) that was freshly prepared in PBS, and incubated on ice for 30 min. Reaction was quenched by adding 5 ml PBS containing 10 mM Tris-HCI pH 8.0 and 0.1% (w/v) BSA and washing the cells twice in the same solution. Cells were resuspended in 200 µl PBS and transferred to a 1.5 ml microfuge tube for subsequent applications.

2.3.3.6 Preparation of protein A sepharose beads

Protein A sepharose (PAS) beads (GE Healthcare) (1g) was swelled by rotating in an excess of PBS overnight at 4°C. The swelled PAS beads, which occupied a bed volume of ~ 4 ml, was sedimented by centrifugation (1000 g, 5 min, 4°C), washed twice, and finally resuspended to a 25% (v/v) suspension in PBS. The protein A sepharose was stored at 4°C.

2.3.3.7 Immunoprecipitation of cell lysates

For standard immunoprecipitation, ~2.5 x 10^6 cells were lysed by adding 0.5 ml lysis buffer with the addition of protease inhibitors (Roche, Basel, Switzerland) and incubated on ice for 20 min. Cell debris were removed by centrifugation at 14000 rpm at 4°C for 10 min, and the cell lysates were transferred to fresh microfuge tubes. Cell lysates (0.5 ml) were precleared by adding 3 µg of irrelevant mAb as appropriate with 40 µl Protein A sepharose and incubated at 4°C for 2 h with rotation. The Protein A sepharose was sedimented by centrifugation (10000 g, 2 min, 4 °C) and the supernatant was transferred to a fresh tube. 3 µg of appropriate mAb and 70 µl Protein A sepharose suspension were added to the precleared cell lysates and incubated at 4°C for 2 h with rotation. The Protein A sepharose was sedimented by centrifugation (10000 g, 4°C, 2 min) and the supernatant was discarded. The Protein A sepharose was washed in 500 µl lysis buffer containing 500 mM NaCl for three times. Thereafter, 100 µl protein solubilisation buffer containing 40 mM DTT was added to the Protein A sepharose precipitate which was then vortexed, short spun, and heated at

100°C for 5 min. The immunoprecipitated proteins were resolved by SDS-PAGE, or were stored at -20°C.

For reporter monoclonal antibody (mAb) immunoprecipitation analyses, the labeled or unlabelled cells were incubated in DMEM medium containing 5% (v/v) heat-inactivated FBS and 10 mM HEPES with the relevant mAb (3 μg each) in the presence or absence of 2 mM $MnCl_2$ for 30 min at 37°C. The unbound mAbs were removed by washing the cells twice in the DMEM, and lysed in lysis buffer with protease inhibitors (Roche, Basel, Switzerland) for 30 min at 4°C. Proteins bound to the mAbs were precipitated with protein-A-Sepharose beads. Precipitated proteins were resolved on SDS-PAGE under reducing conditions (+DTT).

For the cross-linking study, transfectants were incubated in PBS containing 0.5 mg/ml of the cross-linker 3,3'-Dithiobis (sulfosuccinimidylpropionate) (DTSSP) (Pierce) for 30 min at room temperature. The reaction was quenched by washing cells in PBS containing 1 mM Tris (pH 7.5). Cells were incubated in DMEM with 3 μg each of control mouse IgG or appropriate mAbs for 30 min at 37°C. Unbound antibodies were removed by washing cells twice in DMEM. Cells were lysed and bound mAbs precipitated as described above. Precipitated proteins were resolved on SDS-PAGE under non-reducing (-DTT) conditions or reducing (+DTT) conditions.

2.3.3.8 Sodium dodecyl sulphate polyacrylamide gel electrophoresis (SDS-PAGE)

SDS-PAGE was performed as described (Laemmli 1970) with slight modifications. Protein sample (15 µl for minigel system) was mixed with an equal volume of sample solubilisation buffer (2x) under non-reducing conditions or in the presence of 40 mM DTT under reducing conditions. Electrophoresis was carried out at 200V in a Mini Electrophoresis Set (Biorad) in SDS-PAGE eletrophoresis buffer.

2.3.3.9 Western blotting

Proteins separated by SDS-PAGE were transferred onto a PVDF membrane (Immobilon-P, Millipore) by electro blotting. The PVDF membrane was prepared according to the manufacturer's instructions: the membrane was equilibrated by washing in ethanol for 10 sec, followed by water for 10 min, and then in blotting buffer (12 mM Tris-HCl, 95 mM Glycine, 10% (v/v) ethanol) for 5 - 10 min. The SDS-PAGE gel was equilibrated by washing in blotting buffer once. Electro blotting was performed at 25 V for 30 min. After protein transfer, the PVDF membrane was transferred to blocking buffer and was rotated at RT for an hour or overnight at 4°C.

2.3.3.10 ECL detection of proteins blotted onto PVDF membrane

After biotinylated proteins had been transfered onto PVDF membranes, the membrane was removed from blocking buffer and were washed three times in PBS-T (PBS, 0.1% (v/v) Tween-20 (Sigma)) at RT for 10 min. Membrane was then incubated with the streptavidin-HRP conjugate (1:1000 dilution in PBS-T) at RT for 60 min with

gentle agitation, and was washed again for three times in PBS-T at RT for 10 min. Thereafter, the membrane was developed using an ECL Plus Detection Kit (Amersham, Buckinghamshire, UK) according to the manufacturer's recommendations. Membrane was then exposed to Kodak X-Omat film and developed using a Kodak X-OMAT ME-1 processor. For detecting uPAR, the membrane was probed with rabbit anti-uPAR antibody 399 or rabbit anti-HA pAb followed by HRP-conjugated donkey anti-rabbit IgG (Amersham). For detecting actin, anti-actin (BD) was used for the primary antibody.

2.3.3.11 Coating microtitre wells with ICAM-1 for cell adhesion assay

Goat anti-human IgG (Fc specific) (Sigma) was diluted to 5 μg/ml in sodium bicarbonate buffer (pH 9.2) and 50 μl was added to each well of a microtitre plate (Polysorb, Nunc Immuno-Plate). The microtitre plates were left at 4 °C overnight. The solution was discarded and the wells were washed twice with 150 μl PBS per well. A solution of 0.2% (w/v) PVP10 (Sigma) in PBS was added to each well (150 μl per well) and the plates were incubated at 37°C for 30 min. The plates were washed with PBS once (150 μl per well) before the addition of 50 μl per well of ICAM-1/Fc (1 μl /ml in PBS containing 0.05% (w/v) PVP10). After 2-3 h incubation at RT, the plates were washed twice in RPMI/HEPES/FBS (RPMI1640 supplemented with 10 mM HEPES, pH 7.4 and 5% (v/v) heat inactivated FBS) before use. ICAM-1/FC used for the coating of microtitre plates was prepared by Miss Manisha Cooray (SBS, NTU). Briefly, 10 large flasks of COS-7 cells were transfected with human

ICAM-1/FC in expression plasmid πH3M using the DEAE Dextran method of cell transfection. 8-12 days after transfection the tissue culture supernatant was spun and stored at 4°C. Purified ICAM-1/FC was prepared by passing the tissue culture supernatant through protein A sepharose column (GE Healthcare) and eluting the ICAM-1/FC according to the manufacturer's instructions.

2.3.3.12 Coating microtitre plates with BSA or fibrinogen for cell adhesion assay

Microtitre wells (Polysorb, Nunc Immuno-Plate) were coated with 100 μg /ml BSA or 250 μg /ml fibrinogen in 50 μl of sodium bicarbonate buffer pH 9.2 for 2 h at RT. Plates were washed once in PBS (150 μl per well), and blocked with 0.2% (w/v) PVP10 (Sigma) in PBS (150 μl per well) for 30 min at 37°C. Before use, the wells were washed twice with 150 μl RPMI/HEPES/FBS (RPMI1640 supplemented with 10 mM HEPES, pH 7.4 and 5% (v/v) heat inactivated FBS).

2.3.3.13 Cell adhesion assay

Plates were prepared as described in 2.3.3.11 and 2.3.3.12. Cells were then incubated with 1 μg/ml BCECF (2',7'-bis-(2-carboxyethyl)-5-(and-6) carboxy fluorescein, acetoxymethyl ester) (Molecular Probes) in RPMI/HEPES/FBS (RPMI1640 supplemented with 10 mM HEPES, pH 7.4 and 5% (v/v) heat inactivated FBS) for 20 min at 37°C. Labeled cells were transferred to wells (2 x 10^4 cells/well) without or with additional reagents (mAbs or cation additives) and incubated for 30 min at 37°C. Nonadherent cells were removed by washing three times with 100 μl

RPMI/HEPES/FBS (RPMI1640 supplemented with 10 mM HEPES, pH 7.4 and 5% (v/v) heat inactivated FBS). Cell fluorescence, which corresponds to the number of cells adhering to the ligand-coated wells, was measured using a FL600 fluorescence plate reader (Bio-Tek, Winooski, VT).

2.3.3.14 Cell migration assay

Transwell motility assay was performed by coating the undersides of 8μm pore size polycarbonate transwell (Millipore) insert with fibrinogen (250 μg/mL) in PBS 2 h at RT. Cells (5 x 10^5) in 200 μl DMEM without FBS were added to the upper compartment and allowed to migrate for 20 h at 37°C under culture conditions. Non-migrated cells were removed from the upper compartment using a cotton swap. Cell that migrated through the pores to the underside of the transwell were collected by gentle washing in PBS containing typsin. Dislodged cells were collected and counted using flow cytometry.

2.3.3.15 Fluorescence Resonance Energy Transfer (FRET) analyses

K562 transfectants expressing FRET fluorophore pair conjugated to integrin cytoplasmic tails were cytospun onto glass slides. FRET detection by acceptor photobleaching was performed on a Zeiss LSM510 confocal microscope (Carl Zeiss, Thornwood, NY) to detect integrin cytoplasmic tails separation. The following parameters were used for analyses: (i) mCFP: excitation wavelength 458 nm; emission filter BP 470-500 nm. (ii) mYFP: excitation wavelength 514 nm; emission

filter LP 530 nm. (iii) oil immersion 63 x objective. Photobleaching of mYFP of an entire cell within was achieved by scanning the region 20 times using the 514 argon laser line set at the maximum intensity. The cell membrane was selected as region of interest (ROI). mCFP signals within the ROI pre- and post-mYFP bleaching were acquired. FRET efficiency (E_F) was calculated as a percentage using the equation $E_F = (I_6 - I_5) \times 100/I_6$, where I_n is the mCFP intensity at the n^{th} time point. Bleaching was performed between the 5^{th} and 6^{th} time points. Similar analyses of unbleach cells using the equation $C_F = (I_6 - I_5) \times 100/I_6$ were made. The mean noise computed as $N_F = (I_5 - I_4) \times 100/I_5$ in which the mCFP signals at the 4^{th} and 5^{th} time points before the bleaching process was close to zero in all cases.

2.3.3.16 Model of integrin αMβ2

The model of αMβ2 was generated by Dr. Kong Lesheng (Yong Loo Lin School of Medicine, NUS) using the software program Modeller8v1. The overall bent conformation of αMβ2 was genereated using integrin αVβ3 crystal coordinates 1L5G (Xiong et al. 2002). The αM I domain was incorporated into the model with structural coordinates 1JLM (Lee et al. 1995b). The structure of αVβ3 PSI/hybrid domain/I-EGF-1 was not well resolved (Xiong et al. 2002); therefore, the coordinates of integrin β2 subunit PSI/hybrid domain/I-EGF-1 were used 1YUK (Shi et al. 2005). I-EFG-2 and I-EFG-3 folds of the αMβ2 model were generated based on NMR coordinates of the β2 1L3Y (Beglova et al. 2002).

2.4 Plasmid construction details

2.4.1 *Integrin plasmids*

The β2 cDNA in J8.1E (Douglass et al. 1998) was used as a template for construction of the β2 in mammalian expression vector pcDNA3.0 (Invitrogen) (Fig. 2.1). KpnI and SpeI were used to digest β2 cDNA from J8.1E and the fragment was ligated into pcDNA3.0 vector which was digested with KpnI and XbaI (SpeI and XbaI digested DNA fragments have compatible ends). αL, αM and αX cDNA plasmids were in pcDNA 3.0 vector with the restriction sites KpnI and XbaI. The β2/β7 chimera known as β2BN7 was reported previously (Hyland et al. 2001) as depicted in Figure 2.2 and this plasmid was provided by my supervisor Dr. Tan Suet Mien.

The αML cytoplasmic tail chimera was a gift from my ex-colleague Dr. Tang Renhong. It was generated by exchanging the αM cytoplasmic tail with αL cytoplasmic tail. Restriction enzymes SspbI and XbaI were used for digestion. Because wild type αL cDNA in pcDNA3.0 has two SspbI cut sites, the one at the position of 1652 in αL cDNA was removed by point mutation before digestion with SspbI and XbaI (Fig. 2.3). Thereafter, cytoplasmic tails of αL was digested with SspbI and XbaI and ligated into wild type αM plasmid which was also digested by the same enzymes. Point mutations were made by using QuikChange Site-Directed Mutagenesis Kit (Stratagene), and following the manufacturer's protocols. Wild type

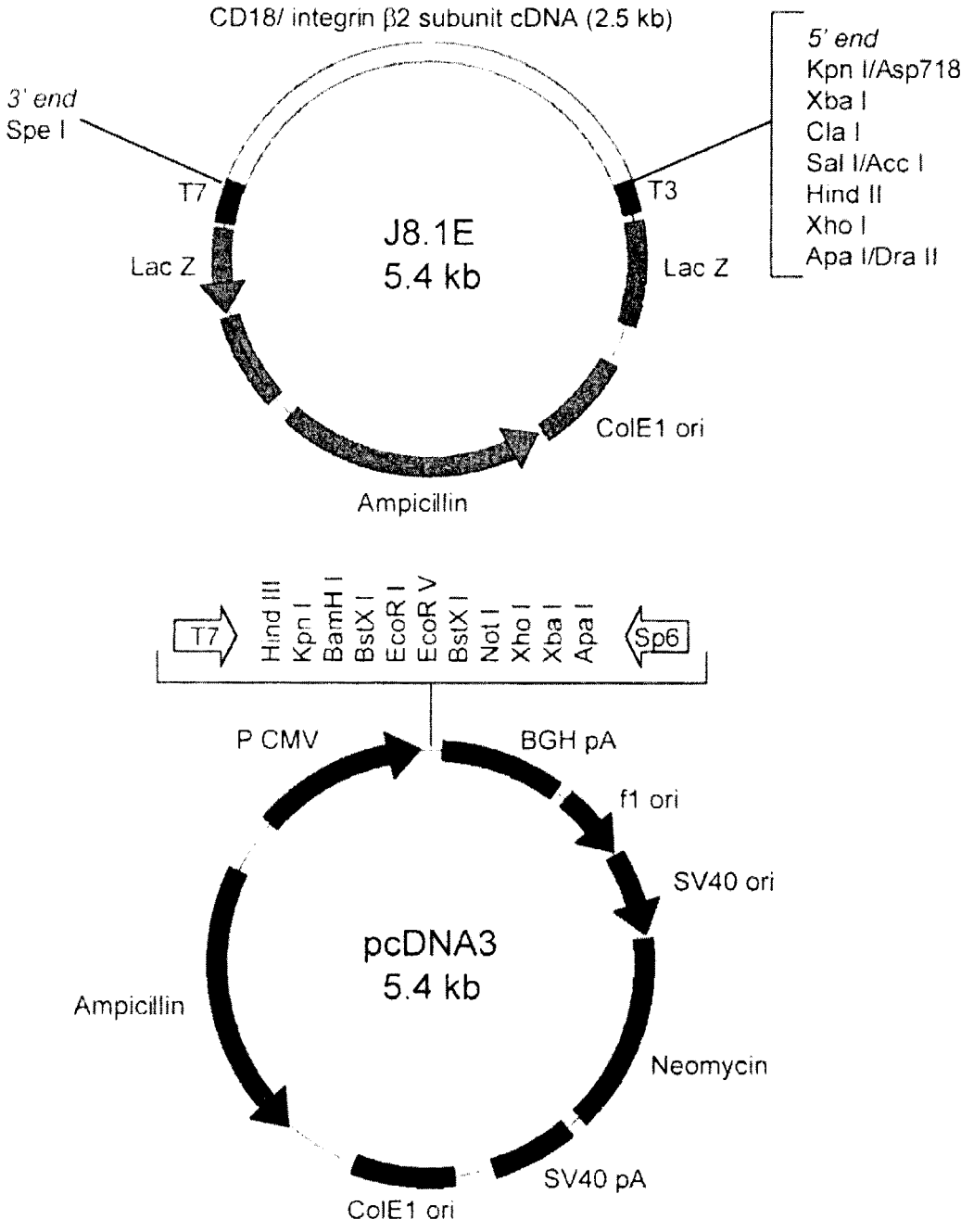

FIG 2.1 Schematic illustration of plasmid J8.1E and pcDNA3.0. The β2 cDNA in J8.1E (Douglass et al. 1998) was used as a template for construction of the β2 in mammalian expression vector pcDNA3.0. Kpn/SpeI was used to digest β2 cDNA from J8.1E and the fragment was ligated into pcDNA3.0 vector which was digested with KpnI and XbaI (SpeI and XbaI digested DNA fragments have compatible ends). αL, αM and αX cDNA plasmids were in pcDNA3.0 vector with the restriction sites KpnI and XbaI.

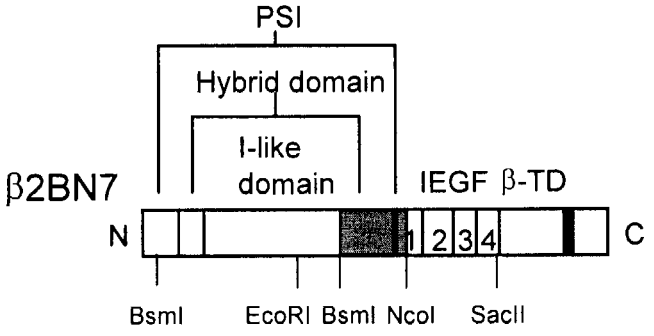

FIG 2.2 Schematic illustration of the integrin β2/β7 chimera β2BN7. The chimera was generated by replacing the β2 sequence Tyr^{338}–Cys^{437} with the corresponding segment from integrin β7 (shaded gray) (Hyland et al. 2001). The restriction sites in the cDNA used to construct the chimera are shown.

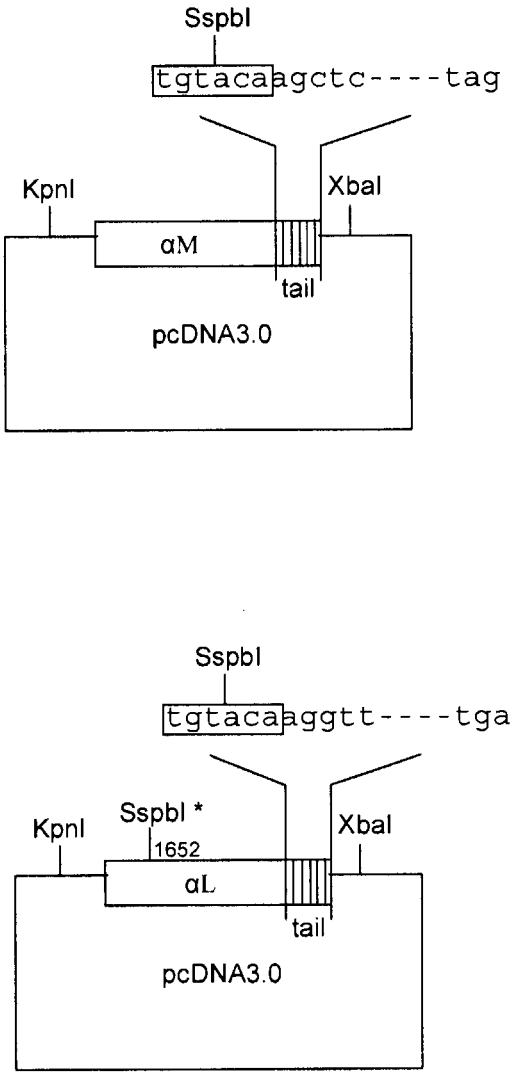

FIG 2.3 Schematic illustration of plasmid construction of αML chimera. The αML cytoplasmic tail chimera was generated by exchanging the αM cytoplasmic tail with αL cytoplasmic tail. Restriction enzymes SspbI and XbaI were used for digestion. There are two SspbI sites on αL cDNA, the SspbI* site at the position 1652 was removed by point mutation before digestion.

plasmids were used as templates.

For FRET experiments, the mammalian expression vectors pEYFP-N1 and pECFP-N1 (clontech, Moutain View, CA) were used. However, to inhibit their inherent tendency to form hetero- or homodimers, monomeric CFP (mCFP) and YFP (mYFP) were generated by replacing Leu-221, at the crystallographic dimer interface, with Lysine (Zacharias et al. 2002). mCFP and mYFP were subcloned into integrin expression vectors to generate αL-mCFP, αM-mCFP, αML-mCFP, αL-mYFP, αML-mYFP and β2-mYFP, in which mCFP or mYFP were tethered to the C-terminus of the integrin cytoplasmic tails. Five amino acids linker (GPVAT) was introduced between all α subunits and mCFP or mYFP, and six amino acids linker (GGPVAT) was inserted between β2 and mYFP based on previous observation that αL-mCFP and β2-mYFP containing 5 and 6 residues linkers exhibited high FRET efficiency (Kim et al. 2003) (Fig. 2.4). All these plasmids are generous gifts from my colleague Dr Ardcharaporn Vararattanavech.

Cysteine mutations in αML-mCFP, β2-mYFP and αM were made by using QuikChange Site-Directed Mutagenesis Kit (Stratagene) with relevant primers, and following the manufacturer's protocols. Wild type plasmids were used as templates.

Specific primers used are listed below:

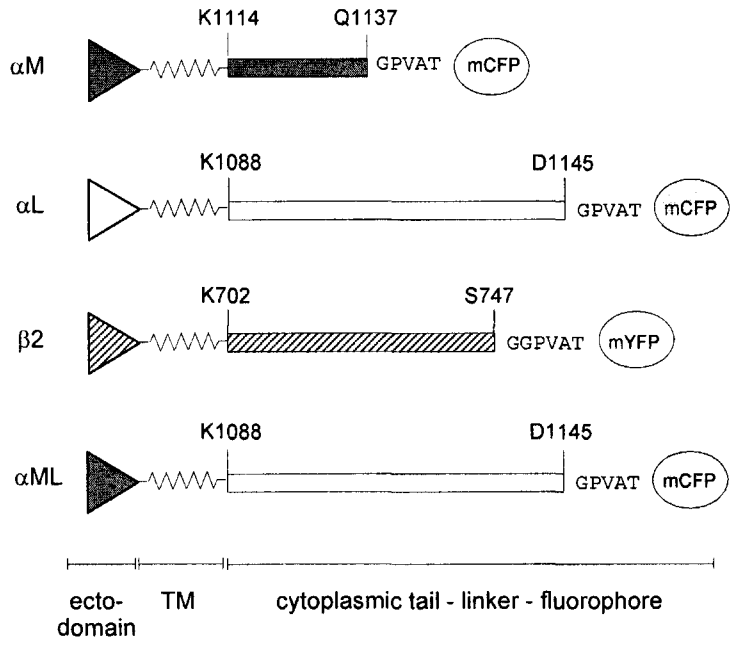

FIG 2.4 Schematic illustration of integrins with different mCFP and mYFP fusions. The linker residues between the cytoplasmic tails and the FRET pair fluorophores are shown. For ease of reference, the amino acids flanking each cytoplasmic tail are numbered according to the mature protein (Barclay A. N. 1997).

1. αML L1091C
   F 5' GAGGTCCCCAACCCCTGCCCGCTCATCGTGGG 3'
   R 5' CCCACGATGAGCGGGCAGGGGTTGGGGACCTC 3'

2. αML P1092C
   F 5' GTCCCCAACCCCCTGTGCCTCATCGTGGGCAGC 3'
   R 5' GCTGCCCACGATGAGGCACAGGGGGTTGGGGAC 3'

3. αML L1093C
   F 5' CCAACCCCCTGCCGTGCATCGTGGGCAGCTC 3'
   R 5' GAGCTGCCCACGATGCACGGCAGGGGGTTGG 3'

4. β2 I679C
   F 5' GGCAGGCCCCAACTGCGCCGCCATCGTCG 3'
   R 5' CGACGATGGCGGCGCAGTTGGGGCCTGCC 3'

5. β2 A680C
   F 5' CAGGCCCCAACATCTGCGCCATCGTCGGGGG 3'
   R 5' CCCCCGACGATGGCGCAGATGTTGGGGCCTG 3'

6. β2 A681C
   F 5' GCCCCAACATCGCCTGCATCGTCGGGGGCAC 3'
   R 5' GTGCCCCCGACGATGCAGGCGATGTTGGGGC 3'

7. β2 I682C
   F 5' CCAACATCGCCGCCTGCGTCGGGGGCACCG 3'
   R 5' CGGTGCCCCCGACGCAGGCGGCGATGTTGG 3'

* Mutated bases are underlined

Cycling parameters for the QuikChange Site-Directed Mutagenesis (based on the manufacturer's protocols)

Segment	**Cycles**	**Temperature**	**Time**
1	1	95°C	1 minute
2	18	95°C	50 seconds
		60°C	50 seconds
		68°C	1 minute/kb of plasmid length
3	1	68°C	7 minutes

2.4.2 *uPAR plasmids*

Full length human uPAR cDNA in expression construct pCEP4 was a gift from Dr. H.A. Chapman (Department of California, San Francisso, CA) and used for a template for construction of the uPAR in pcDNA3.0. The uPAR full length sequences was amplified by PCR using oligonucleotide primers engineered to contain the EcoRI and XhoI restriction enzyme sites. The PCR products were digested with EcoRI and XhoI in EcoRI buffer (NEB) and cloned into the similarly digested pCDNA3.0 vector. The uPAR Domain 1 (D1) deleted mutant, lacking the first 92 amino acids corresponding to domain 1, referred to as D2D3 was constructed by first replacing the EcoRI-NsiI fragment (containing the entire D1 coding region) of the pBluescipt uPAR sub-clone with a PCR product generated by amplification of the uPAR signal peptide and digested with the same enzymes in NsiI buffer (NEB) (thereby restoring the desired signal-peptide/D2D3 junction amino acid -1/92). Finally the modified uPAR D2D3 was transferred to the pcDNA3 vector as described for the full length cDNA. A N-terminal hemagglutinin (HA)-tag uPAR (HA-uPAR) construct was generated by inserting the intact uPAR cDNA (encoding Leu^{1}-Thr^{313} including the stop condon), devoid of its signal peptide, into the BglII and SacII restriction enzyme sites of the multi-cloning sites (MCS) of mammalian expression vector pDisplay (Invitrogen, Carlsbad, CA, USA), which has a murine Ig kappa-chain V-J2-C signal peptide followed by a HA tag before its MSC and was similarly digested with BglII and SacII in NEBuffer 2 (NEB). This provides ease in the detection of uPAR by Western

blotting with anti-HA antibody. HA-D2D3 (Leu^{92}-Thr^{313}) was generated similarly (Fig. 2.5).

Specific primers used are listed below:

1. uPAR full length
   F 5' CGGAATTCGCCGCCACCATGGGTCACCCGCCGCTG 3'
   R 5' CCGCTCGAGCAGAGAGGGGGATTTCAGGTTTAG 3'

2. uPAR signal peptide
   F 5' CGGAATTCGCCGCCACCATGGGTCACCCGCCGCTG 3'
   R 5' AATGCATTCGAGGCCCCAAGAGGCTGGGA 3'

Cycling parameters for uPAR full length and signal peptide PCR

Segment	**Cycles**	**Temperature**	**Time**
1	1	94°C	1 minute
2	30	94°C	1 minute
		61°C	1 minute
		72°C	1 minute
3	1	72°C	7 minutes

3. HA-uPAR
   F 5' GAAGATCTCTGCGGTGCATGCAGTG 3'
   R 5' CCGCTCGAGCAGAGAGGGGGATTTCAGGTTTAG 3'

2. HA-D2D3
   F 5' GAAGATCTCTCGAATGCATTTCCTGTGGC 3'
   R 5' CCGCTCGAGCAGAGAGGGGGATTTCAGGTTTAG 3'

Cycling parameters for HA-uPAR and HA-D2D3 PCR

Segment	**Cycles**	**Temperature**	**Time**
1	1	94°C	1 minute
2	30	94°C	1 minute
		56°C	1 minute
		72°C	1 minute
3	1	72°C	7 minutes

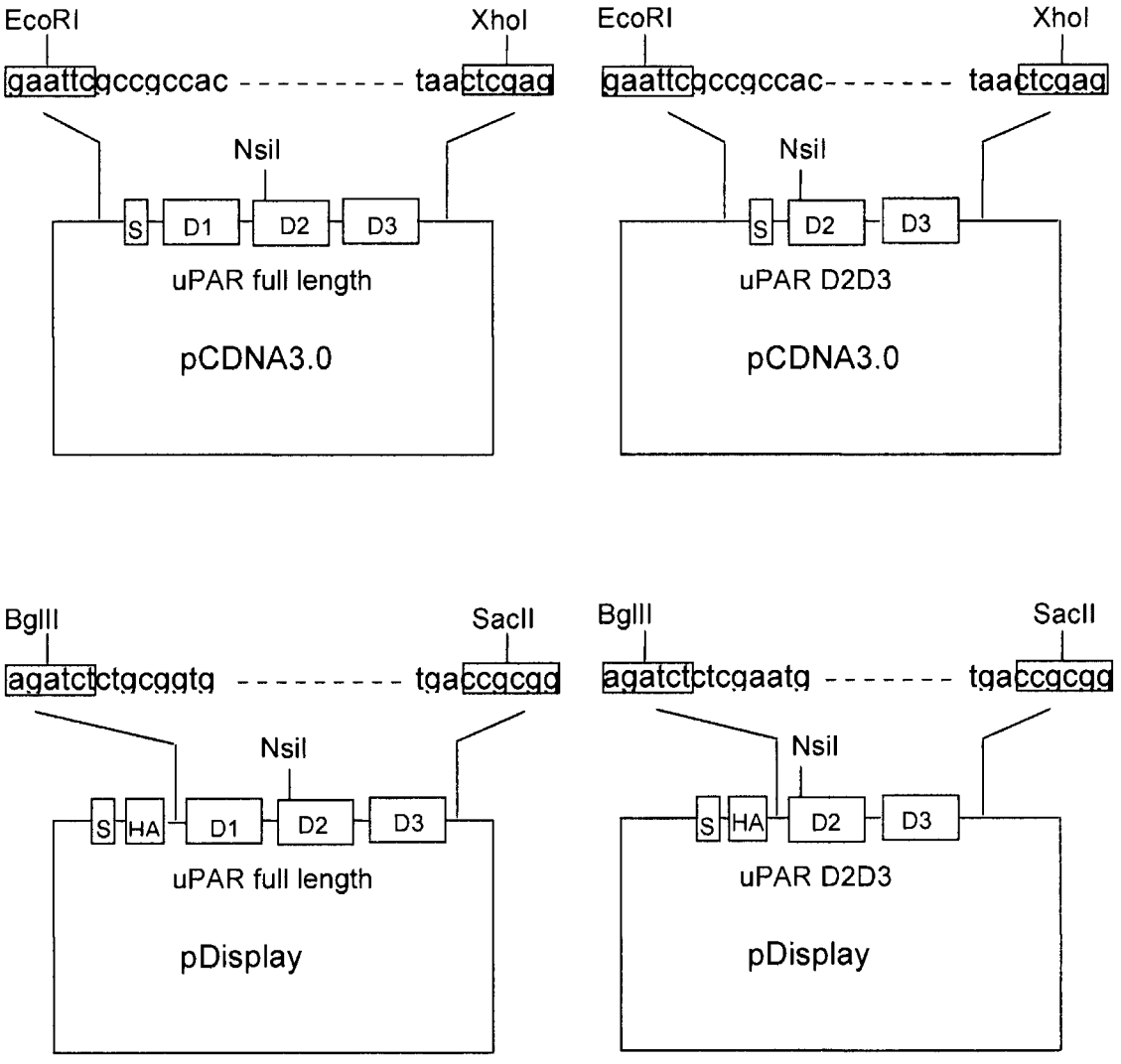

FIG 2.5 Schematic illustration of uPAR plasmid constructions. Full length uPAR was cloned between the EcoRI and XhoI sites of the pcDNA3.0 vector. The uPAR D2D3 was constructed by first replacing the EcoRI-NsiI fragment (containing the entire D1 coding region) of the pBluescipt uPAR sub-clone with a PCR product generated by amplification of the uPAR signal peptide and digested with the same enzymes (thereby restoring the desired signal-peptide/D2D3 junction amino acid -1/92). Finally the modified uPAR D2D3 was transferred to the pcDNA3 vector as described for the full length cDNA. HA-tagged uPAR (full length) and D2D3 were generated by inserting the corresponding coding regions into the BglII and SacII sites of the pDisplay expression vector. S represents signal peptide.

Chapter Three: Down regulation of integrin αMβ2 ligand-binding function by uPAR

3.1 Background

The ligand-binding properties of αMβ2 are known to be modulated by its association with uPAR (Simon et al. 2000; Sitrin et al. 1996; Zhang et al. 2003). uPAR binds to kininogen, extracellular matrix protein vitronectin, and the serine protease urokinase-type plasminogen activator (uPA) (Preissner et al. 2000). uPAR can also associate with integrins α3β1, α4β1, α5β1, α6β1, α9β1, and αVβ3 (Pluskota et al. 2003; Simon et al. 2000; Tarui et al. 2003; Tarui et al. 2001; Wei et al. 2001; Xue et al. 1994; Xue et al. 1997). The association of αMβ2 and uPAR was demonstrated by co-purification, immunolocalization, and fluorescence energy transfer experiments (Bohuslav et al. 1995; Kindzelskii et al. 1996; Xue et al. 1994). The β propeller of the integrin αM subunit contains a critical sequence required for effective association with uPAR (Simon et al. 2000). It is widely accepted that an activated integrin adopts an extended conformation whilst the bent conformer depicts a resting state (Hynes 2002). In an extended integrin, the β propeller would be distal from the comparatively short uPAR, which conceivably argues against its interaction with uPAR. This may, however, be reconciled by a model of a uPAR and bent-integrin complex as proposed for uPAR and α5β1 (Wei et al. 2005).

Integrin αMβ2 and uPAR are required for fibrinolysis by myeloid cells (Plow et al. 1995; Pluskota et al. 2004; Pluskota et al. 2003; Simon et al. 1993). Therefore, the influence of uPAR on αMβ2 binding to fibrinogen warrants investigation. It was reported that αMβ2-dependent binding to fibrinogen was abrogated in HEK-293 cells transfected with αMβ2 and uPAR as compared to transfectants expressing only αMβ2 (Simon et al. 2000). In contrast, uPAR was reported to promote αMβ2 binding to fibrinogen using the same surrogate cell system in another study (Zhang et al. 2003). What accounts for these apparently conflicting observations is not known. In humans, nine of the twenty-four integrins described contain an I domain (Hynes 2002). αMβ2 contains an I domain but α3β1, α4β1, α5β1, α6β1, α9β1, and αVβ3 that interact with uPAR do not. The I domain is the primary ligand-binding site in I domain-containing integrins. Integrins that do not contain the I domain utilize the α subunit β propeller and the β subunit I-like domain for direct ligand-recognition (Hynes 2002). Thus, the influence of uPAR on integrins with or without I domain may be different. In this chapter, data are presented to demonstrate the masking of αMβ2 ligand-binding site by its association with uPAR. The ligand-binding function of αMβ2 was down-regulated in HEK-293 transfectants bearing αMβ2 and uPAR. Similarly, expression of uPAR attenuated the ligand-binding function of a constitutively active αMβ2 mutant. In addition, uPAR expression reduced the migration rate of αMβ2 transfectants as determined by haptotatic assays.

3.2 Results

3.2.1 Analyses of integrin αMβ2 and uPAR interaction interface by immunoprecipitation

The β propeller of the αM subunit was reported to interact with uPAR (Simon et al. 2000). However, the extent of the interaction interface between αMβ2 and uPAR is not well defined because the structure of an intact αMβ2 with uPAR is lacking. Using the method of immunoprecipitation, we sought to examine the molecular interface between αMβ2 and uPAR. The rationale of this approach is that when the epitope of an αMβ2-specific mAb lies in the association interface between αMβ2 and uPAR, the binding of the mAb to αMβ2 could be sterically hindered. Co-precipitation of uPAR with αMβ2, in this case, would be minimal. On the other hand, if the epitope does not reside in the association interface, co-precipitation of uPAR with αMβ2 can therefore be detected. Because the epitopes of a panel of αMβ2-specific mAbs are known, it is possible to "footprint" the molecular surface on αMβ2 that may be in close proximity with uPAR.

Full-length human uPAR cDNA expression vector was constructed (Fig. 3.1A) and full-length uPAR together with integrin αMβ2 expression plasmids were transfected into HEK-293 cells. Cell surface expressions of uPAR and αMβ2 were verified by flow cytometry. High level of αMβ2 and uPAR expression was detected using

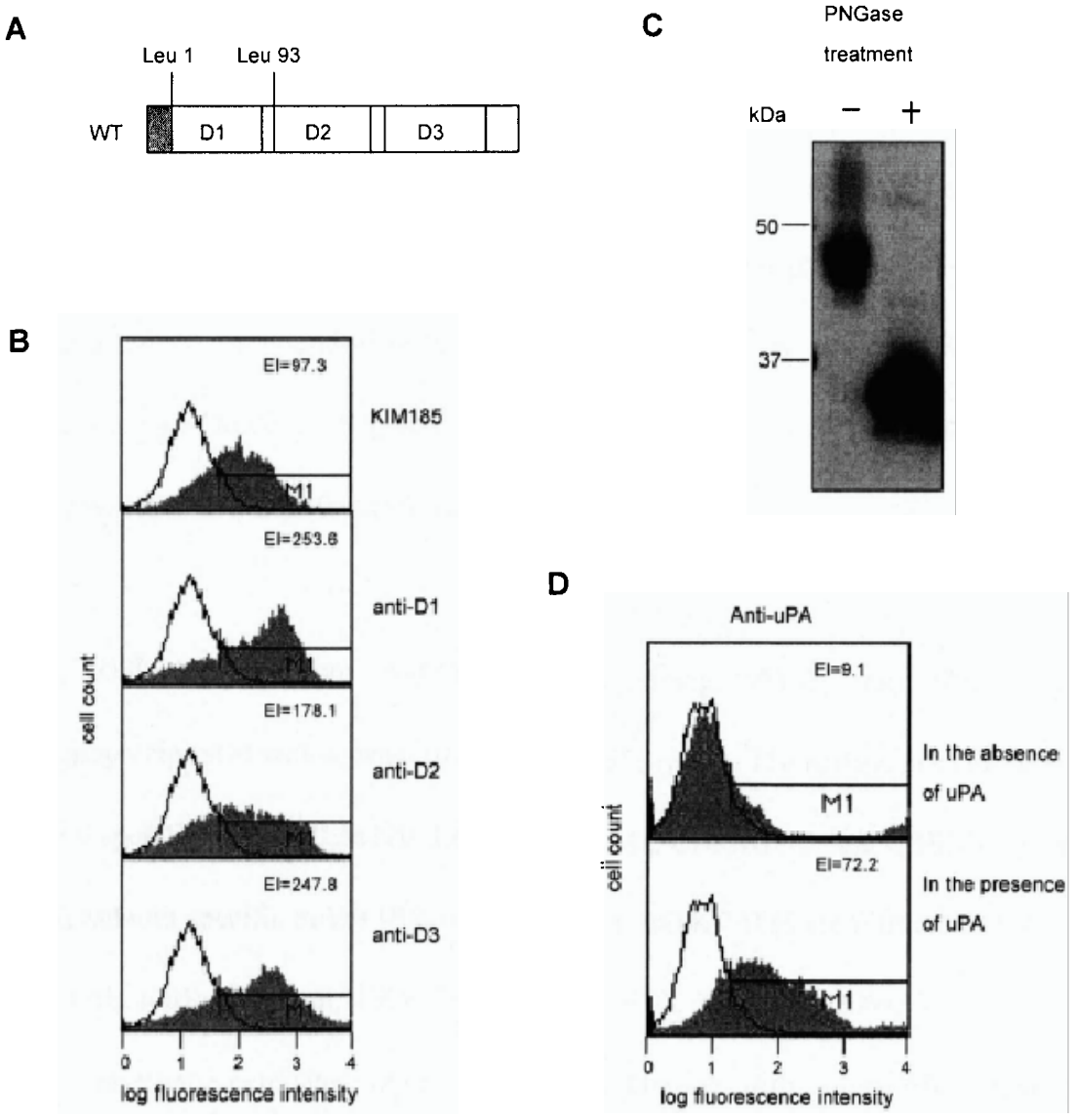

FIG 3.1 (A) Schematic representation of full-length human uPAR. The signal peptide is shaded gray. The boundaries of D1, D2, and D3 are indicated. (B) Flow cytometry analyses of αMβ2 and full-length uPAR expression on HEK-293 transfectants. Open histogram represents staining with an irrelevant mAb. Shaded histogram represents staining with mAbs recognizing αMβ2 or different domain of uPAR. The expression index (EI) was calculated by % gated positive x geo-mean fluorescence intensity (Cheng et al. 2007). M1 denotes region gated to be positive staining. (C) Untreated and PNGase-treated uPAR were resolved by SDS-PAGE. (D) Transfectants expressing full-length uPAR were incubated in media containing 100nm uPA followed by staining with anti-uPA mAb and flow cytometry analyses. High level of uPA bound to uPAR expressing HEK-293 transfectants. Open histogram represents staining with an irrelevant mAb. Shaded histogram represents staining with anti-uPA mAb.

anti-integrin or three uPAR specific mAbs that recognize D1, D2 or D3 of uPAR (Fig. 3.1B). Peptide N-glycosidase F-treated uPAR exhibited a marked increase in electrophoretic mobility as compared to untreated uPAR, which corroborates well with its extensive N-linked glycosylations (Fig. 3.1C). Further, transfectants expressing uPAR showed significant binding of its ligand uPA as determined by immunostaining of bound-uPA followed by flow cytometry analyses (Fig. 3.1D). Therefore, the folding, N-glycosylations, and function of uPAR expressed in surrogate HEK-293 transfectants were intact.

Next, cell lysates from transfectants expressing αMβ2 and uPAR were immunoprecipitated with a panel of αMβ2-specific mAbs. The epitope sites of the αM subunit specific mAbs MEM170, LPM19c, OKM1, CBRM1/10, and CBRM1/23, and the β2 subunit specific mAbs IB4, MHM23, 7E4, and KIM185 are illustrated (Fig. 3.2) (Lu et al. 2001a; Lu et al. 1998; Poloni et al. 2001; Tng et al. 2004; Violette et al. 1995). Immunoprecipitates were subjected to blotting with anti-uPAR polyclonal antibody 399 to detect co-precipitated uPAR. Noteworthy, significant level of uPAR was detected only in samples immunoprecipitated with mAbs KIM185, 7E4, OKM1, and CBRM1/23 (Fig. 3.3A). The lack of uPAR co-precipitated with other αMβ2-specific mAbs could not be due to weaker reactivity of these mAbs towards αMβ2. This was verified by immunoprecipitating cell surface-biotinylated αMβ2 of transfectants using the same panel of mAbs (Fig. 3.3B). All mAbs precipitated significant amount of biotinylated αMβ2. The control mAb MHM24 that is specific

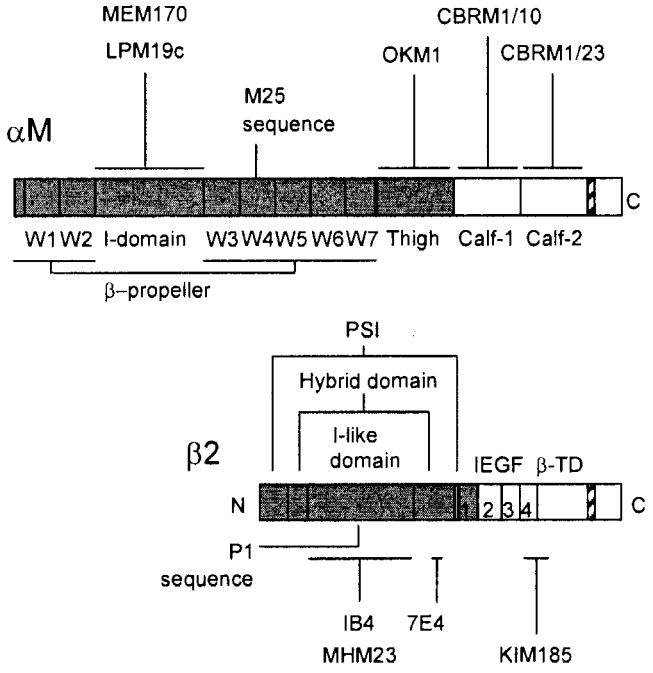

FIG 3.2 Schematic illustration of the linear organization of the integrin αM and β2 subunits. The sites or regions of the mAbs' epitopes are indicated: LPM19c (Violette *et al.*, 1995); OKM1, CBRM1/10, CBRM1/23 (Lu *et al.*, 1998); MHM23 (Poloni *et al.*, 2001); 7E4 (Tng *et al.*, 2004); KIM185 (Lu *et al.*, 2001a); IB4 (Lys^{174} of the β2 subunit) and MEM170 (epitope residing in αM I domain) are unpublished data. The location of the M25, uPAR interacting sequence, in the αM propeller (Simon *et al.*, 2000) and the corresponding P1 sequence in the β2 I-like domain as reported for integrin β1 subunit (Wei *et al.*, 2005) is shown. Regions representing the integrin "headpiece" are shaded.

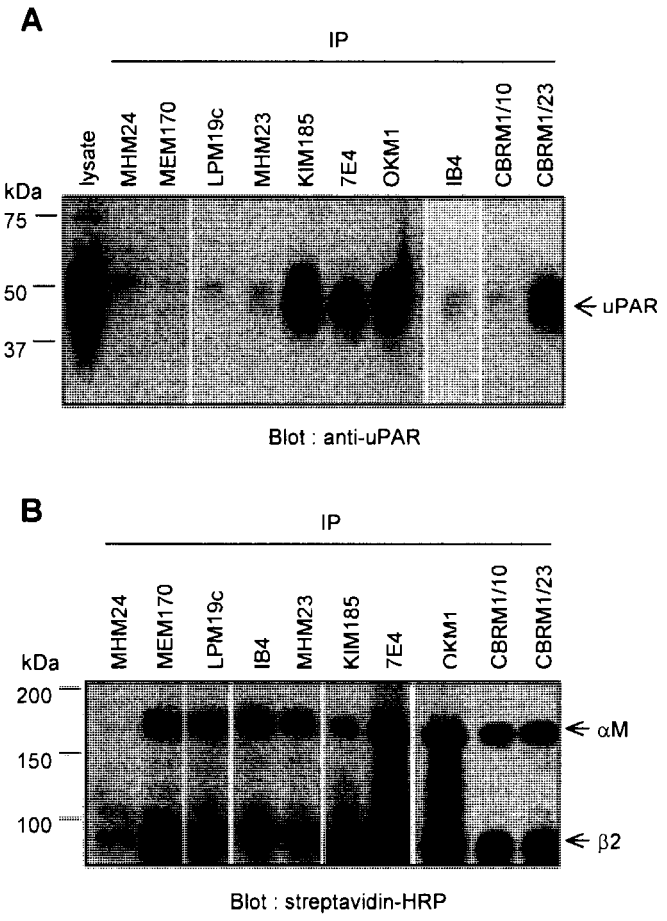

FIG 3.3 (A) Co-immunoprecipitation of uPAR with αMβ2 using a panel of αMβ2-specific mAbs. The mAb MHM24 (integrin αL-specific) was included as negative control. uPAR was detected by immunoblotting with rabbit anti-uPAR antibody. (B) Transfectants were surface-labeled with biotin and αMβ2 immunoprecipitated with relevant mAbs. Protein samples were resolved by SDS-PAGE on a 10% gel under reducing conditions. The αM and β2 subunit were detected by streptavidin-HRP.

for integrin αLβ2 failed to precipitate αMβ2. The lack of uPAR co-precipitated with αMβ2 in immunoprecipitated samples of mAbs MEM170, LPM19c, MHM23, IB4, and CBRM1/10 may be due to disruption of the association of uPAR with αMβ2 when the mAbs bind to αMβ2. This was unlikely because in a competition experiment, the inclusion of increasing amount of mAb IB4 in lysate samples containing the same concentration of mAb KIM185, for example, did not diminish the level of uPAR precipitated (Fig. 3.4). Therefore, these data suggest that the epitopes of mAb MEM170, LPM19c, MHM23, IB4, and CBRM1/10 may be shielded by steric factors when αMβ2 associates with uPAR.

The integrin ectodomain can be segregated into two collective regions referred to as the headpiece and the tailpiece (Hynes 2002). The headpiece contains the β-propeller, the I domain in I-domain-containing integrins, and the thigh domain from the α subunit and the plexin-semaphorin-integrin (PSI) domain, hybrid domain, and I-like domain from the β subunit (Fig. 3.2). In integrins lacking I domain, the β-propeller and the I-like domain participate in ligand recognition. I domain-containing integrins, however, utilizes only the I domain for direct ligand-binding whilst the I-like domain serves as an allosteric regulator of the I domain (Hynes 2002). In the absence of intact αMβ2 structural data, a model of a bent αVβ3 was generated by software Modeller8v1 using the crystal coordinates of αVβ3 as template for a bent integrin conformation (Fig. 3.5). The αM I domain, using available crystal structure data, was tethered to the W2 and W3 of the αM β-propeller in an orientation permissible for the

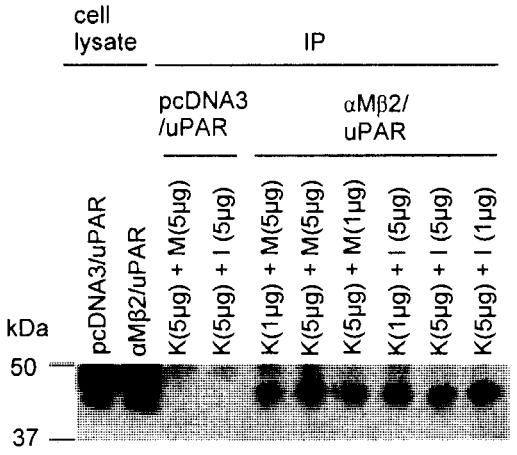

FIG 3.4 IB4 did not show the ability to disrupt the interaction of uPAR and αMβ2. The lysate was immunoprecipitated with KIM185 (K) in combination with different amount of IB4 (I) or irrelevant Ab MHM24 (anti-αL), and then blotted with anti-HA pAb.

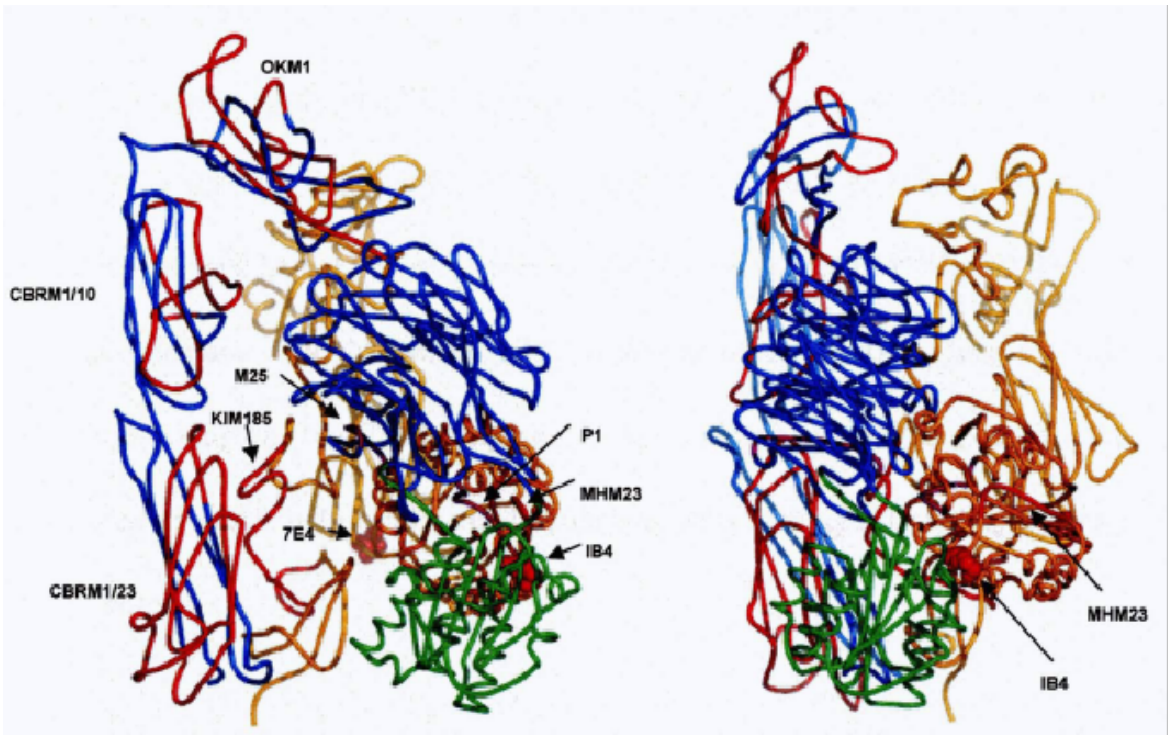

FIG 3.5 A structural model of integrin αMβ2. The αMβ2 is presented as backbone ribbon trace with two views. The polypeptide backbones of αM (blue), αM I domain (green), and β2 (gold) are shown. The location of the epitopes of the mAbs used in this study is highlighted as red backbone traces for regions or a stretch of sequence, and red space-filled atomic spheres for specific amino acids. Specific epitopes of mAbs LPM19c and MEM170 in the αM I domain have not been fully characterized and therefore are not indicated. The M25 sequence in the αM β-propeller (Simon *et al.*, 2000) and the corresponding P1 sequence in β2 with respect to that reported in integrin β1 (Wei *et al.*, 2005) are highlighted as magenta backbone traces.

interaction of αM I domain residue Glu^{320} with the MIDAS of the β2 I-like domain as suggested for integrin αLβ2 (Yang et al. 2004). The regions and sites of the epitopes of the mAbs employed are highlighted in the model. The M25 sequence in W4 of the β-propeller and the P1 sequence in the I-like domain of integrin are reported to be specific interaction sites of uPAR (Simon et al. 2000; Wei et al. 2005). From the model, these sites are in proximity of the I domain and I-like domain. It was noted that all mAbs used herein that recognize the αMβ2 I domain (MEM170, LPM19c) or the I-like domain (IB4, MHM23) failed to co-precipitate uPAR. These are also function-blocking mAbs. Combining these observations, we conjectured that the association of uPAR with αMβ2 could potentially affect the ligand-binding property of the I domain.

3.2.2 The ligand-binding property of integrin αMβ2 was attenuated by uPAR expression

We next tested whether uPAR expression could affect the function of αMβ2 in HEK-293 transfectants. The D1 of uPAR is known to be the major recognition site for integrins whilst D2 has been suggested to contain a second integrin association site (Degryse et al. 2005). Therefore, a mutant uPAR (hereafter referred to as D2D3) was generated without D1 but it retained all other regions of the uPAR (Fig. 3.6A). αMβ2 and D2D3 was highly expressed on HEK-293 transfectants as determined by flow cytometry analyses using anti-integrin or anti-uPAR domain-specific antibodies (Fig.

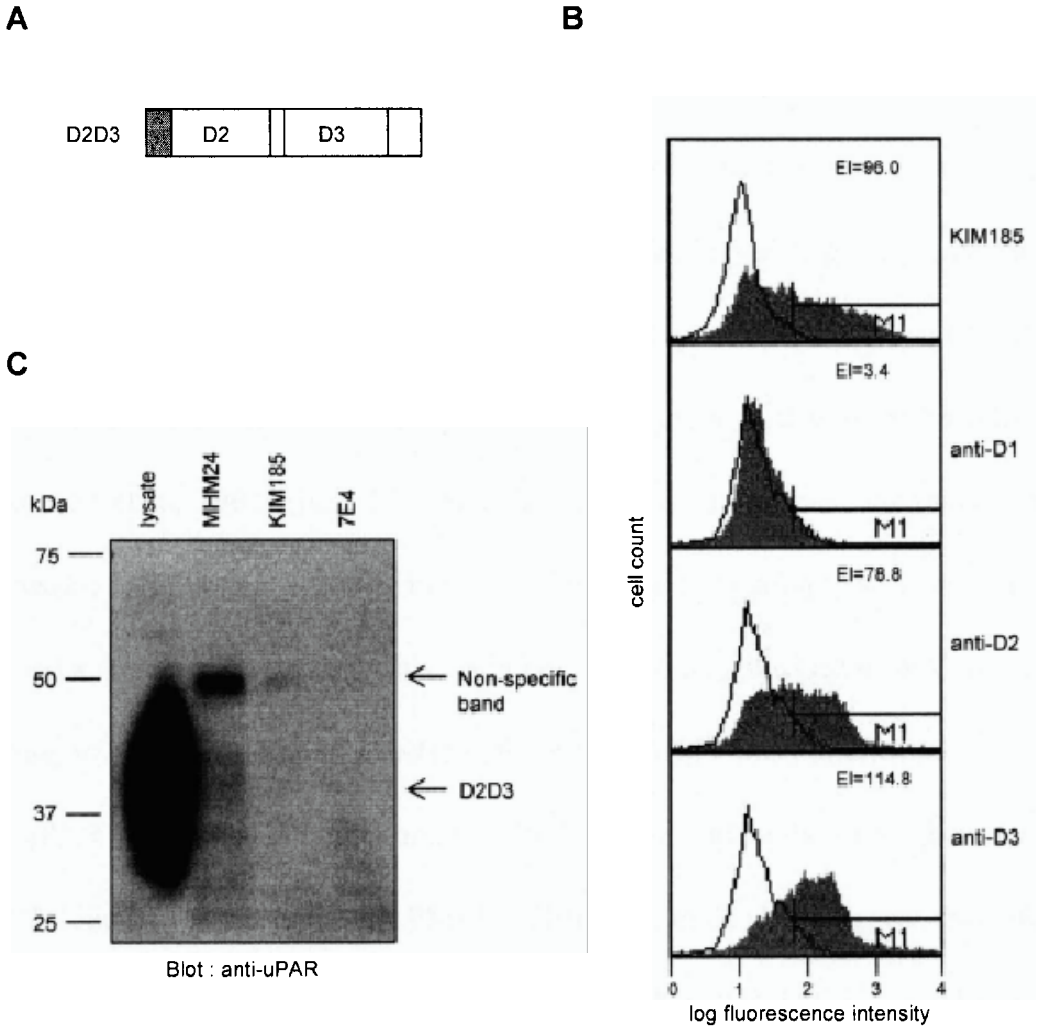

FIG 3.6 (A) Schematic representation of uPAR truncated variant D2D3. The signal peptide is shaded gray. The sequence Leu^{1}-Leu^{93} of D1 was deleted and the signal peptide sequence fused in-frame with the start of D2. (B) Flow cytometry analyses of αMβ2 and D2D3 expression on HEK-293 transfectants using anti-integrin mAb or specific mAbs against different domains of uPAR. Open histogram represents staining with an irrelevant mAb. Shaded histogram represents staining with mAbs recognizing integrin or different domain of uPAR. High level of staining was detected using anti-D2 and D3 mAbs but not anti-D1 mAb confirming the expression of properly folded mutant D2D3 lacking D1. The expression index (EI) was calculated by % gated positive x geo-mean fluorescence intensity. M1 denotes region gated to be positive staining. (C) Transfectants expressing D2D3 and αMβ2 were subjected to co-immunoprecipitation with control mAb MHM24 (anti-αL) and mAbs KIM185 and 7E4. D2D3 detected using rabbit anti-uPAR antibody followed by ECL.

3.6B). Further, D2D3 failed to co-precipitate with αMβ2 using mAb KIM185 or 7E4, suggesting that D1 of uPAR is the primary interaction domain with αMβ2 (Fig. 3.6C). Cell adhesion assays were performed on transfectants expressing αMβ2, αMβ2 with full-length uPAR, and αMβ2 with D2D3. Expression levels of αMβ2, uPAR, and D2D3 were assessed by flow cytometry (Fig. 3.7). Binding of αMβ2 transfectants to BSA (Davis 1992; Tan et al. 2000), fibrinogen (Simon et al. 1993), and ICAM-1 (Diamond et al. 1990) were promoted by the β2 integrin activating mAb KIM185 (Robinson et al. 1992) (Fig. 3.8). Similar profiles were observed for transfectants expressing αMβ2 and D2D3. However, transfectants bearing αMβ2 and uPAR showed a reduction in binding. This could not be attributed to a lack of mAb KIM185 binding to αMβ2 because epitope recognition by KIM185 was not affected by αMβ2 and uPAR association aforementioned. In all cases, binding was abrogated by the αMβ2 function-blocking mAb LPM19c. Therefore, these data suggest that uPAR down-regulates the ligand-binding activity of αMβ2. D2D3 failed to modulate the ligand-binding property of αMβ2 because D2D3 does not associate with αMβ2. It appears intriguing as to why only a reduction but not a complete abrogation of αMβ2 ligand-binding was detected in transfectants co-expressing uPAR. It is plausible that not all αMβ2 expressed are in association with uPAR. These unassociated αMβ2 may account for the residual binding observed and could therefore be activated by KIM185 to bind ligands and similarly be abrogated by αMβ2 function-blocking LPM19c. Taken together, our data are in line with reported observation that uPAR disrupts activated αMβ2 binding to fibrinogen (Simon et al. 2000). Further, we observed that

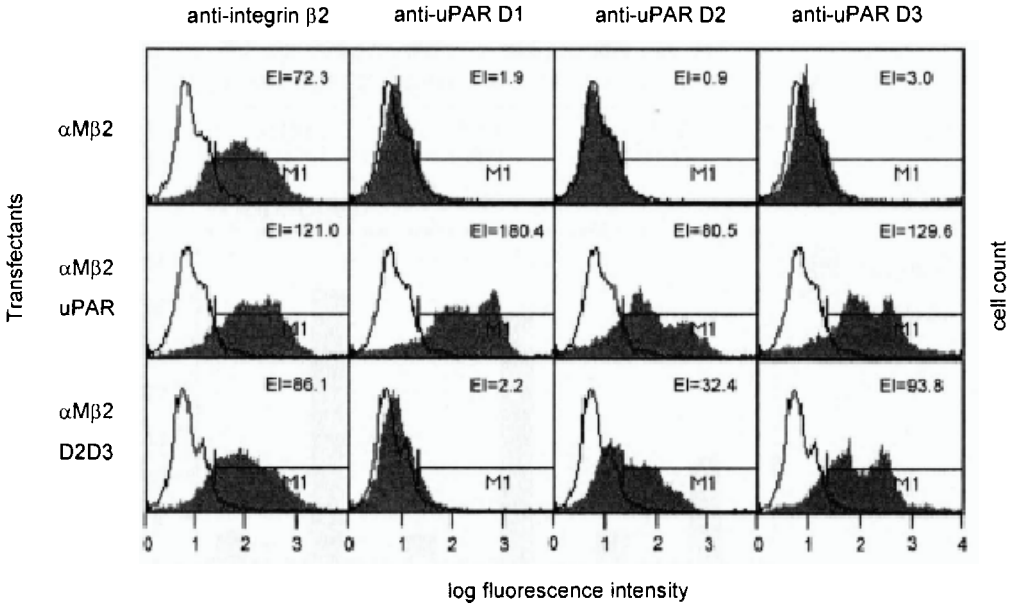

FIG 3.7 Flow cytometry analyses of transfectants expressing αMβ2 only, αMβ2 with uPAR, and αMβ2 with D2D3 using relevant mAbs as indicated. Open histogram represents staining with an irrelevant mAb. Shaded histogram represents staining with anti-integrin or anti-uPAR mAbs as indicated. The expression index (EI) was calculated by % gated positive x geo-mean fluorescence intensity. M1 denotes region gated to be positive staining.

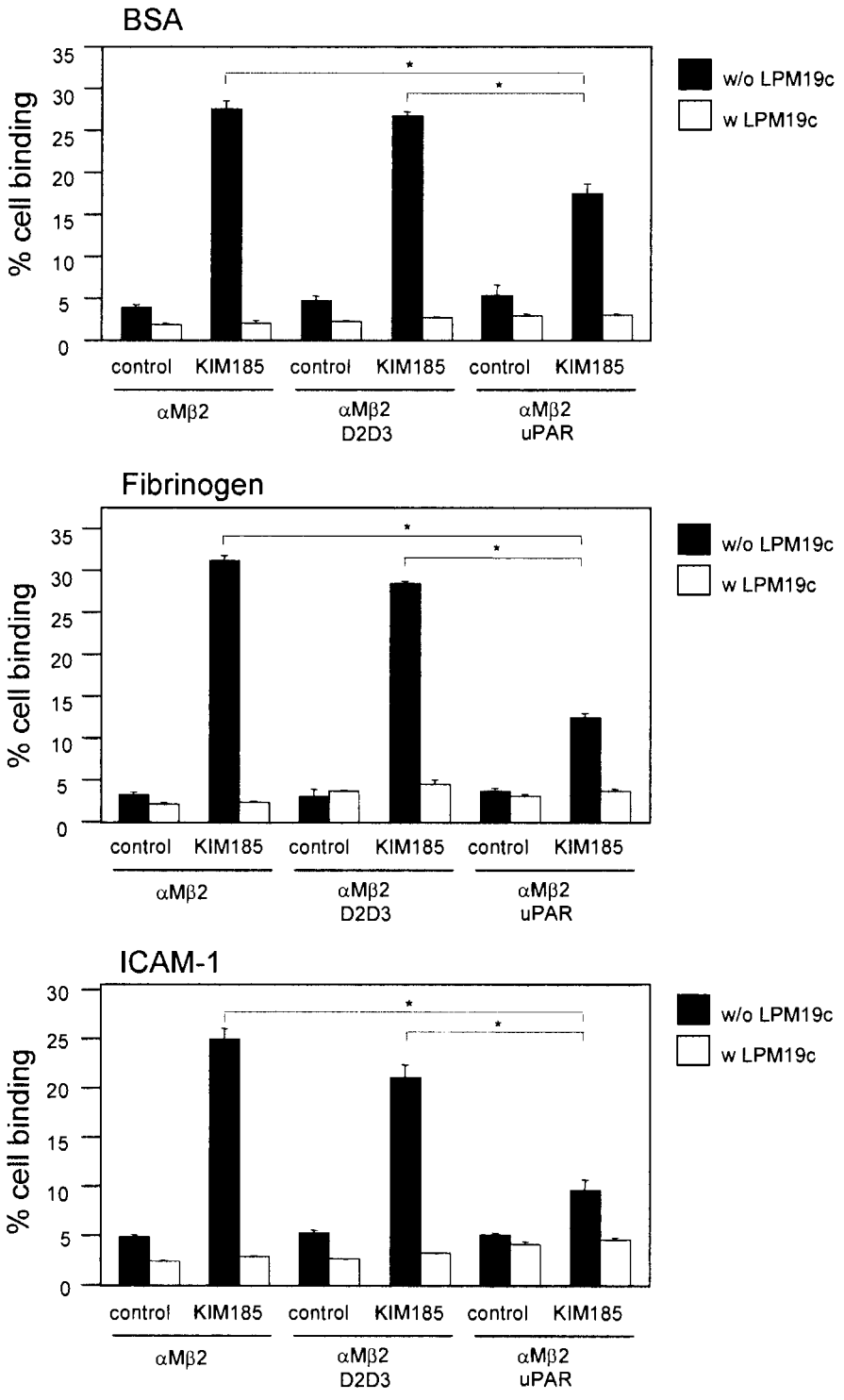

FIG 3.8 Cell adhesion assays using transfectants expressing αMβ2 only, αMβ2 with D2D3, and αMβ2 with uPAR on BSA (100 μg/ml), fibrinogen (250 μg/ml), and ICAM-1 (1 μg/ml). The activating mAb KIM185 and the function-blocking mAb LPM19c were used at 10 μg/ml. Control represents the condition without any additives. Triplicate determination (mean ± SD) representative of three separate experiments is shown. *, $p < 0.05$.

αMβ2 ICAM-1 binding was significantly reduced in the presence of uPAR. These findings are in contrast to one study suggesting that uPAR up-regulates αMβ2 binding to fibrinogen and has no effect on ICAM-1 binding (Zhang et al. 2003). In the same study, it is also not known why uPAR has no effect on αMβ2 binding to biotinylated-fibrinogen as compared to immobilized fibrinogen (Zhang et al. 2003).

We also extended our investigations by performing migration assays using fibrinogen. Transfectants were allowed to migrate for 20 h across transwell inserts coated on the underside with fibrinogen and migrated cells scored using flow cytometry (Fig. 3.9). In contrast to transfectants expressing αMβ2 or αMβ2 and D2D3, the number of migrated cells was reduced substantially in αMβ2 transfectants co-expressing uPAR, which was comparable to αMβ2 transfectants treated with function-blocking mAb.

3.2.3 uPAR expression reduced the ligand-binding capacity of a constitutively active integrin αMβ2 mutant

To provide additional evidence that uPAR can down modulate αMβ2 ligand-binding property, we made use of a constitutively active αMβ2 mutant. This was achieved by using a β2/β7 chimera (β2BN7) (Fig. 3.10A) that was reported previously to generate a constitutively active integrin αMβ2 (Hyland et al. 2001). The β2BN7 chimera has the Tyr^{338}-Cys^{437} of the β2 sequence replaced by the corresponding segment from integrin β7.

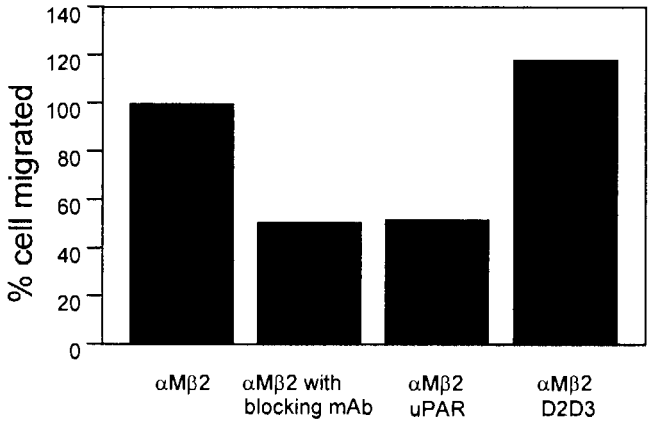

FIG 3.9 Haptotatic transwell motility assay on fibrinogen. Each transwell was coated with fibrinogen (250 μg/ml). Each group of transfectants expressing αMβ2, αMβ2 with uPAR, and αMβ2 with D2D3 was seeded into one transwell. An additional sample having transfectants expressing αMβ2 in the presence of function-blocking mAb was included as a control. The migrated cells were scored by flow cytometry. Number of migrated cells from transfectants expressing αMβ2 only was expressed as 100% cell migrated. Significant reduction of migrated cells was detected for αMβ2 transfectants in the presence of function-blocking mAb or co-expressed uPAR. Representative experiment from two independent experiments is shown.

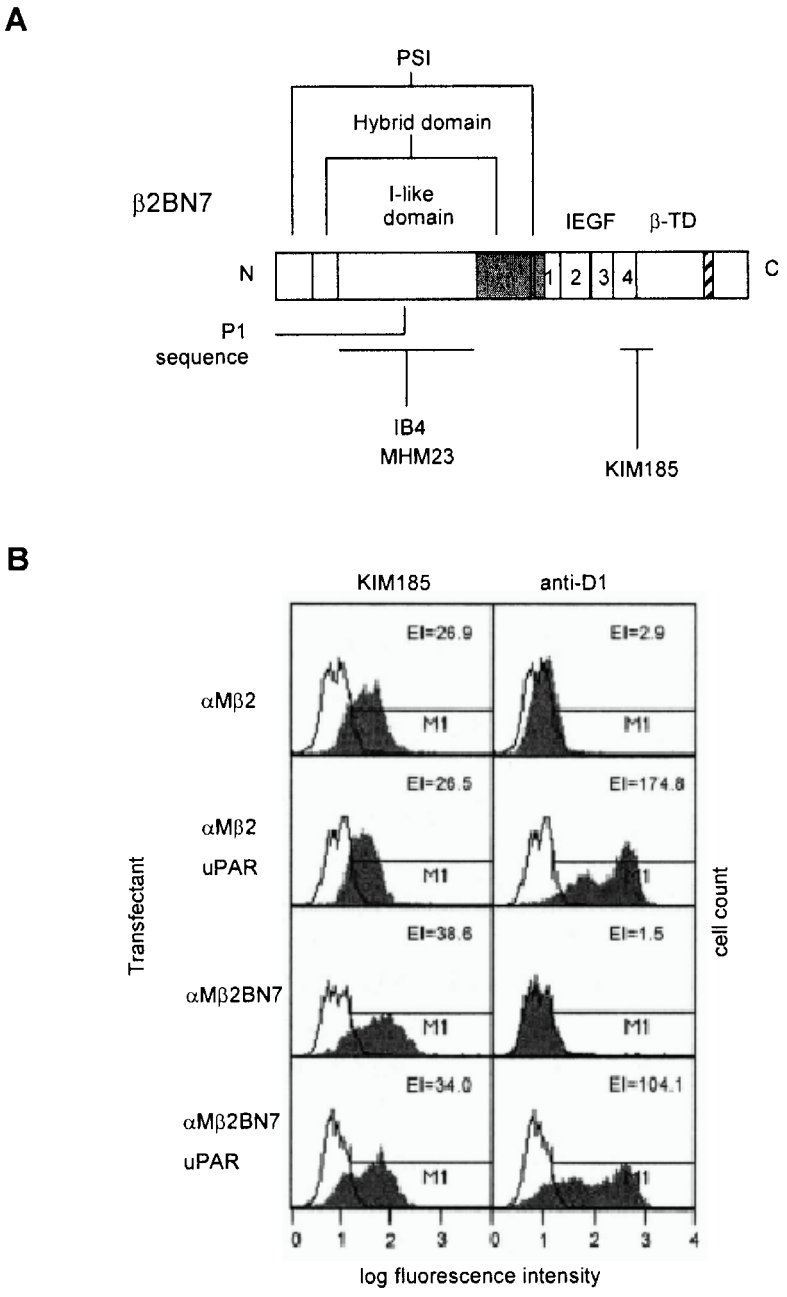

FIG. 3.10 (A) Schematic illustration of the integrin β2/β7 chimera β2BN7. The chimera was generated by replacing the β2 sequence Tyr^{338}-Cys^{437} with the corresponding segment from integrin β7 (shaded gray) (Hyland et al. 2001). The epitope of mAb 7E4 is absent in this chimera. (B) Flow cytometry analyses of transfectants expressing αMβ2 or αMβ2BN7 with or without uPAR using mAbs KIM185 and VIM5 (anti-uPAR D1). Open histogram represents staining with an irrelevant mAb. Shaded histogram represents staining with anti-integrin or anti-uPAR mAbs as indicated. High level of expressions was detected for αMβ2, αMβ2BN7, and uPAR. The expression index (EI) was calculated by % gated positive x geo-mean fluorescence intensity. M1 denotes region gated to be positive staining.

The expression and association of uPAR with αMβ2BN7 was comparable to wild-type αMβ2 as verified by flow cytometry and co-immunoprecipitation respectively (Fig. 3.10B & 3.11). Adhesion assays were performed comparing wild-type αMβ2 with uPAR and αMβ2BN7 with uPAR (Fig. 3.12). αMβ2BN7 transfectants showed constitutive adhesion to ligands BSA, fibrinogen, and ICAM-1 as compared to wild-type αMβ2. Adhesion specificity was demonstrated by its abrogation in the presence of function-blocking mAb in all cases. In the presence of uPAR, a substantial reduction in adhesion was observed for both transfectants on all ligands. Therefore, it is apparent that uPAR can down-regulate αMβ2 that was made constitutively active (in this case αMβ2BN7). This observation also brought about a potentially interesting extrapolation on the conformation of αMβ2BN7. Because it is most likely that a bent integrin associate with uPAR, it may also be conjectured that the constitutively active αMβ2BN7 adopts a relatively bent conformation instead of a highly extended conformation, which allows its association with uPAR.

3.3 Conclusion and discussion

Integrin αMβ2 is required for the adhesive and migratory responses of mononuclear phagocytes and PMNs. The function of αMβ2 can be regulated by cytoplasmic factors, extracellular divalent cations concentrations, and membrane associated proteins (Altieri 1991; Elemer et al. 1994; Petty et al. 1996). Modulation of αMβ2 ligand-binding function by uPAR has been widely reported. However, the precise

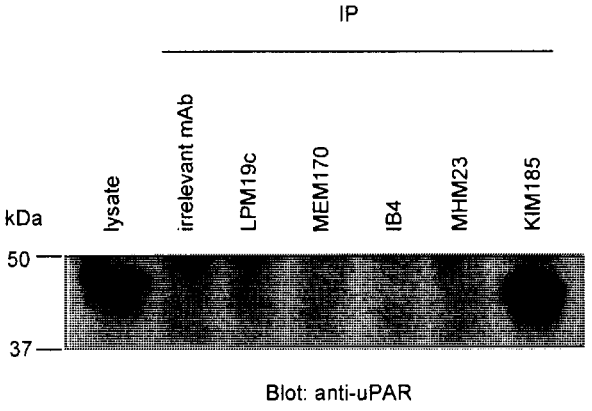

FIG. 3.11 Co-immunoprecipitation of full-length uPAR with αMβ2BN7. The lack of uPAR co-precipitated with αMβ2BN7 using mAb LPM19c, MEM170, IB4, and MHM23 but not KIM185 was similar to that of uPAR with wild-type αMβ2.

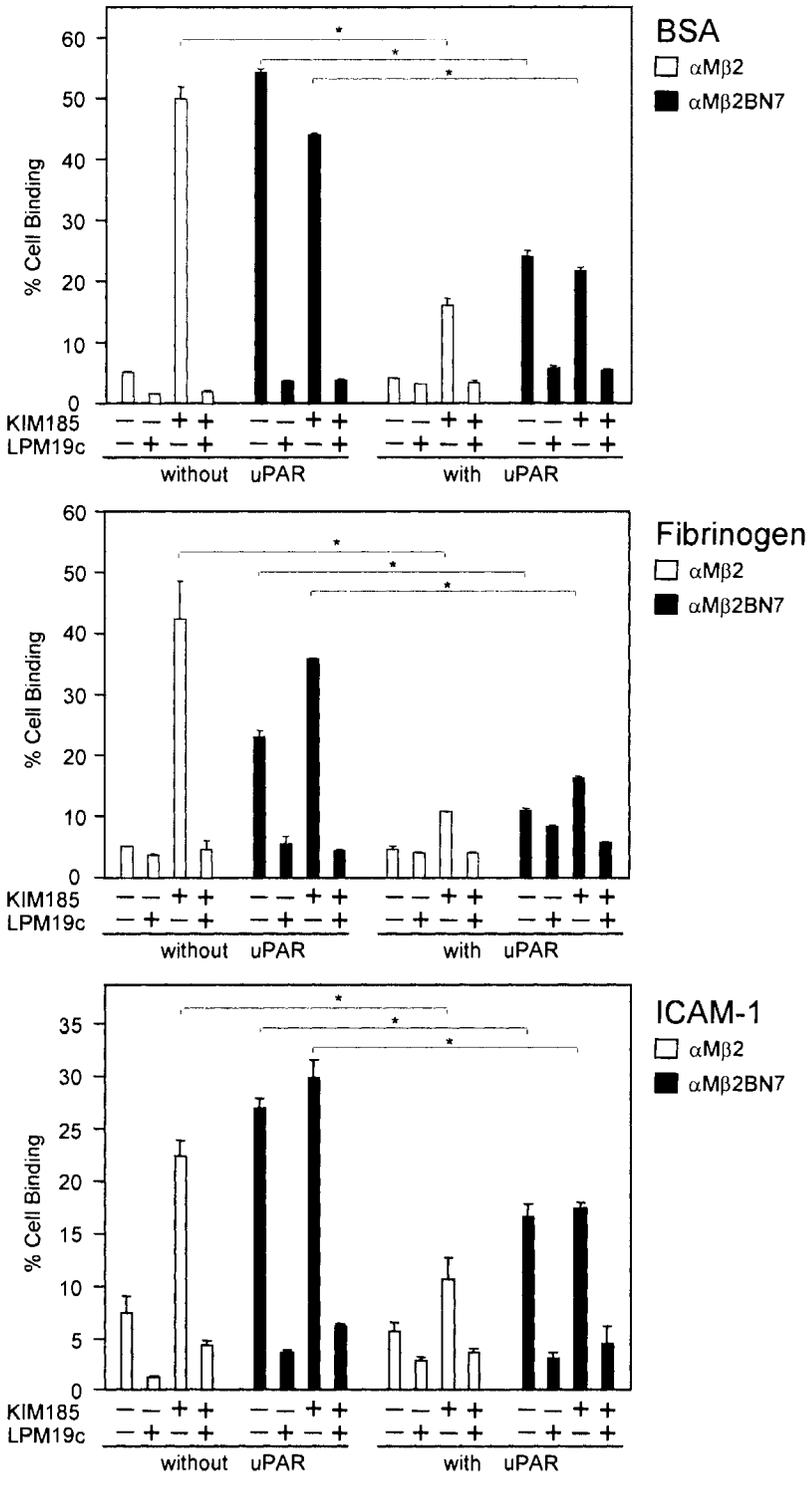

FIG 3.12 Cell adhesion assays of transfectants expressing αMβ2 (open bars) or αMβ2BN7 (filled bars) with or without uPAR on BSA, fibrinogen, and ICAM-1. Transfectants expressing αMβ2BN7 without uPAR co-expression showed constitutive ligand-binding activity as compared to αMβ2 transfectants. uPAR substantially attenuated the constitutive ligand-binding property of αMβ2BN7 on all ligands. The activating mAb KIM185 and the function-blocking mAb LPM19c were used at 10 μg/ml. Triplicate determination (mean ± SD) representative of three separate experiments is shown. *, $p < 0.05$.

mechanism of regulation requires further investigations. Based on the structural data of integrins and uPAR, it was proposed that integrin adopts a modified bent conformation when in association with uPAR (Wei et al. 2005).

In phorbol ester PMA-treated monocytes, uPAR was shown to enhance the adhesive properties of αMβ2 to ligands, in particular fibrinogen (Sitrin et al. 1996). A functional complex of αMβ2, uPAR, and uPA was proposed to serve in the fibrinolytic system (Pluskota et al. 2003; Simon et al. 1996). Further, uPAR-deficient mice exhibited impaired αMβ2-mediated neutrophil phagocytosis and recruitment to sites of infection (Gyetko et al. 2004; Gyetko et al. 2000). However, it was also observed that there was no apparent abrogation of the invasive property of macrophages in $uPAR^{-/-}$ mice when thioglycollate was injected into the peritoneal cavities (Dewerchin et al. 1996). Similarly, macrophages from $uPAR^{-/-}$ mice did not exhibit significantly defective migration on fibrin as compared to macrophages from $uPAR^{+/+}$ mice (Cao et al. 2006). In our study and that of Simon and co-workers (Simon et al. 2000), uPAR had a down-regulating effect on the ligand-binding function of αMβ2 in transfectants. This was further supported using the constitutively active mutant αMβ2BN7 and by showing that deleting D1 from uPAR, which is the primary interaction domain with αMβ2, nullified this effect. From the co-immunoprecpitation analyses, this may be attributed to the shielding of the αMβ2 I domain and I-like domain ligand-recognition site(s) by uPAR, which are reported to interact with critical sequences M25 and P1 of the integrin αM β-propeller and β1

I-like domain respectively (Simon et al. 2000; Wei et al. 2005). The extensive N-linked glycosylations of uPAR may also contribute in part to this effect. Alternatively, the association of uPAR with αMβ2 may alter the conformation of the I domain and I-like domain rendering them ineffective in ligand-binding.

It was proposed that only a small fraction of uPAR is associated with integrins in primary cells in contrast to ectopic cell expression system (Kjoller 2002; Simon et al. 2000). Despite the lack of cytoplasmic domain, uPAR can trigger cell signaling by associating with integrins that are capable of recruiting signaling molecules. For example, the complex formation of uPA, uPAR, and integrin α5β1 triggers α5β1-mediated MAPKs activation, and it was suggested that MAPKs activation may induce activation of unoccupied integrins via inside-out signaling (Tarui et al. 2003). Hence, in primary cells, a small number of uPAR associated with αMβ2 may allow localization of signaling molecules required for cell migration while unassociated αMβ2 mediates adhesive functions of cell locomotion. The src family tyrosine kinase $p56/59^{hck}$ was reported to have an important role in uPAR-mediated cell motility (Trigwell et al. 2000). Interestingly, $p56/59^{hck}$ was shown to interact with αMβ2 (Arias-Salgado et al. 2003). Whether a similar mode of uPAR, αMβ2, and Hck cooperativity exists as proposed for that of uPAR, α5β1, and MAPKs requires further investigations.

Chapter Four: uPAR induces conformational changes in the integrin headpiece and re-orientation of its transmembrane domains

4.1 Background

It is evident, based on the overall dimensions, that uPAR associates with a bent integrin (Arnaout et al. 2005; Llinas et al. 2005) (Fig. 4. 1). The uPAR-integrin complex is important in tumor biology and metastasis because of the proteolytic activity of uPA-uPAR, and importantly the signaling capacity of the uPAR-integrin complex (Blasi & Carmeliet 2002). Although uPAR does not contain a cytoplasmic domain, it can trigger cytosolic signaling by changing the shape of its integrin partner. uPAR changes the conformation of integrin α5β1, which promotes RGD-independent adhesion to fibronectin (Wei et al. 2005). Further, the uPAR-α5β1 complex induces ERK signaling in tumor cells (Wei et al. 2007).

uPAR changes the conformation of the β1 ectodomain when it interacts with a bent α5β1 (Wei et al. 2005). Presumably, this leads to integrin-mediated intracellular signaling. But the molecular details of signal transmission at the C-terminal halve of the integrin remain unclear. It was reported that the separation of the integrin αIIbβ3 TMs is an important event for outside-in signaling (Zhu et al. 2007). Here, we showed that the association of uPAR with a bent αMβ2 induces movement of the hybrid domain in the β2 subunit, and the re-orientation of the αMβ2 TMs.

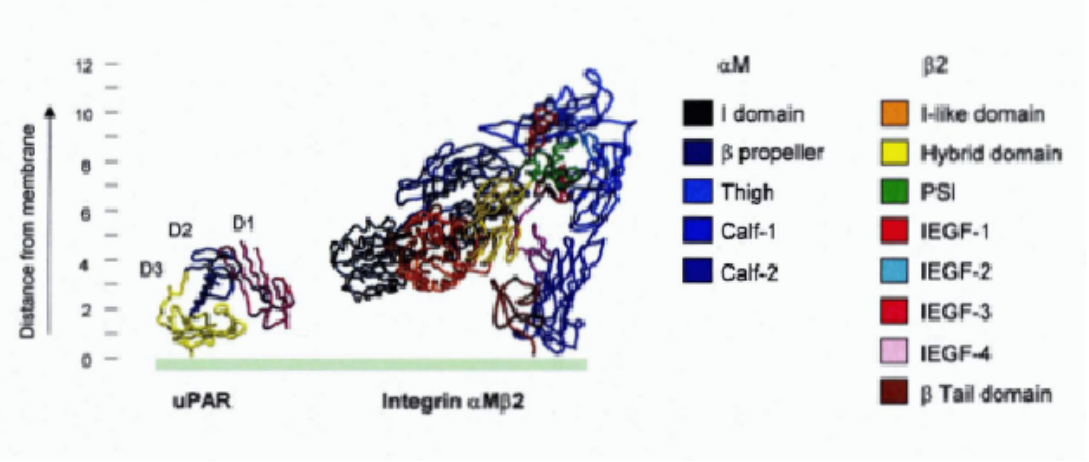

FIG 4.1 An illustration of the domain organization in αMβ2 and uPAR. The model of αMβ2 was built using Modeller8v1 and PyMOL (W.L. DeLano 2002) using these structure coordinates. The bent αMβ2 was generated using αVβ3 coordinates 1L5G as template (Xiong et al. 2002). The αM I domain 1BHO (Baldwin et al. 1998) was included. The structures of β2 PSI, hybrid, I-EGF1, 2, and 3 were from 2P26 and 2P28 (Shi et al. 2007). uPAR coordinates were from 2FD6 (Huai et al. 2006). The αMβ2 model only serves as an illustration in the absence of a complete structure of an I domain-containing integrin. The detail position of the I domain in an intact integrin has not been determined.

4.2 Results

4.2.1 Interaction with uPAR induces the movement of the αMβ2 hybrid domain.

The association of uPAR with αMβ2 has been reported by others and our group (Bohuslav et al. 1995; Simon et al. 1996; Simon et al. 2000; Tang et al. 2006; Xue et al. 1994). Here, we further verified the association of uPAR with αMβ2 in 293T transfectants. 293T cells were transiently transfected with αMβ2 alone, αMβ2 with HA-uPAR, or αMβ2 with HA-D2D3 (uPAR without domain 1, D1). HA-D2D3 was included as a control because we showed in chapter three that D1 of uPAR is critical for its association with αMβ2 (Tang et al. 2006). Flow cytometry was performed, and the expression of αMβ2 was detected by mAb KIM185 that is β2 subunit-specific and an activating mAb (Andrew et al. 1993), and the expressions of HA-uPAR and HA-D2D3 were detected by anti-uPAR D2-specific mAb (Fig. 4.2A). Comparable levels of αMβ2 were detected in all transfectants, and high level of HA-uPAR and HA-D2D3 detected in respective transfectants.

Next, we performed chemical cross-linking experiment using the water soluble and membrane impermeable compound 3,3'-Dithiobis (sulfosuccinimidyl proprionate) (DTSSP) containing two NHS-ester functional groups that react with primary amines, and has a thiol cleavable spacer with an arm length of 12Å. The close proximity of uPAR with αMβ2 when they interact would allow cross-linking of both molecules by

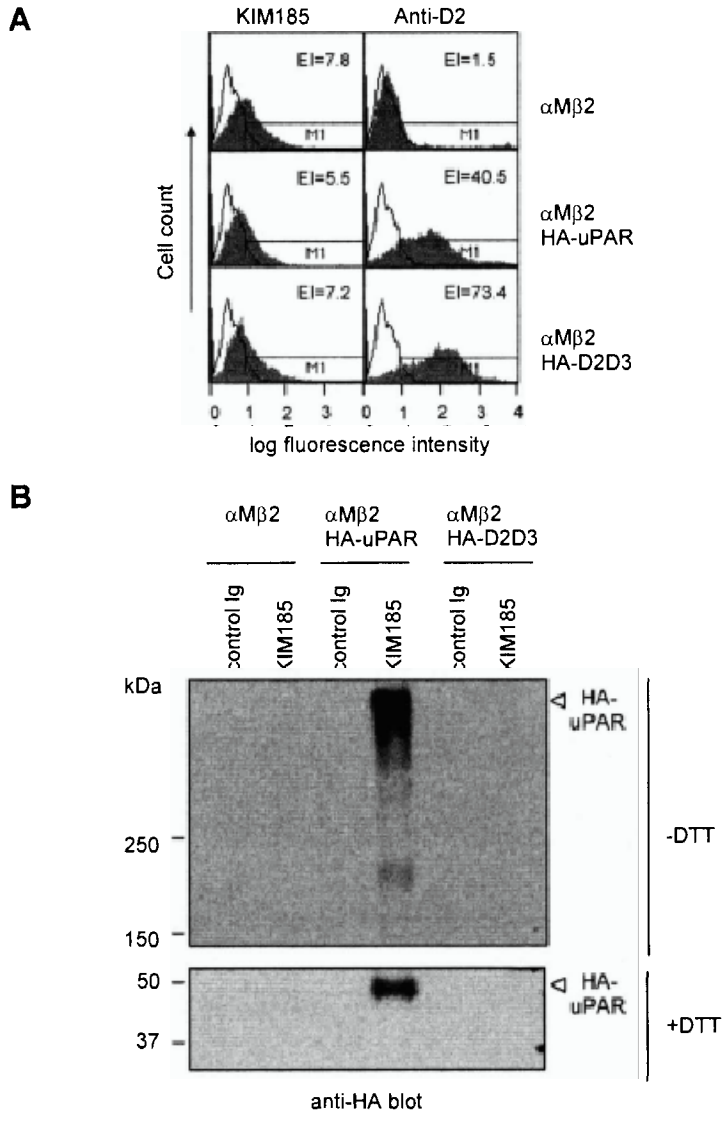

FIG 4.2 (A) Flow cytometry analyses of 293T cells transiently transfected with αMβ2, αMβ2 with HA-uPAR, or αMβ2 with HA-D2D3. To detect αMβ2 expression, cells were stained with mAb KIM185 (β2-specific). To detect HA-uPAR and HA-D2D3 expressions, cells were stained with anti-uPAR mAb (D2-specific). Cells were subsequently stained with FITC-conjugated secondary antibody followed by flow cytometry analyses. Shaded histograms represent staining with KIM185 or anti-D2 (uPAR). Open histogram (irrelevant mAb). The expression index (EI) was calculated by % gated positive x geo-mean fluorescence intensity. M1 denotes region gated to be positive staining. (B) Cross-linking of αMβ2 and HA-uPAR on 293T transfectants. Cells expressing αMβ2, αMβ2 with HA-uPAR, or αMβ2 with HA-D2D3 were incubated in PBS containing the chemical DTSSP for 30 min at room temperature. Thereafter, cells were subjected to immunoprecipitation with KIM185 as described under Materials and Methods. An irrelevant mAb was included as control. Precipitated proteins were resolved on a 6% SDS-PAGE under non-reducing conditions (-DTT) or on a 10% SDS-PAGE under reducing conditions (DTT). Detection of HA-uPAR was performed by anti-HA immunoblotting followed by ECL.

DTSSP. 293T transfectants were incubated in PBS containing DTSSP followed by immunoprecipitation as described under Materials and Methods (Fig. 4.2B). Immunoprecipitated proteins were resolved on denaturing SDS-PAGE under non-reducing (-DTT) or reducing (+DTT) conditions. Under non-reducing conditions, an apparent high molecular weight HA-uPAR was detected only in the KIM185 precipitate of αMβ2/HA-uPAR transfectants. We conjectured that the high molecular weight signal detected for HA-uPAR was due to its association with αMβ2 covalently cross-linked by DTSSP (uPAR~50 kDa, αM~170 kDa, β2~95 kDa; uPAR-αMβ2~315 kDa). When DTT was included, HA-uPAR was dissociated from the KIM185-immunoprecipitated αMβ2 and it migrated as an ~50 kDa protein band. By contrast, HA-D2D3 was not detected in the KIM185 precipitate of αMβ2/HA-D2D3 transfectants, which was consistent with the requirement of D1 for the interaction of uPAR with αMβ2 (Tang et al. 2006). Thus, the physical association of uPAR with αMβ2 was further verified in the 293T transfection system.

As discussed in the previous section, the integrin headpiece comprises from the α subunit the inserted (I) domain (for I domain-containing integrins that include αMβ2; this domain is also referred to as the A domain), β-propeller, and thigh domain, and from the β subunit the I-like domain, hybrid domain, plexin-semaphorin-integrin (PSI), and integrin epidermal growth factor (IEGF)-1 (Luo et al. 2007) (Fig. 4.1). Three distinct integrin conformations have been reported based on electron microscopy analyses of αLβ2 and αXβ2. These are the bent conformer, the extended

conformer with a closed headpiece, and an extended conformer with an open headpiece (Nishida et al. 2006). One of the key features distinguishing a closed headpiece from an open headpiece lies in the orientation of the hybrid domain. In the closed headpiece, the hybrid domain and PSI are in juxtaposition to the α subunit, and in the open headpiece, they "swing-out" (Mould et al. 2003) by ~62 Å in the crystal structure of ligand-mimetic bound platelet integrin αIIbβ3 (Xiao et al. 2004).

We examined whether αMβ2 interaction with uPAR induces conformational change to the integrin headpiece. 293T cells were transfected with αMβ2 or αMβ2/HA-uPAR. Cell surface expressions of αMβ2 and HA-uPAR were determined by flow cytometry analyses using the mAb KIM185, and mAb VIM5, another uPAR-specific mAb but it recognizes D1 of uPAR (Fig. 4.3A). Comparable expressions of αMβ2 were detected in both transfectants, and high-level of HA-uPAR was detected in αMβ2/HA-uPAR transfectants.

We then performed immunoprecipitation analyses with β2 integrin activation reporter mAbs. 293T cells expressing αMβ2 or αMβ2/HA-uPAR were surface labeled with biotin, and αMβ2 immunoprecipitated with mAbs MEM148, KIM127, and KIM185. The mAb MEM148 was shown to recognize a neo-epitope in the hybrid domain of the β2 subunit that is masked in the absence of hybrid domain movement (Tang et al. 2005). Hybrid domain movement is a key feature of an integrin with an open headpiece (Luo et al. 2007). The mAb KIM127 recognizes a neo-epitope in the

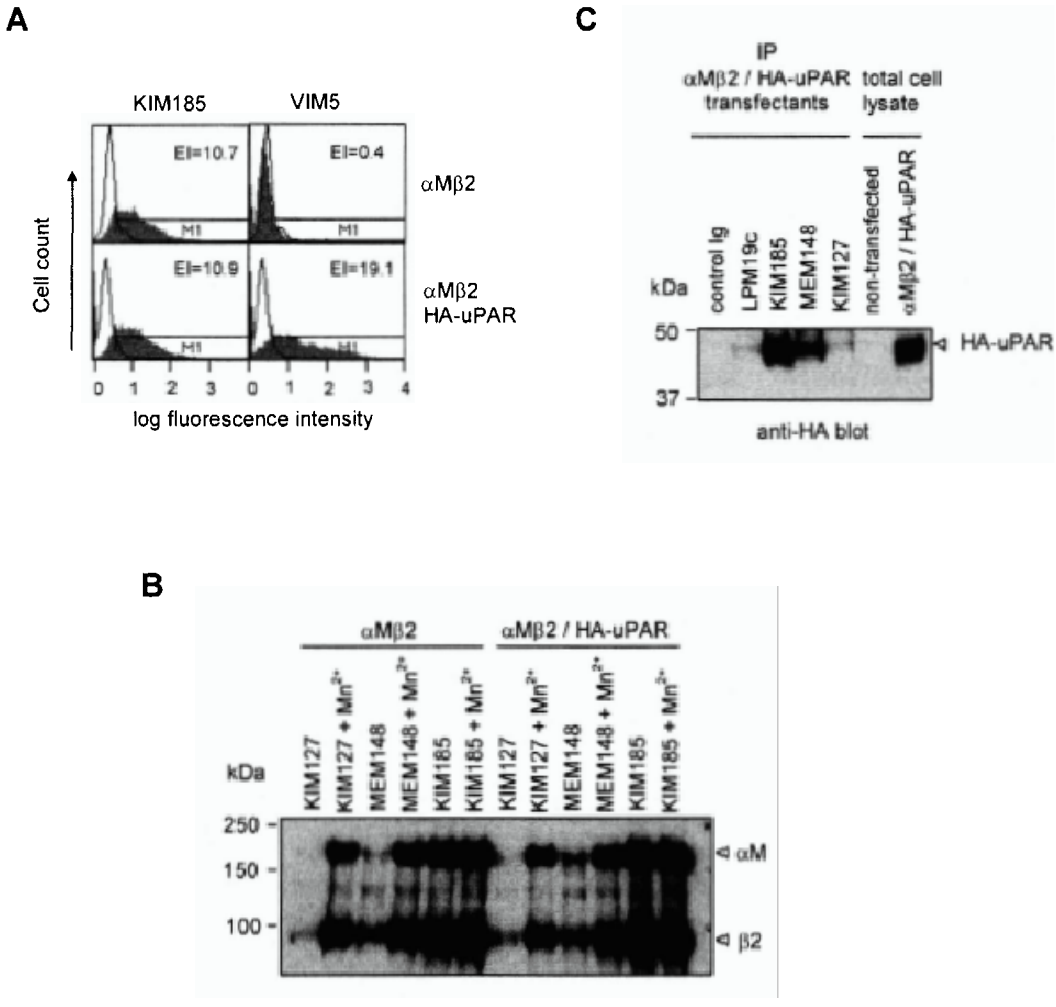

FIG 4.3 Conformation of αMβ2 when it interacts with uPAR. (A) Flow cytometry analyses of 293T transfectants expressing αMβ2 with or without HA-uPAR. mAb KIM185 was employed to detect αMβ2 expression and mAb VIM5 (D1-specific) was used for HA-uPAR detection. Shaded histograms represent staining with KIM185 or VIM5. Open histogram (irrelevant mAb). The expression index (EI) was calculated by % gated positive x geo-mean fluorescence intensity. M1 denotes region gated to be positive staining. (B) The conformation of αMβ2 interacting with uPAR was assessed by immunoprecipitation analyses. 293T transfectants expressing αMβ2 or αMβ2 and HA-uPAR were surface biotinylated, lysed, immunoprecipitated with mAbs KIM127, MEM148 or KIM185. Immunoprecipitated proteins were resolved on a 7.5% SDS-PAGE gel under reducing conditions. Biotin-labeled αMβ2 subunits were probed with streptavidin-HRP, and detected by ECL. (C) Conformational change in αMβ2 when it interacts with uPAR was assessed by a different approach. 293T transfectants bearing αMβ2 and HA-uPAR were immunoprecipitated with the indicated mAbs, and HA-uPAR that co-precipitated with αMβ2 was detected by immunoblotting with anti-HA antibody. Proteins were resolved on a 10% SDS-PAGE under reducing conditions. IP: immunoprecipitation.

I-EGF2 of the β2 subunit, and is masked in the bent conformation but expressed in the extended conformation (Beglova et al. 2002; Stephens et al. 1995). KIM185 was also included in the analysis as a control, and its epitope lies in the β2 I-EGF4/βTD region (Lu et al. 2001a). Transfectants were incubated in media containing these mAbs with or without Mn^{2+}, which activates αMβ2 (Altieri 1991), for 30 min at 37°C before immunoprecipitation was performed. KIM127 and MEM148 did not immunoprecipitate a significant level of αMβ2 heterodimer from lysate of cells transfected with αMβ2 (Fig. 4.3B). The β2 signal detected in the MEM148 sample was attributed to unassociated β2 as described previously (Cheng et al. 2007). When supplemented with Mn^{2+}, high level of αMβ2 was precipitated by KIM127 and MEM148. The control mAb KIM185 precipitated αMβ2 without requirement of Mn^{2+} treatment. These data showed that under resting condition, αMβ2 is in a bent conformation with a closed headpiece because of the lack of reactivity of αMβ2 with KIM127 and MEM148. When cells co-expressing αMβ2 and HA-uPAR were analyzed, the profiles of KIM127 and KIM185 samples were similar to that of cells expressing αMβ2 only, but significant αMβ2 signal was detected by MEM148 even without Mn^{2+} treatment. Addition of Mn^{2+} further increased the amount of αMβ2 precipitated by MEM148. These data suggest that when uPAR interacts with αMβ2, the hybrid domain of β2 was displaced as reported by MEM148, although it was also apparent that the population of αMβ2 with hybrid domain displacement was relatively small in the presence of uPAR interaction.

To further verify that the interaction with uPAR induces hybrid domain movement in αMβ2, co-immunoprecipitation analysis was performed (Fig. 4.3C). The rationale of this experiment was that if the interaction with uPAR induces shape changes in αMβ2, uPAR would be co-precipitated with the αMβ2 that has undergone conformational change using the relevant reporter mAb. 293T cells transfected with αMβ2 and HA-uPAR were lysed and subjected to immunoprecipitation with the indicated mAbs. HA-uPAR that co-precipitated was probed and detected with anti-HA immunoblotting. The mAb LPM19c that recognizes an epitope in the αM I domain was also included as a control (Violette et al. 1995). Expression of HA-uPAR was detected in total cell lysate of transfectants but not untransfected cells. HA-uPAR was not detected in the control Ig lane, and poorly detected in lanes of LPM19c and KIM127. The lack of interacting HA-uPAR with αMβ2 in samples containing LPM19c was consistent with previous data shown in chapter three, and possibly due to the masking of αM I domain by the partner uPAR (Tang et al. 2006). The lack of HA-uPAR co-precipitating with αMβ2 in the sample of KIM127, and the presence of significant HA-uPAR in samples of KIM185 and MEM148 were consistent with that aforementioned.

Thus, these data lend support to the concept that uPAR interaction with αMβ2 induces an open headpiece with hybrid domain displacement but it retains an overall bent conformation.

4.2.2 Interaction with uPAR induces the separation of the αMβ2 TMs.

We next examined whether interaction of uPAR with αMβ2 could induce the separation or re-orientation of the αMβ2 TMs, which is an important event in integrins αLβ2 and αIIbβ3 outside-in signaling (Kim et al. 2003; Zhu et al. 2007), and this is relevant to the possible mechanism by which uPAR signal through its partner integrins. To test this hypothesis, we made use of photo-bleach FRET detection method by fusing monomeric(m)CFP and mYFP to the C-termini of integrin cytoplasmic tails (Kim et al. 2003) (Fig. 4.4). mCFP and mYFP will be referred to as CFP and YFP henceforth. In the integrin α subunit expression construct, a five amino acid linker was engineered between the mCFP and the last amino acid of the cytoplasmic tail. In the integrin β subunit, a six amino acid linker was introduced. It was conceived that the close proximity of the cytoplasmic tails, which suggest proximity of the TMs, would allow effective FRET. A decrease in FRET would ensue if the TMs are separated, which leads to the separation of cytoplasmic tails.

When first tested, we observed that the integrin FRET pair αMCFP and β2YFP in a K562 transfectant system described previously (Kim et al. 2003; Vararattanavech et al. 2008) failed to show significant increase in the fluorescence intensity of CFP after YFP photo-bleached when compared to cells that were not subjected to photo-bleach (unbleach) (Fig. 4.5A). This could be attributed to the marked length difference of the αM and β2 cytoplasmic tails. We noted that FRET was used to demonstrate

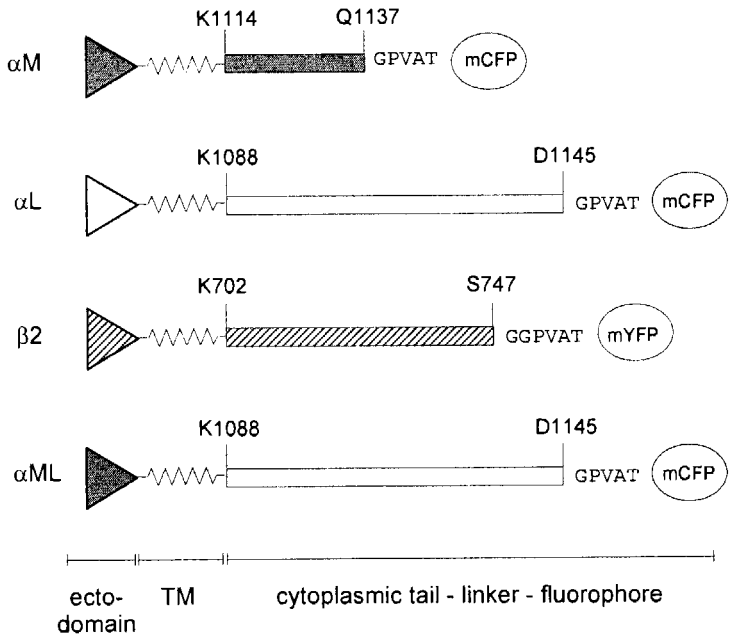

FIG 4.4 Schematic illustrating integrins with different mCFP and mYFP fusions. The linker residues between the cytoplasmic tails and the FRET pair fluorophores are shown. For ease of reference, the amino acids flanking each cytoplasmic tail are numbered according to the mature protein (Barclay A. N. 1997).

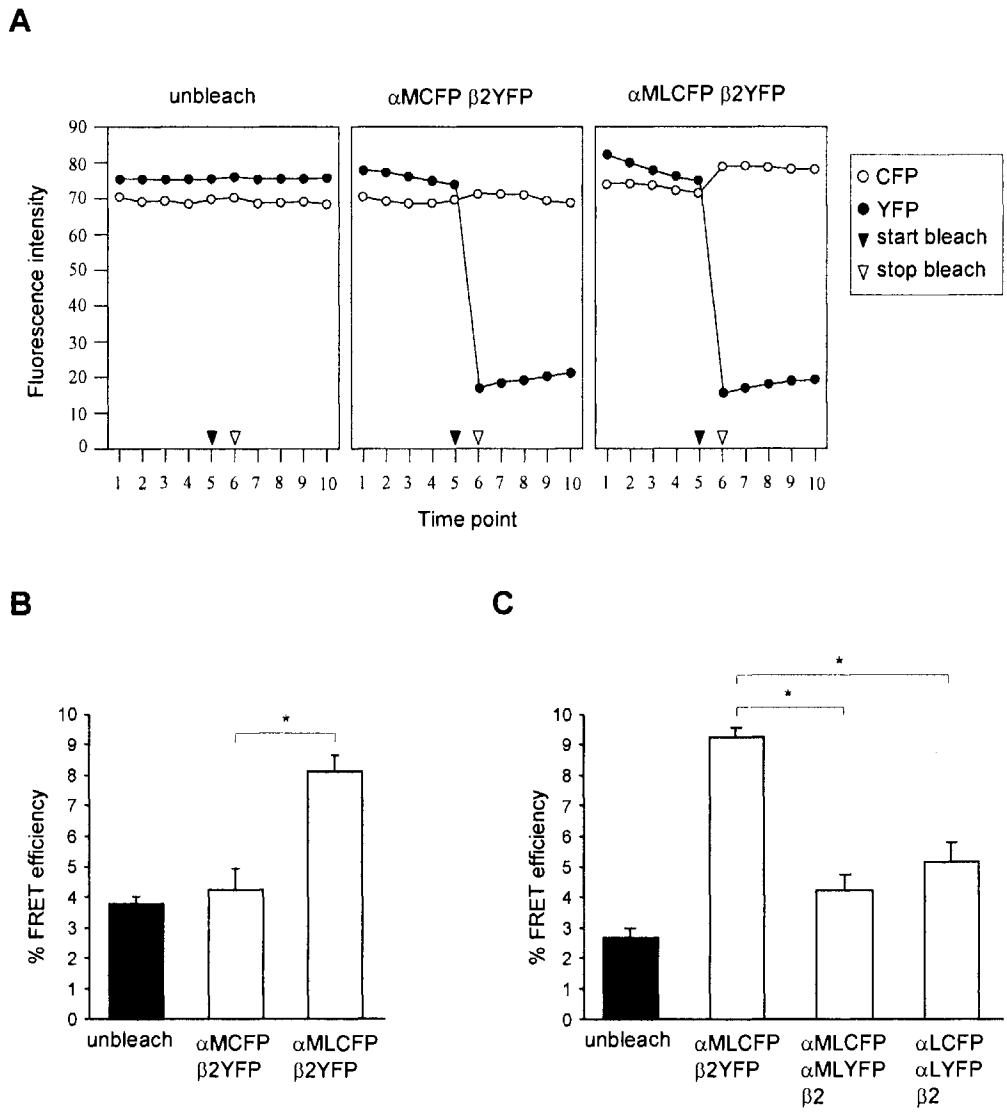

FIG 4.5 FRET analyses to detect αMβ2 TM movement. (A) Representative fluorescence intensity plots of K562 transfectants expressing integrins with FRET pair fusions pre- and post-YFP photobleach. The time interval between each point is 3s, except that between the 5th and 6th timepoints when the photobleaching was conducted, the duration was ~60s as it varies with cell size. (B & C) % FRET efficiency plots of integrin cytoplasmic tail mutants. Data are representative of two independent experiments. Data show mean ± SEM for 15 cells analyzed. Student's *t* test, assuming unequal variance, was used for statistical analyses. *, $p < 0.001$.

constitutive heterodimerization of αMβ2 in adherent CHO and 293T cells, and was proposed to be cell-type independent (Fu et al. 2006). However, in our hands, we were unable to obtain interpretable plasma membrane FRET data because of the uneven morphology of 293T cells. Further, the authors also reported possible conformational differences between αMβ2 expressed in CHO and 293T (Fu et al. 2006). Thus, we retained the use of non-adherent K562 cells but with re-engineered integrin cytoplasmic tails. Previously, we analyzed FRET of αLβ2 cytoplasmic tails in transfected K562 (Vararattanavech et al. 2008). Hence, we re-engineered αM with its cytoplasmic tail substituted with that of αL having a C-terminus CFP, referred to as αML (Fig. 4.4). Cells transfected with αMLCFPβ2YFP showed an increase in CFP signal when YFP was photobleached (Fig. 4.5A), suggesting proximity of the cytoplasmic tails, and reasonably the association of the αMβ2 TMs. To provide ease in comparison, and with more cells analyzed, we plotted % FRET efficiency as described in Materials and Methods, and these plots were used in all subsequent figures. When compared to cells expressing αMCFPβ2YFP, cells expressing αMLCFPβ2YFP showed higher FRET (Fig. 4.5B). Unbleach sample was also plotted for comparison. To exclude the possibility that FRET was detected due to micro-clustering of the integrins in K562 or due to sample preparation, we transfected K562 cells with αMLCFP, αMLYFP, and β2. If micro-clustering occurs, it is likely that the close proximity of αMLCFPβ2 and αMLYFPβ2 will lead to detectable FRET. Included for comparison were cells transfected with αLCFP, αLYFP, and β2. Whereas significant FRET was detected for cells expressing αMLCFPβ2YFP, markedly less

FRET was detected in cells expressing αMLCFP, αMLYFP, β2 and αLCFP, αLYFP, β2. These data suggest that the FRET detected in αMLCFPβ2YFP was due primarily to intra-molecular cytoplasmic tails interaction rather than microclustering. In addition, we could infer that the TMs of the integrin are in close juxtaposition.

We then analyzed the effect of uPAR on αMβ2 TMs. uPAR contains three domains, D1, D2, and D3 (Fig. 4.1). We showed previously that D1 is required for uPAR interaction with αMβ2 because the deletion of D1 abrogated association between uPAR and αMβ2 (Tang et al. 2006). The expression and identity of full-length HA-uPAR and HA-D2D3 were re-assessed in K562 transfectants with a panel of uPAR domain-specific mAbs followed by flow cytometry analyses (Fig. 4.6A). Whilst cells expressing full-length HA-uPAR stained positive with all three mAbs, cells bearing HA-D2D3 only showed positive staining with anti-D2 and anti-D3 mAbs. Next, FRET analyses were performed on K562 expressing full-length HA-uPAR or HA-D2D3 with αMLCFPβ2YFP (Fig. 4.6B). Cells expressing only the integrins and cells expressing integrins with HA-D2D3 showed comparable level of FRET. By contrast, a significant diminution of FRET was observed for cells expressing integrins with full-length HA-uPAR. These data suggest the separation of the integrin cytoplasmic tails in uPAR co-expressing cells, and they suggest re-orientation or separation of the αMβ2 TMs in these cells.

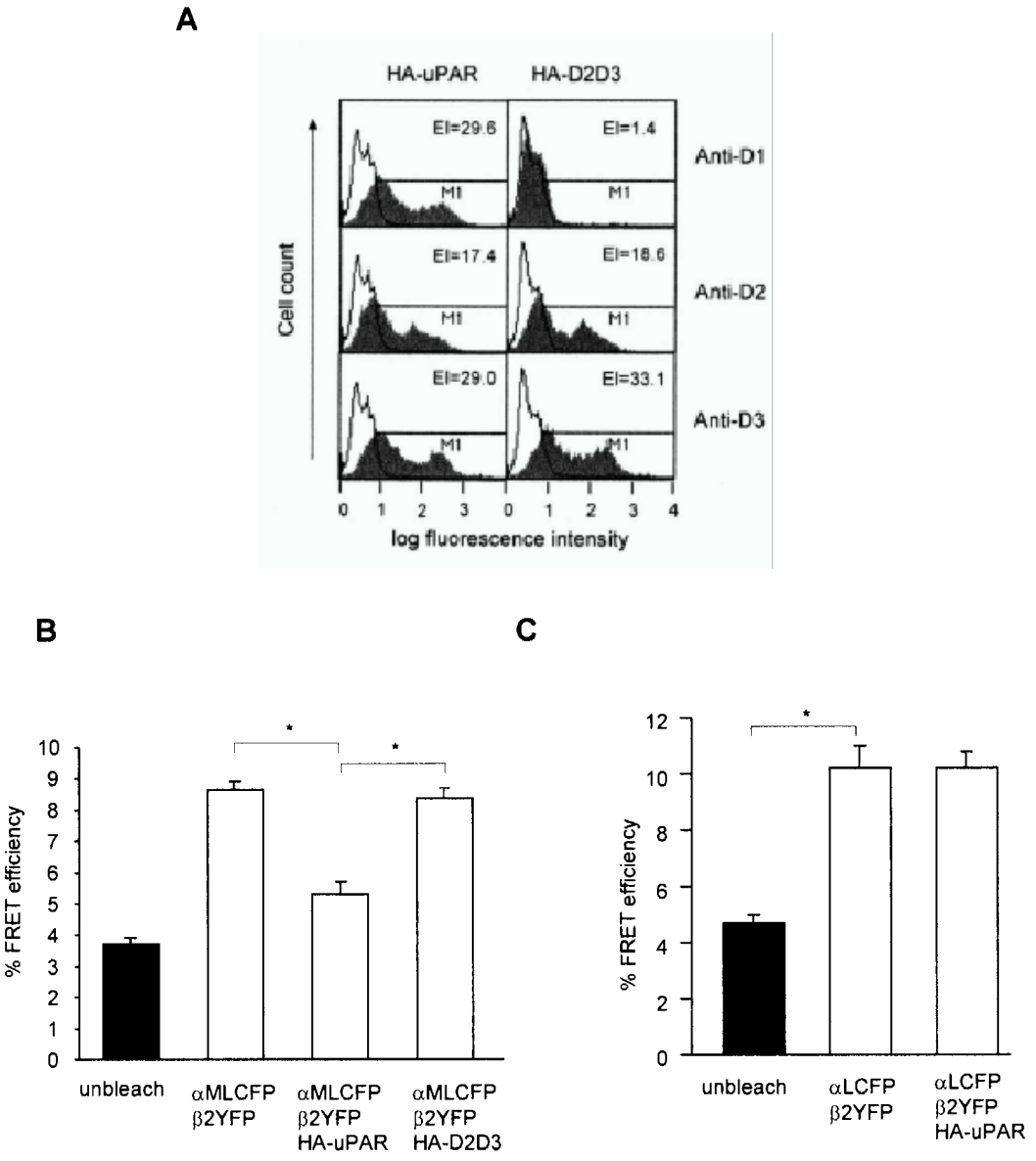

FIG 4.6 uPAR induces re-orientation or separation of the αMβ2 TMs. (A) Expressions of HA-uPAR and HA-D2D3 on 293T transfectants were determined by immunostaining with domain-specific mAbs (shaded histograms) followed by flow cytometry analyses. Open histogram (irrelevant mAb). The expression index (EI) was calculated by % gated positive x geo-mean fluorescence intensity. M1 denotes region gated to be positive staining. (B) FRET analyses of αMβ2 TM re-orientation or separation in K562 transfectants. Cells were transiently transfected with αMCFPβ2YFP followed by FRET detection. Included in the analyses was co-expression of HA-uPAR or HA-D2D3 with αMCFPβ2YFP. Data show mean ± SEM for 20 cells analyzed. (C) FRET analyses of K562 cells transfected with αLCFPβ2YFP in the presence or absence of HA-uPAR co-expression. Data show mean ± SEM for 14 cells analyzed. *, $p < 0.001$.

The reduction in FRET signal of αMLCFPβ2YFP in the presence of HA-uPAR was not an aberrant effect of HA-uPAR on the αL cytoplasmic tail that was engineered into αM because HA-uPAR had minimal effect on the FRET signal of αLCFPβ2YFP on K562 transfectants (Fig. 4.6C). It was also noted that in αMLCFPβ2YFP, the cytoplasmic tail substitution was made from αM Lys1114 onwards (Fig. 4.4 & 4.7). Recently, NMR studies reveal that the first charged residue Lys on the intracellular side of αIIb and β3 does not demarcate the C-terminal end of the transmembrane domains (Lau et al. 2008a; Lau et al. 2008b). In αIIb, two residues that are located after Lys989, namely Phe992 and Phe993, loop back into the intracellular side of the plasma membrane (Lau et al. 2008a). Comparison of αM and αL membrane proximal sequences reveals an amino acid difference (shaded in black) between αM Lys1114-Arg1120 and αL Lys1088-Arg1094 (Fig. 4.7). The αMLCFP may have a disrupted membrane insertion due to the substitution of αM Leu1115 with Val. This may complicate the analyses of αMLCFPβ2YFP interacting with uPAR. Thus, we have generated an additional chimera αML*CFP in which the cytoplasmic tail exchange between αM and αL was made after the GFFKR sequence. FRET analyses of αML*CFPβ2YFP in the presence of HA-uPAR or HA-D2D3 were performed. The FRET profile of αML*CFPβ2YFP (Fig. 4.7) was similar to that of αMLCFPβ2YFP (Fig. 4.6B). Thus, we reasoned that αM Leu1115 replaced by Val in αMLCFP had minimal precocious effect at least on the αMLCFPβ2YFP FRET studies performed herein.

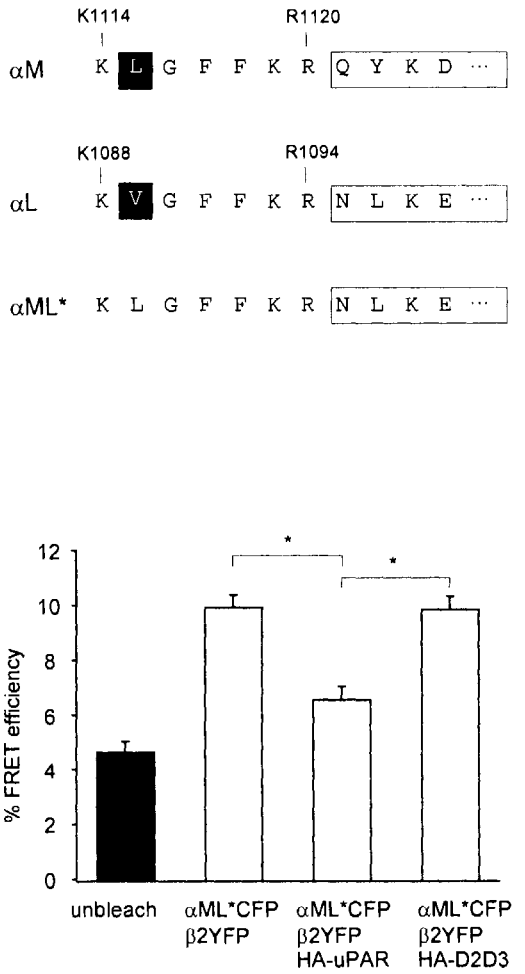

FIG 4.7 FRET analyses of K562 cells expressing αML*CFPβ2YFP with the co-expression of HA-uPAR or HA-D2D3. In αML*CFP, the cytoplasmic tail substitution of αM with that of αL was made after Arg1120. Data show mean ± SEM for 15 cells analyzed. In the schematic illustrating the membrane proximal sequences of αM and αL cytoplasmic tail, αM Leu1115 and αL Val1089 are in black boxes. Amino acid numbers according to the mature protein are shown. *, $p < 0.001$.

uPA forms a trimolecular complex with uPAR and αMβ2, and it initiates Ca^{2+} signaling in neutrophils (Cao et al. 1995). Addition of uPA to cells expressing αMLCFPβ2YFP and HA-uPAR did not show any significant FRET difference from cells without uPA albeit avid uPA binding on these cells (Fig. 4.8A) and data not shown. We went further to examine the effect of uPA on αMβ2 that is associated with HA-uPAR by the method of immunoprecipitation with the reporter mAbs MEM148 and KIM127 (Fig. 4.8B). The profile of the immunoprecipitation data was similar to that of αMβ2/HA-uPAR transfectants in the absence of uPA (Fig. 4.3C). However, we do not preclude uPA inducing further structural changes in the αMβ2 TMs and ectodomain that may not be detected using our present method of FRET analyses and immunoprecipitation assays with the reporter mAbs available to us.

Next, the expression of uPAR is low on αMβ2-expressing monocytes, but its expression can be up-regulated markedly when these cells are treated with E. coli lipopolysaccharide (LPS) or M. tuberculosis lipoarabinomannan (LAM) (Juffermans et al. 2001). In this study, the expression of uPAR is comparatively high. We asked whether reduction of uPAR expression would also exert a similar effect on the conformation of αMβ2 as shown in previous sections, but at a reduced level. To this end, we performed FRET analyses of K562 expressing αMLCFPβ2YFP and different levels of HA-uPAR (by transfecting the same amount of αMLCFPβ2YFP but different amounts of HA-uPAR). A reduction of HA-uPAR expressed was detected in cell lysates of transfectants with decreasing amount of plasmid HA-uPAR transfected

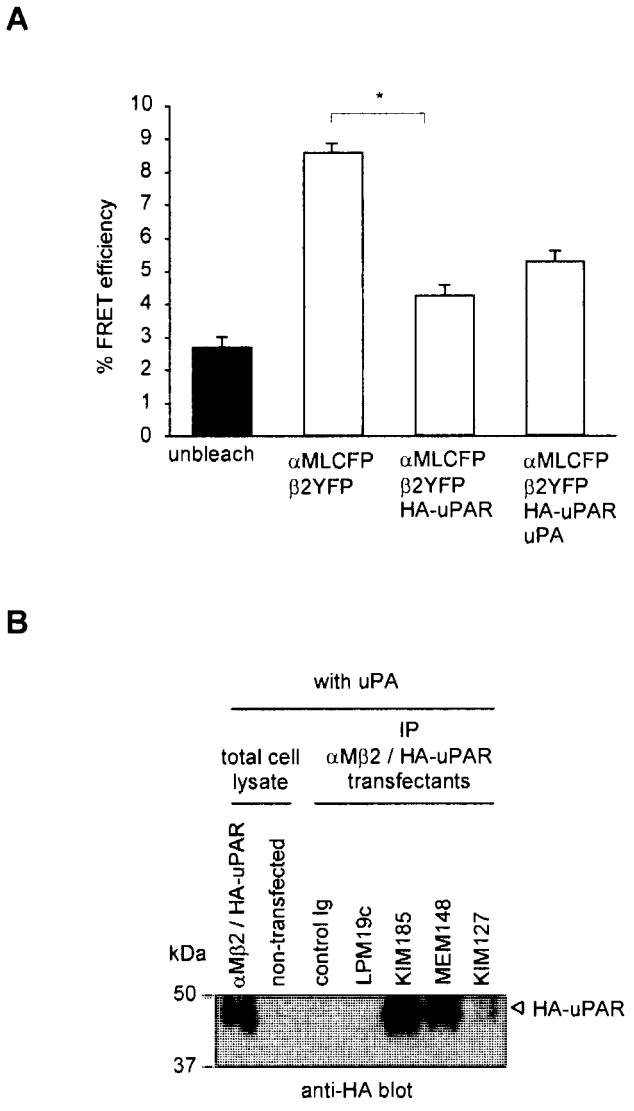

FIG 4.8 (A) FRET analyses of K562 cells expressing αMLCFPβ2YFP and HA-uPAR in the presence of uPA (100 nM). Data show mean ± SEM for 20 cells analyzed. Data are representative of two independent experiments. Student's *t* test, assuming unequal variance, was used for statistical analyses. (B) 293T transfectants expressing αMβ2 and HA-uPAR were incubated in medium containing uPA (100 nM) for 45 min at 37°C. Immunoprecipitation analyses were performed with the indicated mAbs, and HA-uPAR that co-precipitated with αMβ2 was detected by immunoblotting with anti-HA antibody. Proteins were resolved on 10% SDS-PAGE under reducing conditions. IP: immunoprecipitation. *, $p < 0.001$.

(Fig. 4.9A). An anti-actin blot was included as a control. The expressions of αMLCFPβ2YFP in these transfectants were comparable as determined by confocal microscopy analyses (data not shown). When these cells were subjected to FRET analyses, a decrease in HA-uPAR expression had a lesser effect on αMLCFPβ2YFP FRET signal (Fig. 4.9B). We extended the analyses by performing reporter mAbs immunoprecipitation of αMβ2 when co-expressed with HA-uPAR using 293T transfectants. A reduction in HA-uPAR plasmid transfected led to a decrease in HA-uPAR expression in 293T transfectants as determined by flow cytometry analyses using mAb VIM5 and immunoblotting with anti-HA antibody (Fig. 4.10A). The anti-actin control blot was included. The expressions of αMβ2 in these transfectants were comparable as determined by flow cytometry using KIM185. When immunoprecipitations using mAbs MEM148 and KIM185 were performed with αMβ2 transfectants bearing different levels of HA-uPAR, accordingly a reduction in HA-uPAR was co-precipitated from transfectants expressing reduced amounts of HA-uPAR (Fig 4.10B). The reduced level of αMβ2 conformational changes detected with a reduction in uPAR expression may be explained by a lesser number of uPAR-associated αMβ2.

4.2.3 Disulphide clasp in the αMβ2 TMs prevent their separation induced by uPAR.

To further validate the separation of the αMβ2 TMs induced by uPAR, we sought to generate disulphide clasp αMβ2 mutants. In these mutants, the extracellular

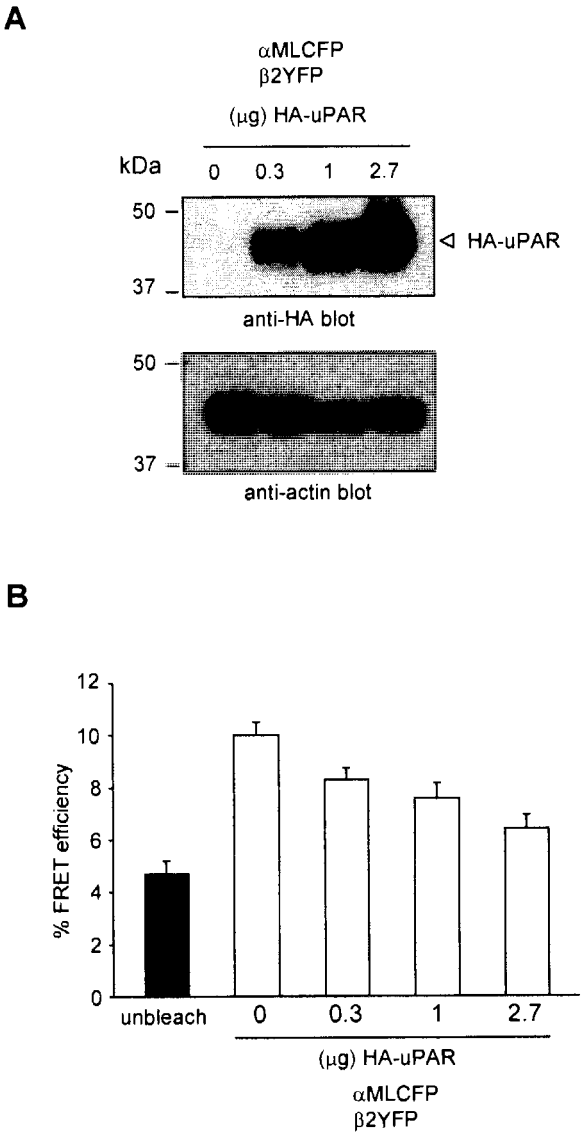

FIG 4.9 The effect of reduced uPAR expression on αMβ2 conformational changes. (A) K562 cells were transfected with the same amount of αMLCFPβ2YFP and varying amounts of HA-uPAR (0, 0.3, 1, 2.7 μg). Cell lysates were immunoblotted with anti-HA antibody to detect the expression of HA-uPAR. Protein bands were visualized by ECL. An anti-actin immunoblot was included as protein loading control. (B) K562 cells transfected with αMLCFPβ2YFP but with different levels of HA-uPAR were subjected to FRET analyses. Data show mean ± SEM for 40 cells analyzed.

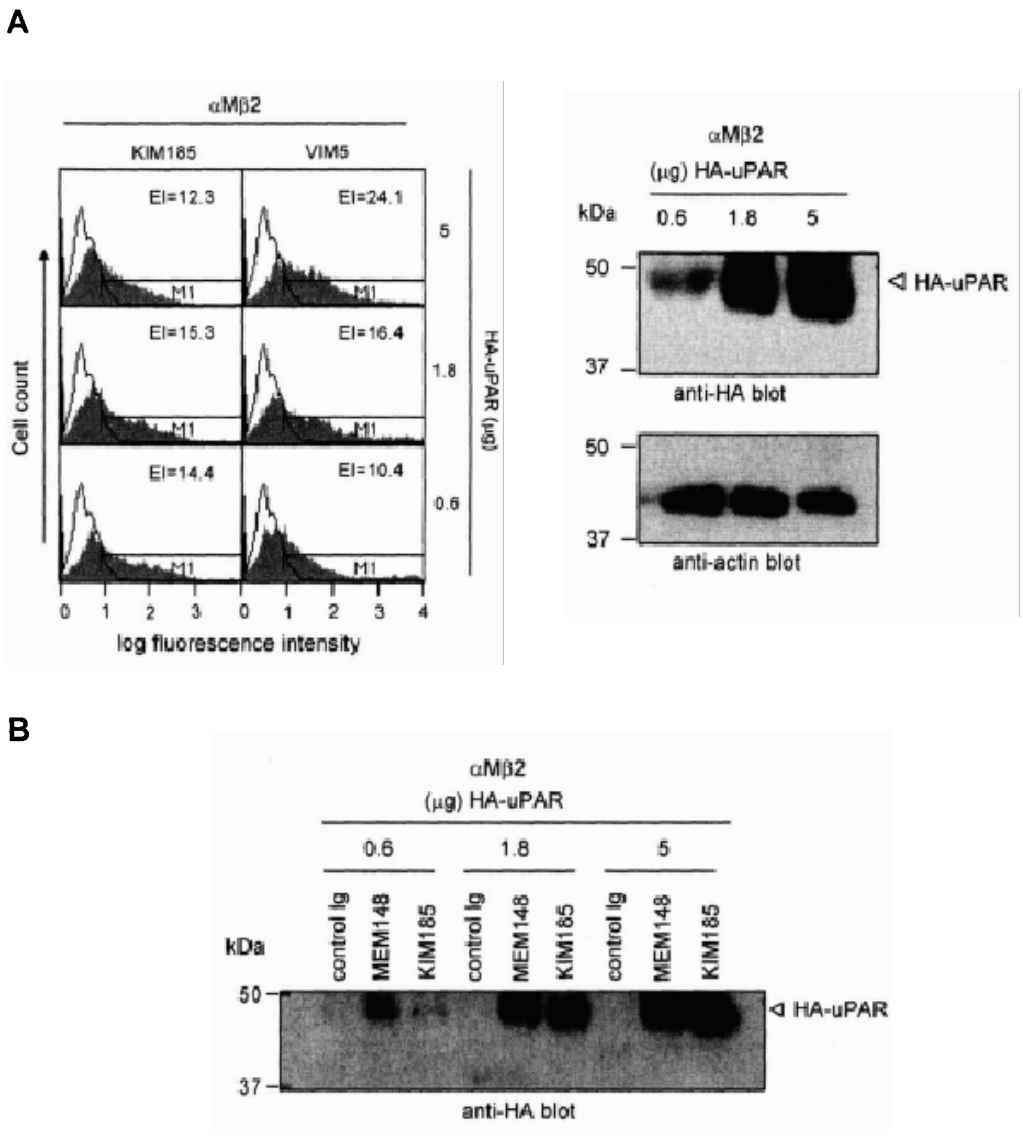

FIG 4.10 The effect of reduced uPAR expression on αMβ2 conformational changes. (A) 293T cells were transfected with the same amount of αMβ2 and varying amounts of HA-uPAR (0.6, 1.8, 5 μg). The expression levels of αMβ2 and HA-uPAR were determined by flow cytometry using mAbs KIM185 and VIM5 respectively (shaded histograms). Open histogram (irrelevant mAb). The expression index (EI) was calculated by % gated positive x geo-mean fluorescence intensity. M1 denotes region gated to be positive staining. The expressions of HA-uPAR in these transfectants were also detected by anti-HA immunoblot and ECL. The anti-actin immunoblot was included as protein loading control. (B) 293T cells expressing αMβ2 with varied levels of HA-uPAR were subjected to co-immunoprecipitation analyses with the indicated mAbs. HA-uPAR was detected by anti-HA immunoblotting and ECL. In all immunoblotting experiments above, proteins were resolved on 10% SDS-PAGE under reducing conditions.

membrane proximal residues of αMβ2 TMs were mutated singly to Cys in order to allow disulphide bond formation between permissible pairs of introduced Cys as indicated (Fig. 4.11A). Clasping of TMs by engineered disulphide bond has been shown to attenuate αIIbβ3 outside-in signaling (Luo et al. 2004; Zhu et al. 2007). Transfectants bearing the αMLCFPβ2YFP Cys mutants were surface labeled with biotin, lysed, and immunoprecipitated with the mAb IB4 that is specific to heterodimeric β2 integrins (Tang et al. 2006). Integrins precipitated were resolved on SDS-PAGE under non-reducing (-DTT) or reducing (+DTT) conditions (Fig. 4.11B). Under non-reducing conditions, high molecular weight protein bands were detected that corresponded to integrin heterodimers that were covalently-linked. Except for cysteine mutant pair that contained αMLL1091C, the αMLP1092C and αMLL1093C showed propensity to form disulphide bonded heterodimer with β2I679C, β2A680C, β2A681C, and β2I682C. Under reducing conditions, only three of these heterodimers were separated into their individual αMLCFP and β2YFP subunits. It was not clear why the others showed much lower level of individual subunits. However, one of these pairs αMLL1093C β2A680C was selected for subsequent analyses. This cysteine clasp will be referred to as c-c in subsequent discussion.

Before proceeding to test the effect of c-c clasp on the αMβ2 TMs induced by uPAR, we verified that the clasp did not alter the ligand-binding function and conformation of the αMβ2. K562 cells transfected with wild-type αMβ2 or αMβ2c-c (Fig. 4.12A) were allowed to adhere to the αMβ2 ligand fibrinogen (Fig. 4.12B). Cells expressing

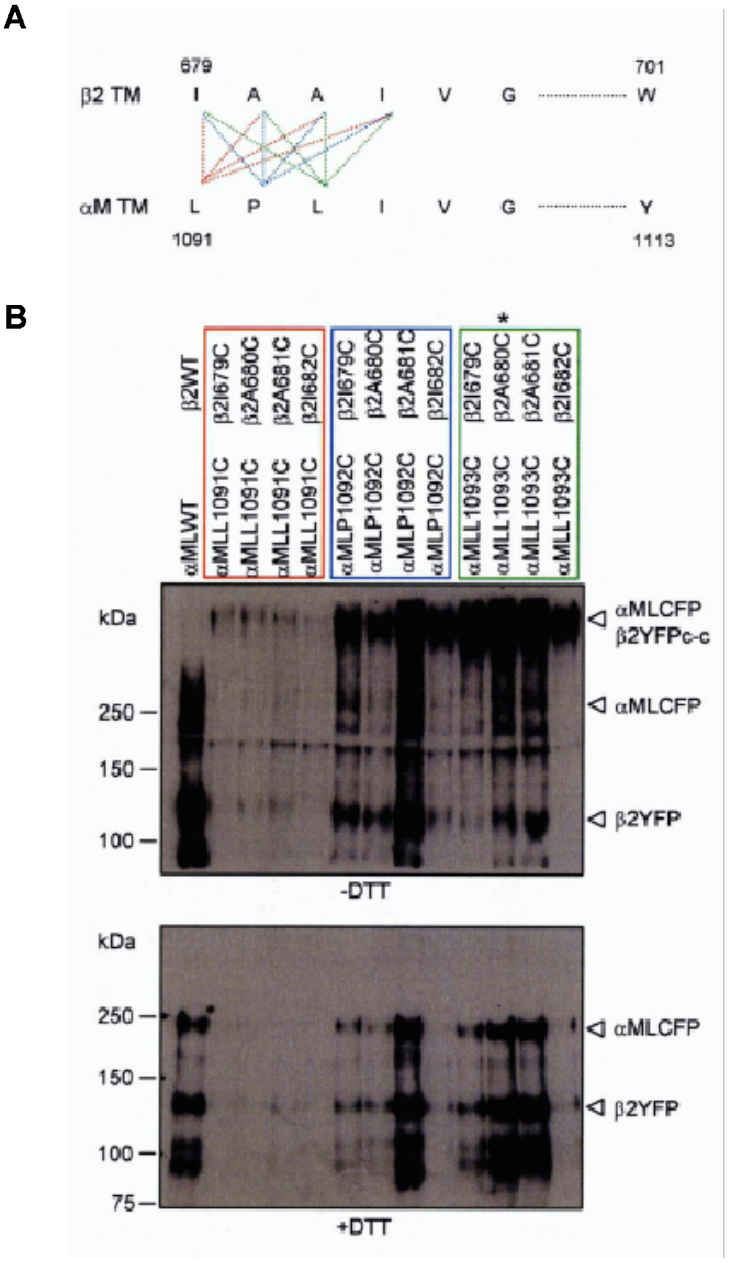

FIG 4.11 Generation of an αMβ2 with a disulphide clasp in its TM. (A) Illustration of possible disulphide bonds that can be formed between the 4 β2 and 3 αM membrane proximal TM residues when mutated to Cys. For ease of reference, amino acid numbering is shown based on the mature protein. (B) Assessing the formation of disulphide bond in integrin TM mutants. Cell surface biotinylated αMLCFP β2YFP TM mutants were immunoprecipitated with the β2 integrins heterodimer-specific mAb IB4. Proteins were resolved on a 6% SDS-PAGE gel under non-reducing conditions (-DTT) and on a 7.5% SDS-PAGE gel under reducing conditions (+DTT). Proteins were probed with streptavidin-HRP, and detected by ECL. * denotes the pair of integrin TM mutants that were used in subsequent analyses. This disulphide clasp is referred to as c-c henceforth.

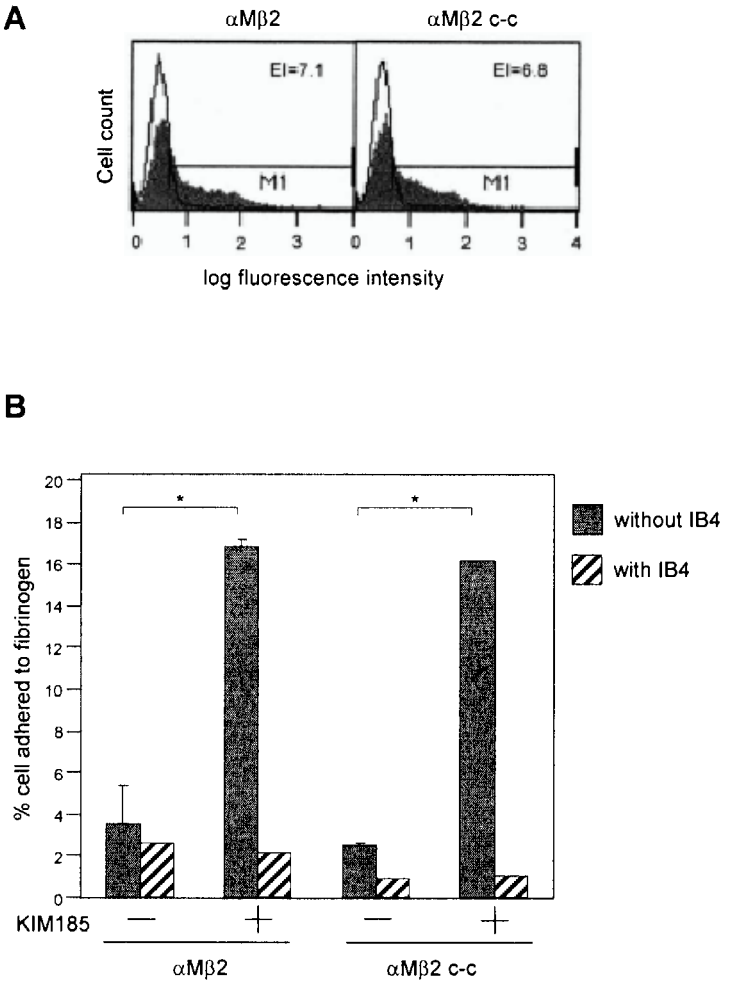

FIG 4.12 (A) Flow cytometry analyses of K562 transfectants expressing αMβ2 or αMβ2 with the disulphide clasp c-c. The mAb used was IB4 (shaded histogram). Open histogram (irrelevant mAb). The expression index (EI) was calculated by % gated positive x geo-mean fluorescence intensity. M1 denotes region gated to be positive staining. (B) K562 transfectants were examined for their adhesive properties to fibrinogen. For activation of αMβ2, the activating mAb KIM185 was used. Cell adhesion specificity was demonstrated using mAb IB4, which is also a function-blocking mAb. Triplicate determination (mean ± SD) representative of two separate experiments is shown. *, $p < 0.05$.

αMβ2c-c showed a similar adhesion profile to cells expressing wild-type αMβ2 with minimal adhesion to fibrinogen in the absence of activation, and high level of adhesion was detected when the β2 activating mAb KIM185 was included. Adhesion specificity was demonstrated with the heterodimeric-specific and function-blocking mAb IB4. Thus, the c-c clasp did not affect the cell surface expression and the ligand-binding function of the αMβ2 ectodomain.

Next, we analyzed the ectodomain conformation of the αMβ2c-c co-expressed with HA-uPAR (Fig. 4.13A). The profile of HA-uPAR co-precipitating with αMβ2c-c was similar to that with wild-type αMβ2 (Fig. 4.3C). αMβ2c-c interacting with HA-uPAR most possibly retained a bent conformation because KIM127 failed to co-precipitate HA-uPAR, and it adopted an open headpiece conformation because it showed reactivity with MEM148. Thus, the introduction of the c-c clasp had also no apparent effect on the ectodomain conformation of αMβ2 interacting with HA-uPAR. We then examined whether c-c clasp prevents re-orientation of the αMβ2 TMs induced by HA-uPAR (Fig. 4.13B). K562 transfectants expressing the indicated constructs were subjected to FRET analyses. Cells expressing αMLCFPβ2YFP showed a significant reduction in FRET efficiency in the presence of HA-uPAR co-expression. Cells expressing αMLCFPβ2YFP with c-c clasp showed comparable FRET to those without the clasp. However, co-expressing HA-uPAR with αMLCFPβ2YFP c-c clasp did not show significant reduction in FRET signal. This was not attributed to poor interaction of HA-uPAR with the c-c clasp integrin because HA-uPAR was co-precipitated

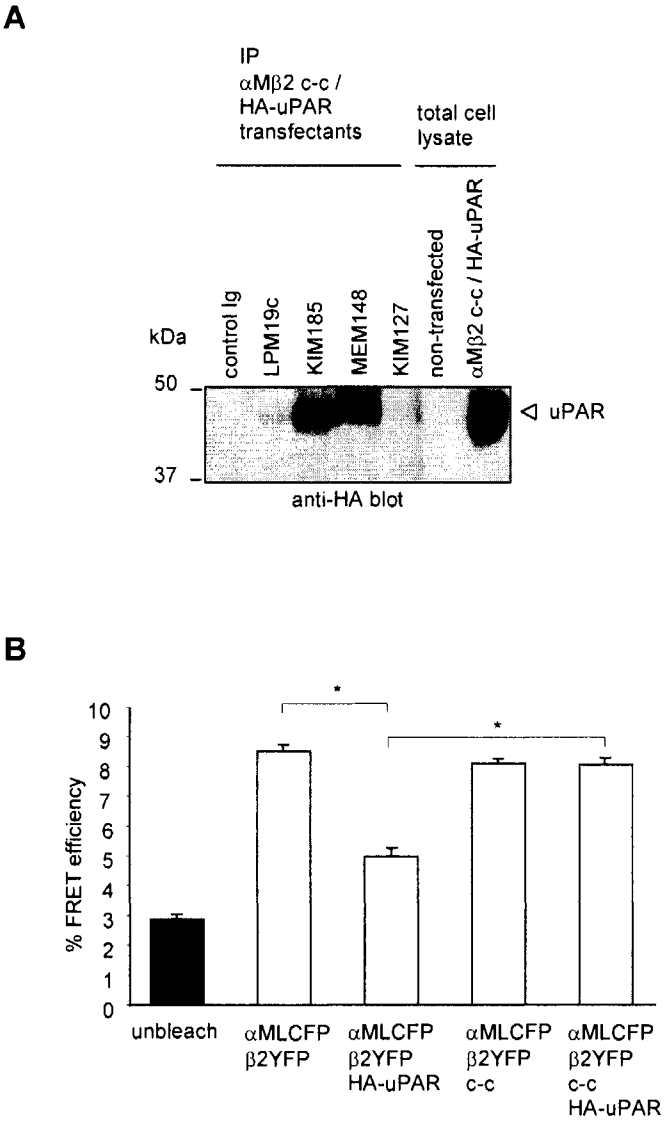

FIG 4.13 The disulphide clasp prevented re-orientation or separation of the αMβ2 TMs but did not attenuate the conformational changes in the αMβ2 ectodomain induced by uPAR. (A) The ectodomain conformation of the αMβ2c-c interacting with HA-uPAR was analyzed by co-immunoprecipitation analyses. Cell lysate of transfectants were immunoprecipitated with the mAbs indicated, and HA-uPAR detected by immunoblotting with anti-HA antibody. Proteins were resolved on a 10% SDS-PAGE gel under reducing conditions. IP: immunoprecipitation. (B) FRET analyses of transfectants co-expressing the indicated integrins with or without the disulphide clasp (c-c), and with or without HA-uPAR. Data are representative of three independent experiments. Data show mean ± SEM for 20 cells. Student's *t* test, assuming unequal variance, was used for statistical analyses. *, $p < 0.001$.

effectively with the integrins by KIM185 and MEM148 aforementioned (Fig. 4.13A). Taken together, these data suggest that the TM c-c clasp prevents the separation or re-orientation of the αMβ2 TMs induced by HA-uPAR, lending further support that uPAR interacting with αMβ2 not only induces the opening of the αMβ2 headpiece, the 'activation' signal is propagated to the C-terminal halve of the αMβ2 that leads to the re-orientation of the TMs.

4.3 Discussion

The integrin αMβ2 is a primary receptor that promotes the adhesion and migration of PMNs and mononuclear phagocytes (Ehlers 2000). The activity of αMβ2 that is conformational dependent is regulated at several levels. Extracellular divalent cation Mn^{2+} stimulates adhesion of monocytes to endothelial cells mediated by αMβ2, and enhances αMβ2 ligand-binding (Altieri 1991). From the intracellular compartment, the large cytoskeletal network protein talin, interacts with the β2 cytoplasmic tail to regulate αMβ2-mediated phagocytosis in mouse macrophage line (Lim et al. 2007). On the plasma membrane, αMβ2 interacts with FcγRIIIB, FcγRIIA, LDL-receptor, and uPAR (Annenkov et al. 1996; Bohuslav et al. 1995; Spijkers et al. 2005; Zhou et al. 1993). uPAR is well reported to form a functional complex with αMβ2 in fibrinolysis, and it modulates the activity of αMβ2 (Pluskota et al. 2004; Pluskota et al. 2003; Simon et al. 1996; Simon et al. 2000; Tang et al. 2006; Zhang et al. 2003). uPAR deficient mice also showed impaired αMβ2-mediated recruitment of

neutrophils in response to infections (Gyetko et al. 2004; Gyetko et al. 2000). However, it is not well characterized how interaction with uPAR affects the conformation of the αMβ2.

Our data suggest that interaction of uPAR with αMβ2 changes the conformation of the integrin headpiece, from a closed to an open conformation. A displaced β2 hybrid domain was detected using the reporter mAb MEM148. Indeed, our observation is in line with a study made on uPAR and integrin α5β1 that showed conformational changes in the integrin using two reporter mAbs HUTS-21 and 9EG7 (Wei et al. 2005). It was observed that suppressing expression of uPAR by siRNA in human fibrosarcoma and breast cancer cell lines enhanced the epitope expressions of HUTS-21 and 9EG7, which recognize ligand-induced epitopes in β1 subunit (Wei et al. 2005). Thus, it was inferred that uPAR directly affects the conformation of its partner α5β1. Interestingly, the epitope of HUTS-21 lies in the region spanning residues 355-425 of the β1 subunit that is in the hybrid domain (Luque et al. 1996). The epitope of 9EG7 lies in region 495-602 of the β1 IEGF-2, 3, and 4 (Bazzoni et al. 1995). Together, these data suggest that conformational changes are transmitted from the headpiece of an integrin involving hybrid domain movement to the C-terminal halve of the integrin ectodomain when it interacts with uPAR.

A key feature of uPAR interaction with an integrin is the overall bent conformation of the integrin because both molecules are juxtaposed on the same membrane, and the

interaction sites on both molecules disfavor association of uPAR with an extended integrin as discussed under Background. Indeed, we were unable to detect extended αMβ2 interacting with uPAR using the reporter mAb KIM127 although association of uPAR with αMβ2 was verified using KIM185. However, uPAR induces displacement of the αMβ2 hybrid domain, which may be reminiscent to that of a ligand-bound α5β1 (Takagi et al. 2003) and αIIbβ3 (Xiao et al. 2004). Thus, uPAR may be considered as an in-cis ligand of αMβ2.

An interesting observation made in this study is the movement of the αMβ2 TMs when it is associated with uPAR. This is inferred from the FRET analyses of αMβ2 with FRET pair fluorophore fused to the cytoplasmic tails, which report movement of the TMs. We were unable to detect significant FRET in αMβ2 with its native cytoplasmic tails, hence we have made substitution of αM cytoplasmic tail with that of αL, which was successful in the FRET system we employed previously (Vararattanavech et al. 2008). We acknowledge that there can be a limitation in the use of αL cytoplasmic tail in an αM construct to report αMβ2 conformational changes; however, we reasoned that this approach is still relevant and useful in demonstrating TM separation of αMβ2. The re-orientation of TMs in αMβ2 interacting with uPAR is further verified by clasping the TMs with a disulphide bond. This also eliminates the possibility of uPAR directly inducing spatial changes in the integrin cytoplasmic tails via other factors, which would complicate the readout and the interpretation of the data with regards to TM movement. The separation of the integrin TMs is important

for outside-in signaling as shown directly in αIIbβ3 (Zhu et al. 2007). Thus, our data suggest that uPAR changes the ectodomain conformation of its partner integrin, which is sufficient to trigger movement of the integrin TMs as illustrated in the model (Fig. 4.14). However, we should be cautious with the interpretation because the re-orientation of the TMs or their complete separation when an integrin is activated remains to be fully characterized by structural studies. Nonetheless, the movement of the integrin TMs induced by uPAR can be one of the mechanisms by which uPAR trigger integrin-mediated cytosolic signaling. Other mechanisms may involved dimerization of uPAR and its potential to partition into membrane rafts (Cunningham et al. 2003).

Our data and that of others (Wei et al. 2005) suggest that uPAR induces shape changes in its integrin partner that retains an overall bent conformation. Although integrin extension is one of the hallmarks of integrin activation, there are also reports of activated bent integrins (Adair et al. 2005; Arnaout et al. 2007; Chigaev et al. 2001; Larson et al. 2005; Luo et al. 2007; Nishida et al. 2006). A model was proposed for non-I domain containing integrins in which engagement of a bent integrin with its ligand induces certain degree of unbending, and in I domain containing integrins, the swing-out of the hybrid domain is an event of outside-in signaling in the deadbolt model of activation (Arnaout et al. 2007). Thus, it will be interesting to obtain structural data of an uPAR-integrin complex in future work to obtain direct measurements of these conformational changes. These will add to the ensemble of

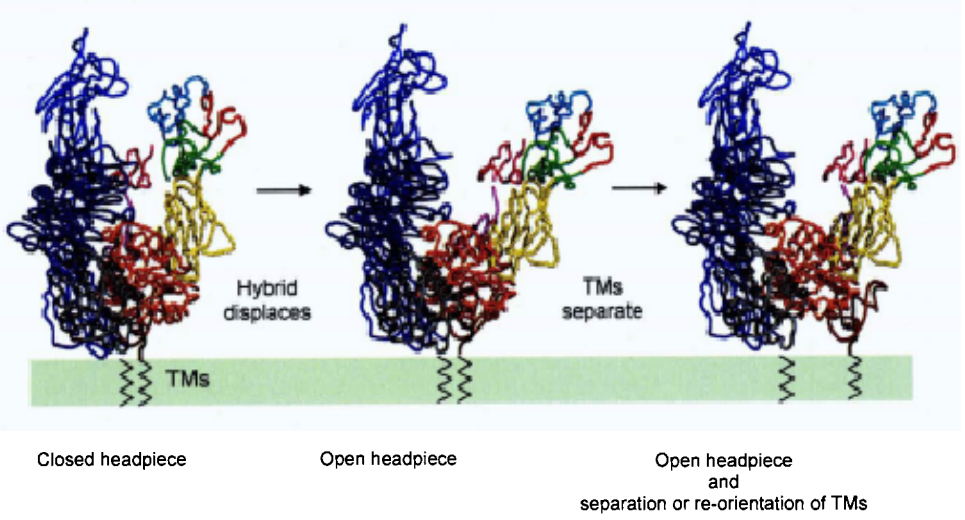

FIG 4.14 Hypothetical model of αMβ2 conformational changes induced by uPAR. *In-cis* interaction of αMβ2 with uPAR induces hybrid domain movement in an overall bent conformer, subsequently triggering the re-orientation or separation of the TMs.

conformations adopted by the integrins under different physiological conditions that are required for fine-regulating integrin-mediated biological processes.

Chapter Five: Discussion

Integrin αMβ2, one of the β2 integrins, is expressed mainly in leukocytes of the myeloid lineage. It binds to a broad spectrum of ligands and contributes toward leukocyte adhesion, migration, and phagocytosis (Ehlers 2000). Interestingly, a number of membrane proteins are reported to associate with αMβ2. These are the FcγRIIIB (Zhou et al. 1993), FcγRIIA (Annenkov et al. 1996), LDL-receptor (Spijkers et al. 2005), and uPAR (Bohuslav et al. 1995). Lateral association of membrane proteins expands the functional diversity of membrane receptors. uPAR, a GPI-anchored membrane protein lacking TM and cytoplasmic domain, is well reported to interact with integrins. Two major functional consequences of this interaction are the modulation of the integrin ligand-binding property and the trigger of uPAR-mediated cytosolic signaling via the integrin partner. To date, the molecular mechanisms underlying these effects remain to be fully characterized.

In the first part of this study, we showed that transfectants bearing αMβ2 and uPAR adhered less effectively than those expressing αMβ2 alone to ligands BSA, fibrinogen, and ICAM-1. This was in line with the disrupted fibrinogen binding by αMβ2 in the presence of uPAR reported previously. We further verified the down-regulating effect of uPAR on αMβ2 ligand-binding function using an αMβ2 that was made constitutively active (αMβ2BN7). uPAR markedly reduced the ligand-binding property of this active αMβ2 mutant. uPAR is comprised of three domains, with the

C-terminus domain 3 containing the GPI-anchoring site. We showed that domain 1 of uPAR (D1) is a critical domain involved in uPAR interaction with αMβ2 because a D1-deleted uPAR mutant (D2D3) failed to associate with αMβ2, and conceivably had no effect on αMβ2 ligand-binding.

An apparent conflicting observation to ours and that of Simon et al. is the report by Zhang et al. that showed enhanced αMβ2 ligand-binding activity in the presence of uPAR. Cell type difference is ruled out for the disparity because in all three studies HEK-293 cells were used. Nonetheless, we sought to explain the negative effect of uPAR on αMβ2 ligand-binding by performing a series of immunoprecipitation analyses using antibodies to αMβ2 available to us. Aforementioned in Chapter 3, mAbs with epitopes residing in the I and I-like domains of the αMβ2 failed to precipitate αMβ2 in association with uPAR. This could explain the poor ligand-binding of αMβ2 in association with uPAR, in which uPAR shielded the αMβ2 ligand-binding site. In fact most of the αM-recognizing mAbs but not the β2-recognizing mAbs we have tested failed to precipitate αMβ2 with uPAR, suggesting that an extensive surface of the αM subunit is shielded by its association with uPAR and that the orientation of uPAR may be tilted more towards to the αM subunit rather than the β2 subunit. The extensive N-linked glycosylations of uPAR may also contribute in part to this effect. It is also possible that interaction of αMβ2 with uPAR changes the conformation of the αM subunit such that its reactivity with conformational sensitive mAbs is attenuated. Our data also corroborate well with the

identification of a critical sequence (M25) within the W4 of the αM β-propeller found to be important for uPAR interaction (Simon et al. 2000).

The second part of my study investigated a potential mechanism by which uPAR triggers cytosolic signaling via the integrin αMβ2. Because the heights of the uPAR and an extended αMβ2 or integrin in general are markedly different, it is unlikely that uPAR interacts with a highly extended αMβ2. It was proposed that integrin α5β1 adopts a modified bent conformation when it associates with uPAR (Wei et al. 2005). The same study also reports shape changes in the headpiece of the integrin α5β1 interacting with uPAR, but it is not clear how 'activation' signal is propagated into the cell's interior. Here, we showed that uPAR induces headpiece opening of the αMβ2 based on reporter mAb immunoprecipitation analyses. Importantly, we have demonstrated for the first time that this conformational change is propagated to the C-terminal half of the αMβ2 and leads to the separation or re-orientation of its TMs by FRET analyses. This could explain how uPAR triggers cytosolic signaling via its integrin partner because the separation of the integrin TMs is a critical event in integrin outside-in signaling. However, we should be cautious with the interpretation because the re-orientation of the TMs or their complete separation when an integrin is activated remains to be fully characterized by structural studies (Rocco et al. 2008).

Our present findings add to the ensemble of integrin conformations with modulated functions reported to date. Although integrin extension is widely recognized as a

hallmark of integrin activation, there is gathering evidence of integrins functioning as bent conformers. A recent model of ligand-binding by bent integrins proposed that ligand engagement induces hybrid domain displacement in the bent integrin, which may lead to downstream cytoplasmic signaling events (Arnaout et al. 2007). Thus, uPAR can be considered as an in-cis ligand of αMβ2, which apparently does not require αMβ2 activation. Rather the association of uPAR with a bent αMβ2 elicits downstream signaling via conformational changes in αMβ2. We rationalized that structural studies are required to fully "visualize" the mode of interaction between uPAR and αMβ2 in the future. However, this approach could be challenging because we were unable to obtain HEK-293 stable cell line that expresses high level of soluble αMβ2 (data not known). This may impede the investigation that requires co-crystallization of soluble αMβ2 with purified uPAR.

This study also highlights the difference in function between an I domain-containing integrin (αMβ2) and an integrin without I domain (α5β1) in association with uPAR. uPAR induces conformational changes in the headpiece of α5β1 such that the ligand-binding property of α5β1 is modulated from an RGD-dependent to RGD-independent mode of binding to its ligand fibronectin (Wei et al. 2005). However, in αMβ2 the ligand-binding property is negatively regulated when it interacts with uPAR. How does this reconcile with the widely reported role of uPAR in promoting cellular processes such as migration and invasion (Bohuslav et al. 1995; Gyetko et al. 1994; May et al. 1998). In these processes, the initial adhesion events are only part of the

machinery in effective cell locomotion. Downstream signaling events such as receptor clustering, cytoskeletal re-modeling, and the release of attachment sites at the rear of the cell are essential. It was proposed that uPAR association with αMβ2 may be a mechanism to enrich and localize integrin clusters and relevant signaling molecules at the expense of decreasing the number of total adhesion site available (Simon et al. 2000). On cell surface, there may exist two populations of αMβ2, the uPAR associated αMβ2, whose conformation change might be a pre-requisite for its cytosolic signaling such as recruitment of signaling molecules, and the free αMβ2 that can be activated to bind ligands (Fig. 5.1). The Src family kinases (SFKs) are important for integrin downstream signaling (Shattil 2005) and for uPAR-mediated cell motility (Trigwell et al. 2000). It was reported that uPAR, β2 integrins, and Hck, one member of Src kinases, were joint components within a single receptor complex of human monocytes by isolation of the monocyte uPAR using its ligand uPAR (Bohuslav et al. 1995). Involvement of these kinases in uPAR signaling is supported by induction of tyrosine phosphorylation upon stimulation of monocytes with uPA, independent of its enzymatic activity (Bohuslav et al. 1995). Thus future investigations of the functional cooperativity of uPAR, αMβ2 and Hck are of particular interest. Other mechanisms of integrin-mediated cytosolic signaling triggered by uPAR may involve dimerization of uPAR and its potential to partition into membrane rafts (Cunningham et al. 2003; Sidenius et al. 2002). The dimerization was reported to be an intrinsic property of soluble uPAR and cell surface uPAR, and

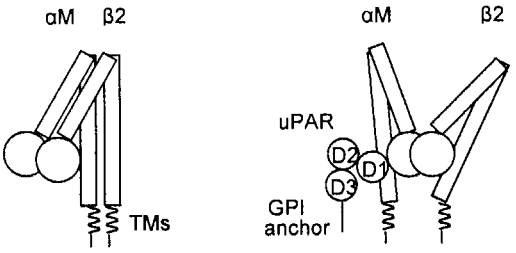

FIG 5.1 Schematic cartoon for the two populations of αMβ2 on cell surface. There may exist two populations of αMβ2 on cell surface, the uPAR associated αMβ2 with modified conformation and free αMβ2 that can be activated to bind ligands.

that it plays a key role in uPAR interaction with vitronectin (Cunningham et al. 2003; Sidenius et al. 2002). It was also demonstrated that the cell surface dimeric uPAR partitions preferentially to detergent-resistant lipid rafts (Cunningham et al. 2003). Thus, it will be interesting to determine whether the dimerization of uPAR and its capacity to partition into lipid rafts could also influence its association with αMβ2.

Finally, this study provides a valuable insight into the mechanism of αMβ2 interaction with uPAR. The larger implication of this study is the possibility of other integrin membrane associated molecules using a similar mechanism to prime or synergize cytosolic signaling cascades with integrins having an overall bent conformation.

References

Adair BD, Xiong JP, Maddock C et al. Three-dimensional EM structure of the ectodomain of integrin {alpha}V{beta}3 in a complex with fibronectin. J Cell Biol 2005; 168 (7):1109-18.

Adair BD, Yeager M. Three-dimensional model of the human platelet integrin alpha IIbbeta 3 based on electron cryomicroscopy and x-ray crystallography. Proc Natl Acad Sci U S A 2002; 99 (22):14059-64.

Aguirre Ghiso JA, Kovalski K, Ossowski L. Tumor dormancy induced by downregulation of urokinase receptor in human carcinoma involves integrin and MAPK signaling. J Cell Biol 1999; 147 (1):89-104.

Altieri DC. Occupancy of CD11b/CD18 (Mac-1) divalent ion binding site(s) induces leukocyte adhesion. J Immunol 1991; 147 (6):1891-8.

Altieri DC, Bader R, Mannucci PM et al. Oligospecificity of the cellular adhesion receptor Mac-1 encompasses an inducible recognition specificity for fibrinogen. J Cell Biol 1988a; 107 (5):1893-900.

Altieri DC, Edgington TS. The saturable high affinity association of factor X to ADP-stimulated monocytes defines a novel function of the Mac-1 receptor. J Biol Chem 1988b; 263 (15):7007-15.

Altieri DC, Morrissey JH, Edgington TS. Adhesive receptor Mac-1 coordinates the activation of factor X on stimulated cells of monocytic and myeloid differentiation: an alternative initiation of the coagulation protease cascade. Proc Natl Acad Sci U S A 1988c; 85 (20):7462-6.

Andrew D, Shock A, Ball E et al. KIM185, a monoclonal antibody to CD18 which induces a change in the conformation of CD18 and promotes both LFA-1- and CR3-dependent adhesion. Eur J Immunol 1993; 23 (9):2217-22.

Annenkov A, Ortlepp S, Hogg N. The beta 2 integrin Mac-1 but not p150,95 associates with Fc gamma RIIA. Eur J Immunol 1996; 26 (1):207-12.

Arias-Salgado EG, Lizano S, Sarkar S et al. Src kinase activation by direct interaction with the integrin beta cytoplasmic domain. Proc Natl Acad Sci U S A 2003; 100 (23):13298-302.

Armulik A, Nilsson I, von Heijne G et al. Determination of the border between the transmembrane and cytoplasmic domains of human integrin subunits. J Biol Chem 1999; 274 (52):37030-4.

Arnaout MA. Leukocyte adhesion molecules deficiency: its structural basis, pathophysiology and implications for modulating the inflammatory response. Immunol Rev 1990a; 114:145-80.

Arnaout MA. Structure and function of the leukocyte adhesion molecules CD11/CD18. Blood 1990b; 75 (5):1037-50.

Arnaout MA, Dana N, Melamed J et al. Low ionic strength or chemical cross-linking of monomeric C3b increases its binding affinity to the human complement C3b receptor. Immunology 1983; 48 (2):229-37.

Arnaout MA, Goodman SL, Xiong JP. Structure and mechanics of integrin-based cell adhesion. Curr Opin Cell Biol 2007; 19 (5):495-507.

Arnaout MA, Mahalingam B, Xiong JP. Integrin structure, allostery, and bidirectional signaling. Annu Rev Cell Dev Biol 2005; 21:381-410.

Bailly P, Tontti E, Hermand P et al. The red cell LW blood group protein is an intercellular adhesion molecule which binds to CD11/CD18 leukocyte integrins. Eur J Immunol 1995; 25 (12):3316-20.

Bainton DF, Miller LJ, Kishimoto TK et al. Leukocyte adhesion receptors are stored in peroxidase-negative granules of human neutrophils. J Exp Med 1987; 166 (6):1641-53.

Bajt ML, Goodman T, McGuire SL. Beta 2 (CD18) mutations abolish ligand recognition by I domain integrins LFA-1 (alpha L beta 2, CD11a/CD18) and MAC-1 (alpha M beta 2, CD11b/CD18). J Biol Chem 1995; 270 (1):94-8.

Baldwin ET, Sarver RW, Bryant GL, Jr. et al. Cation binding to the integrin CD11b I domain and activation model assessment. Structure 1998; 6 (7):923-35.

Barazzone C, Belin D, Piguet PF et al. Plasminogen activator inhibitor-1 in acute hyperoxic mouse lung injury. J Clin Invest 1996; 98 (12):2666-73.

Barclay A. N. BMH, Law S. K., McKnight A. J., Tomlinson M. G., van der Merwe P. A. The leucocyte antigen facts book. Second ed. London, UK: Academic press; 1997.

Barclay AN, Brown MH. Heterogeneity of interactions mediated by membrane glycoproteins of lymphocytes. Biochem Soc Trans 1997; 25 (1):224-8.

Barinka C, Parry G, Callahan J et al. Structural basis of interaction between urokinase-type plasminogen activator and its receptor. J Mol Biol 2006; 363 (2):482-95.

Bazzoni G, Shih DT, Buck CA et al. Monoclonal antibody 9EG7 defines a novel beta 1 integrin epitope induced by soluble ligand and manganese, but inhibited by calcium. J Biol Chem 1995; 270 (43):25570-7.

Beglova N, Blacklow SC, Takagi J et al. Cysteine-rich module structure reveals a fulcrum for integrin rearrangement upon activation. Nat Struct Biol 2002; 9 (4):282-7.

Beller DI, Springer TA, Schreiber RD. Anti-Mac-1 selectively inhibits the mouse and human type three complement receptor. J Exp Med 1982; 156 (4):1000-9.

Bianchi E, Ferrero E, Fazioli F et al. Integrin-dependent induction of functional urokinase receptors in primary T lymphocytes. J Clin Invest 1996; 98 (5):1133-41.

Blasi F. The urokinase receptor. A cell surface, regulated chemokine. Apmis 1999; 107 (1):96-101.

Blasi F, Carmeliet P. uPAR: a versatile signalling orchestrator. Nat Rev Mol Cell Biol 2002; 3 (12):932-43.

Blois S, Tometten M, Kandil J et al. Intercellular adhesion molecule-1/LFA-1 cross talk is a proximate mediator capable of disrupting immune integration and tolerance mechanism at the feto-maternal interface in murine pregnancies. J Immunol 2005; 174 (4):1820-9.

Bohnsack JF, Akiyama SK, Damsky CH et al. Human neutrophil adherence to laminin in vitro. Evidence for a distinct neutrophil integrin receptor for laminin. J Exp Med 1990; 171 (4):1221-37.

Bohuslav J, Horejsi V, Hansmann C et al. Urokinase plasminogen activator receptor, beta 2-integrins, and Src-kinases within a single receptor complex of human monocytes. J Exp Med 1995; 181 (4):1381-90.

Bork P, Doerks T, Springer TA et al. Domains in plexins: links to integrins and transcription factors. Trends Biochem Sci 1999; 24 (7):261-3.

Calderwood DA, Fujioka Y, de Pereda JM et al. Integrin beta cytoplasmic domain interactions with phosphotyrosine-binding domains: a structural prototype for diversity in integrin signaling. Proc Natl Acad Sci U S A 2003; 100 (5):2272-7.

Calderwood DA, Huttenlocher A, Kiosses WB et al. Increased filamin binding to beta-integrin cytoplasmic domains inhibits cell migration. Nat Cell Biol 2001; 3 (12):1060-8.

Campbell ID. The modular architecture of leukocyte cell-surface receptors. Immunol Rev 1998; 163:11-8.

Cao C, Lawrence DA, Li Y et al. Endocytic receptor LRP together with tPA and PAI-1 coordinates Mac-1-dependent macrophage migration. Embo J 2006; 25 (9):1860-70.

Cao D, Mizukami IF, Garni-Wagner BA et al. Human urokinase-type plasminogen activator primes neutrophils for superoxide anion release. Possible roles of complement receptor type 3 and calcium. J Immunol 1995; 154 (4):1817-29.

Carman CV, Springer TA. Integrin avidity regulation: are changes in affinity and conformation underemphasized? Curr Opin Cell Biol 2003; 15 (5):547-56.

Chen WJ, Goldstein JL, Brown MS. NPXY, a sequence often found in cytoplasmic tails, is required for coated pit-mediated internalization of the low density lipoprotein receptor. J Biol Chem 1990; 265 (6):3116-23.

Chen YP, O'Toole TE, Shipley T et al. "Inside-out" signal transduction inhibited by isolated integrin cytoplasmic domains. J Biol Chem 1994; 269 (28):18307-10.

Cheng M, Foo SY, Shi ML et al. Mutation of a conserved asparagine in the I-like domain promotes constitutively active integrins αLβ2 and αIIbβ3. J Biol Chem 2007; 282:18225-32.

Chigaev A, Blenc AM, Braaten JV et al. Real time analysis of the affinity regulation of alpha 4-integrin. The physiologically activated receptor is intermediate in affinity between resting and Mn(2+) or antibody activation. J Biol Chem 2001; 276 (52):48670-8.

Clark EA, Brugge JS. Integrins and signal transduction pathways: the road taken. Science 1995; 268 (5208):233-9.

Colombatti A, Bonaldo P. The superfamily of proteins with von Willebrand factor type A-like domains: one theme common to components of extracellular matrix, hemostasis, cellular adhesion, and defense mechanisms. Blood 1991; 77 (11):2305-15.

Constantin G, Majeed M, Giagulli C et al. Chemokines trigger immediate beta2 integrin affinity and mobility changes: differential regulation and roles in lymphocyte arrest under flow. Immunity 2000; 13 (6):759-69.

Crowley CW, Cohen RL, Lucas BK et al. Prevention of metastasis by inhibition of the urokinase receptor. Proc Natl Acad Sci U S A 1993; 90 (11):5021-5.

Cunningham O, Andolfo A, Santovito ML et al. Dimerization controls the lipid raft partitioning of uPAR/CD87 and regulates its biological functions. Embo J 2003; 22 (22):5994-6003.

D'Souza SE, Ginsberg MH, Plow EF. Arginyl-glycyl-aspartic acid (RGD): a cell adhesion motif. Trends Biochem Sci 1991; 16 (7):246-50.

Davignon D, Martz E, Reynolds T et al. Lymphocyte function-associated antigen 1 (LFA-1): a surface antigen distinct from Lyt-2,3 that participates in T lymphocyte-mediated killing. Proc Natl Acad Sci U S A 1981; 78 (7):4535-9.

Davis GE. The Mac-1 and p150,95 beta 2 integrins bind denatured proteins to mediate leukocyte cell-substrate adhesion. Exp Cell Res 1992; 200 (2):242-52.

de Fougerolles AR, Diamond MS, Springer TA. Heterogenous glycosylation of ICAM-3 and lack of interaction with Mac-1 and p150,95. Eur J Immunol 1995; 25 (4):1008-12.

de Fougerolles AR, Klickstein LB, Springer TA. Cloning and expression of intercellular adhesion molecule 3 reveals strong homology to other immunoglobulin family counter-receptors for lymphocyte function-associated antigen 1. J Exp Med 1993; 177 (4):1187-92.

de Fougerolles AR, Springer TA. Intercellular adhesion molecule 3, a third adhesion counter-receptor for lymphocyte function-associated molecule 1 on resting lymphocytes. J Exp Med 1992; 175 (1):185-90.

Degryse B, Orlando S, Resnati M et al. Urokinase/urokinase receptor and vitronectin/alpha(v)beta(3) integrin induce chemotaxis and cytoskeleton reorganization through different signaling pathways. Oncogene 2001; 20 (16):2032-43.

Degryse B, Resnati M, Czekay RP et al. Domain 2 of the urokinase receptor contains an integrin-interacting epitope with intrinsic signaling activity: generation of a new integrin inhibitor. J Biol Chem 2005; 280 (26):24792-803.

Dewerchin M, Nuffelen AV, Wallays G et al. Generation and characterization of urokinase receptor-deficient mice. J Clin Invest 1996; 97 (3):870-8.

Diamond MS, Garcia-Aguilar J, Bickford JK et al. The I domain is a major recognition site on the leukocyte integrin Mac-1 (CD11b/CD18) for four distinct adhesion ligands. J Cell Biol 1993; 120 (4):1031-43.

Diamond MS, Staunton DE, de Fougerolles AR et al. ICAM-1 (CD54): a counter-receptor for Mac-1 (CD11b/CD18). J Cell Biol 1990; 111 (6 Pt 2):3129-39.

Diamond MS, Staunton DE, Marlin SD et al. Binding of the integrin Mac-1 (CD11b/CD18) to the third immunoglobulin-like domain of ICAM-1 (CD54) and its regulation by glycosylation. Cell 1991; 65 (6):961-71.

Douglass WA, Hyland RH, Buckley CD et al. The role of the cysteine-rich region of the beta2 integrin subunit in the leukocyte function-associated antigen-1 (LFA-1, alphaLbeta2, CD11a/CD18) heterodimer formation and ligand binding. FEBS Lett 1998; 440 (3):414-8.

Dransfield I, Cabanas C, Craig A et al. Divalent cation regulation of the function of the leukocyte integrin LFA-1. J Cell Biol 1992; 116 (1):219-26.

Ehlers MR. CR3: a general purpose adhesion-recognition receptor essential for innate immunity. Microbes Infect 2000; 2 (3):289-94.

Elemer GS, Edgington TS. Microfilament reorganization is associated with functional activation of alpha M beta 2 on monocytic cells. J Biol Chem 1994; 269 (5):3159-66.

Emsley J, King SL, Bergelson JM et al. Crystal structure of the I domain from integrin alpha2beta1. J Biol Chem 1997; 272 (45):28512-7.

Fawcett J, Holness CL, Needham LA et al. Molecular cloning of ICAM-3, a third ligand for LFA-1, constitutively expressed on resting leukocytes. Nature 1992; 360 (6403):481-4.

Fearon DT. Identification of the membrane glycoprotein that is the C3b receptor of the human erythrocyte, polymorphonuclear leukocyte, B lymphocyte, and monocyte. J Exp Med 1980; 152 (1):20-30.

Fu G, Yang HY, Wang C et al. Detection of constitutive heterodimerization of the integrin Mac-1 subunits by fluorescence resonance energy transfer in living cells. Biochem Biophys Res Commun 2006; 346 (3):986-91.

Gahmberg CG. Leukocyte adhesion: CD11/CD18 integrins and intercellular adhesion molecules. Curr Opin Cell Biol 1997; 9 (5):643-50.

Gahmberg CG, Valmu L, Fagerholm S et al. Leukocyte integrins and inflammation. Cell Mol Life Sci 1998; 54 (6):549-55.

Giagulli C, Scarpini E, Ottoboni L et al. RhoA and zeta PKC control distinct modalities of LFA-1 activation by chemokines: critical role of LFA-1 affinity triggering in lymphocyte in vivo homing. Immunity 2004; 20 (1):25-35.

Gogstad GO, Hagen I, Korsmo R et al. Characterization of the proteins of isolated human platelet alpha-granules. Evidence for a separate alpha-granule-pool of the glycoproteins IIb and IIIa. Biochim Biophys Acta 1981; 670 (2):150-62.

Gottschalk KE, Adams PD, Brunger AT et al. Transmembrane signal transduction of the alpha(IIb)beta(3) integrin. Protein Sci 2002; 11 (7):1800-12.

Graff JC, Jutila MA. Differential regulation of CD11b on gammadelta T cells and monocytes in response to unripe apple polyphenols. J Leukoc Biol 2007; 82 (3):603-7.

Graham IL, Gresham HD, Brown EJ. An immobile subset of plasma membrane CD11b/CD18 (Mac-1) is involved in phagocytosis of targets recognized by multiple receptors. J Immunol 1989; 142 (7):2352-8.

Gyetko MR, Aizenberg D, Mayo-Bond L. Urokinase-deficient and urokinase receptor-deficient mice have impaired neutrophil antimicrobial activation in vitro. J Leukoc Biol 2004; 76 (3):648-56.

Gyetko MR, Libre EA, Fuller JA et al. Urokinase is required for T lymphocyte proliferation and activation in vitro. J Lab Clin Med 1999; 133 (3):274-88.

Gyetko MR, Sud S, Kendall T et al. Urokinase receptor-deficient mice have impaired neutrophil recruitment in response to pulmonary Pseudomonas aeruginosa infection. J Immunol 2000; 165 (3):1513-9.

Gyetko MR, Sud S, Sonstein J et al. Antigen-driven lymphocyte recruitment to the lung is diminished in the absence of urokinase-type plasminogen activator (uPA) receptor, but is independent of uPA. J Immunol 2001; 167 (10):5539-42.

Gyetko MR, Todd RF, 3rd, Wilkinson CC et al. The urokinase receptor is required for human monocyte chemotaxis in vitro. J Clin Invest 1994; 93 (4):1380-7.

Harris ES, McIntyre TM, Prescott SM et al. The leukocyte integrins. J Biol Chem 2000; 275 (31):23409-12.

Hermand P, Huet M, Callebaut I et al. Binding sites of leukocyte beta 2 integrins (LFA-1, Mac-1) on the human ICAM-4/LW blood group protein. J Biol Chem 2000; 275 (34):26002-10.

Hildreth JE, August JT. The human lymphocyte function-associated (HLFA) antigen and a related macrophage differentiation antigen (HMac-1): functional effects of subunit-specific monoclonal antibodies. J Immunol 1985; 134 (5):3272-80.

Hildreth JE, Gotch FM, Hildreth PD et al. A human lymphocyte-associated antigen involved in cell-mediated lympholysis. Eur J Immunol 1983; 13 (3):202-8.

Hogg N. The leukocyte integrins. Immunol Today 1989; 10 (4):111-4.

Hogg N, Bates PA. Genetic analysis of integrin function in man: LAD-1 and other syndromes. Matrix Biol 2000; 19 (3):211-22.

Honda S, Tomiyama Y, Pelletier AJ et al. Topography of ligand-induced binding sites, including a novel cation-sensitive epitope (AP5) at the amino terminus, of the human integrin beta 3 subunit. J Biol Chem 1995; 270 (20):11947-54.

Hong SI, Park IC, Son YS et al. Expression of urokinase-type plasminogen activator, its receptor, and its inhibitor in gastric adenocarcinoma tissues. J Korean Med Sci 1996; 11 (1):33-7.

Horgan MJ, Wright SD, Malik AB. Antibody against leukocyte integrin (CD18) prevents reperfusion-induced lung vascular injury. Am J Physiol 1990; 259 (4 Pt 1):L315-9.

Huai Q, Mazar AP, Kuo A et al. Structure of human urokinase plasminogen activator in complex with its receptor. Science 2006; 311 (5761):656-9.

Huang C, Lu C, Springer TA. Folding of the conserved domain but not of flanking regions in the integrin beta2 subunit requires association with the alpha subunit. Proc Natl Acad Sci U S A 1997; 94 (7):3156-61.

Hughes PE, Diaz-Gonzalez F, Leong L et al. Breaking the integrin hinge. A defined structural constraint regulates integrin signaling. J Biol Chem 1996; 271 (12):6571-4.

Humphries MJ. Integrin cell adhesion receptors and the concept of agonism. Trends Pharmacol Sci 2000a; 21 (1):29-32.

Humphries MJ. Integrin structure. Biochem Soc Trans 2000b; 28 (4):311-39.

Hyland RH, Douglass WA, Tan SM et al. Chimeras of the integrin beta subunit mid-region reveal regions required for heterodimer formation and for activation. Cell Commun Adhes 2001; 8 (2):61-9.

Hynes RO. Integrins: bidirectional, allosteric signaling machines. Cell 2002; 110 (6):673-87.

Hynes RO. Integrins: versatility, modulation, and signaling in cell adhesion. Cell 1992; 69 (1):11-25.

Juffermans NP, Dekkers PE, Verbon A et al. Concurrent upregulation of urokinase plasminogen activator receptor and CD11b during tuberculosis and experimental endotoxemia. Infect Immun 2001; 69 (8):5182-5.

Keizer GD, Te Velde AA, Schwarting R et al. Role of p150,95 in adhesion, migration, chemotaxis and phagocytosis of human monocytes. Eur J Immunol 1987; 17 (9):1317-22.

Kim M, Carman CV, Springer TA. Bidirectional transmembrane signaling by cytoplasmic domain separation in integrins. Science 2003; 301 (5640):1720-5.

Kinashi T. Integrin regulation of lymphocyte trafficking: lessons from structural and signaling studies. Adv Immunol 2007; 93:185-227.

Kindzelskii AL, Eszes MM, Todd RF, 3rd et al. Proximity oscillations of complement type 4 (alphaX beta2) and urokinase receptors on migrating neutrophils. Biophys J 1997; 73 (4):1777-84.

Kindzelskii AL, Laska ZO, Todd RF, 3rd et al. Urokinase-type plasminogen activator receptor reversibly dissociates from complement receptor type 3 (alpha M beta 2' CD11b/CD18) during neutrophil polarization. J Immunol 1996; 156 (1):297-309.

Kitching AR, Holdsworth SR, Ploplis VA et al. Plasminogen and plasminogen activators protect against renal injury in crescentic glomerulonephritis. J Exp Med 1997; 185 (5):963-8.

Kjoller L. The urokinase plasminogen activator receptor in the regulation of the actin cytoskeleton and cell motility. Biol Chem 2002; 383 (1):5-19.

Koivunen E, Ranta TM, Annila A et al. Inhibition of beta(2) integrin-mediated leukocyte cell adhesion by leucine-leucine-glycine motif-containing peptides. J Cell Biol 2001; 153 (5):905-16.

Kook YH, Adamski J, Zelent A et al. The effect of antisense inhibition of urokinase receptor in human squamous cell carcinoma on malignancy. Embo J 1994; 13 (17):3983-91.

Lad Y, Harburger DS, Calderwood DA. Integrin cytoskeletal interactions. Methods Enzymol 2007; 426:69-84.

Laemmli UK. Cleavage of structural proteins during the assembly of the head of bacteriophage T4. Nature 1970; 227 (5259):680-5.

Larson RS, Davis T, Bologa C et al. Dissociation of I domain and global conformational changes in LFA-1: refinement of small molecule-I domain structure-activity relationships. Biochemistry 2005; 44 (11):4322-31.

Larson RS, Springer TA. Structure and function of leukocyte integrins. Immunol Rev 1990; 114:181-217.

Lau TL, Dua V, Ulmer TS. Structure of the Integrin αIIb Transmembrane Segment. J Biol Chem 2008a; 283 (23):16162-8.

Lau TL, Partridge AW, Ginsberg MH et al. Structure of the integrin β3 transmembrane segment in phospholipid bicelles and detergent micelles. Biochemistry 2008b; 47 (13):4008-16.

Lee JO, Bankston LA, Arnaout MA et al. Two conformations of the integrin A-domain (I-domain): a pathway for activation? Structure 1995a; 3 (12):1333-40.

Lee JO, Rieu P, Arnaout MA et al. Crystal structure of the A domain from the alpha subunit of integrin CR3 (CD11b/CD18). Cell 1995b; 80 (4):631-8.

Leitinger B, Hogg N. Effects of I domain deletion on the function of the beta2 integrin lymphocyte function-associated antigen-1. Mol Biol Cell 2000; 11 (2):677-90.

Li W, Metcalf DG, Gorelik R et al. A push-pull mechanism for regulating integrin function. Proc Natl Acad Sci U S A 2005; 102 (5):1424-9.

Lim J, Wiedemann A, Tzircotis G et al. An essential role for talin during alpha(M)beta(2)-mediated phagocytosis. Mol Biol Cell 2007; 18 (3):976-85.

Liu S, Calderwood DA, Ginsberg MH. Integrin cytoplasmic domain-binding proteins. J Cell Sci 2000; 113 (Pt 20):3563-71.

Llinas P, Le Du MH, Gardsvoll H et al. Crystal structure of the human urokinase plasminogen activator receptor bound to an antagonist peptide. Embo J 2005; 24 (9):1655-63.

Lluis F, Roma J, Suelves M et al. Urokinase-dependent plasminogen activation is required for efficient skeletal muscle regeneration in vivo. Blood 2001; 97 (6):1703-11.

Loftus JC, Smith JW, Ginsberg MH. Integrin-mediated cell adhesion: the extracellular face. J Biol Chem 1994; 269 (41):25235-8.

Lu C, Ferzly M, Takagi J et al. Epitope mapping of antibodies to the C-terminal region of the integrin beta 2 subunit reveals regions that become exposed upon receptor activation. J Immunol 2001a; 166 (9):5629-37.

Lu C, Oxvig C, Springer TA. The structure of the beta-propeller domain and C-terminal region of the integrin alphaM subunit. Dependence on beta subunit association and prediction of domains. J Biol Chem 1998; 273 (24):15138-47.

Lu C, Shimaoka M, Ferzly M et al. An isolated, surface-expressed I domain of the integrin alphaLbeta2 is sufficient for strong adhesive function when locked in the open conformation with a disulfide bond. Proc Natl Acad Sci U S A 2001b; 98 (5):2387-92.

Lu C, Shimaoka M, Zang Q et al. Locking in alternate conformations of the integrin alphaLbeta2 I domain with disulfide bonds reveals functional relationships among integrin domains. Proc Natl Acad Sci U S A 2001c; 98 (5):2393-8.

Luo BH, Carman CV, Springer TA. Structural basis of integrin regulation and signaling. Annu Rev Immunol 2007; 25:619-47.

Luo BH, Springer TA, Takagi J. A specific interface between integrin transmembrane helices and affinity for ligand. PLoS Biol 2004; 2 (6):e153.

Luque A, Gomez M, Puzon W et al. Activated conformations of very late activation integrins detected by a group of antibodies (HUTS) specific for a novel regulatory region (355-425) of the common beta 1 chain. J Biol Chem 1996; 271 (19):11067-75.

Marlin SD, Springer TA. Purified intercellular adhesion molecule-1 (ICAM-1) is a ligand for lymphocyte function-associated antigen 1 (LFA-1). Cell 1987; 51 (5):813-9.

May AE, Kanse SM, Lund LR et al. Urokinase receptor (CD87) regulates leukocyte recruitment via beta 2 integrins in vivo. J Exp Med 1998; 188 (6):1029-37.

Mazar AP, Henkin J, Goldfarb RH. The urokinase plasminogen activator system in cancer: implications for tumor angiogenesis and metastasis. Angiogenesis 1999; 3 (1):15-32.

Mazzone A, Ricevuti G. Leukocyte CD11/CD18 integrins: biological and clinical relevance. Haematologica 1995; 80 (2):161-75.

Mondino A, Blasi F. uPA and uPAR in fibrinolysis, immunity and pathology. Trends Immunol 2004; 25 (8):450-5.

Morel-Kopp MC, Kaplan C, Proulle V et al. A three amino acid deletion in glycoprotein IIIa is responsible for type I Glanzmann's thrombasthenia: importance of residues Ile325Pro326Gly327 for beta3 integrin subunit association. Blood 1997; 90 (2):669-77.

Mould AP, Barton SJ, Askari JA et al. Conformational changes in the integrin β A domain provide a mechanism for signal transduction via hybrid domain movement. J Biol Chem 2003; 278 (19):17028-35.

Myones BL, Dalzell JG, Hogg N et al. Neutrophil and monocyte cell surface p150,95 has iC3b-receptor (CR4) activity resembling CR3. J Clin Invest 1988; 82 (2):640-51.

Nermut MV, Green NM, Eason P et al. Electron microscopy and structural model of human fibronectin receptor. Embo J 1988; 7 (13):4093-9.

Nishida N, Xie C, Shimaoka M et al. Activation of leukocyte beta2 integrins by conversion from bent to extended conformations. Immunity 2006; 25 (4):583-94.

Nolte M, Pepinsky RB, Venyaminov S et al. Crystal structure of the alpha1beta1 integrin I-domain: insights into integrin I-domain function. FEBS Lett 1999; 452 (3):379-85.

Nurden AT. Glanzmann thrombasthenia. Orphanet J Rare Dis 2006; 1:10.

Nusrat AR, Chapman HA, Jr. An autocrine role for urokinase in phorbol ester-mediated differentiation of myeloid cell lines. J Clin Invest 1991; 87 (3):1091-7.

Nykjaer A, Moller B, Todd RF, 3rd et al. Urokinase receptor. An activation antigen in human T lymphocytes. J Immunol 1994; 152 (2):505-16.

O'Toole TE, Katagiri Y, Faull RJ et al. Integrin cytoplasmic domains mediate inside-out signal transduction. J Cell Biol 1994; 124 (6):1047-59.

Ostermann G, Weber KS, Zernecke A et al. JAM-1 is a ligand of the beta(2) integrin LFA-1 involved in transendothelial migration of leukocytes. Nat Immunol 2002; 3 (2):151-8.

Petty HR, Todd RF, 3rd. Integrins as promiscuous signal transduction devices. Immunol Today 1996; 17 (5):209-12.

Plescia J, Altieri DC. Activation of Mac-1 (CD11b/CD18)-bound factor X by released cathepsin G defines an alternative pathway of leucocyte initiation of coagulation. Biochem J 1996; 319 (Pt 3):873-9.

Ploug M, Ellis V. Structure-function relationships in the receptor for urokinase-type plasminogen activator. Comparison to other members of the Ly-6 family and snake venom alpha-neurotoxins. FEBS Lett 1994; 349 (2):163-8.

Plow EF, Haas TA, Zhang L et al. Ligand binding to integrins. J Biol Chem 2000; 275 (29):21785-8.

Plow EF, Herren T, Redlitz A et al. The cell biology of the plasminogen system. Faseb J 1995; 9 (10):939-45.

Pluskota E, Soloviev DA, Bdeir K et al. Integrin alphaMbeta2 orchestrates and accelerates plasminogen activation and fibrinolysis by neutrophils. J Biol Chem 2004; 279 (17):18063-72.

Pluskota E, Soloviev DA, Plow EF. Convergence of the adhesive and fibrinolytic systems: recognition of urokinase by integrin alpha Mbeta 2 as well as by the urokinase receptor regulates cell adhesion and migration. Blood 2003; 101 (4):1582-90.

Poloni F, Puddu P, Moretti F et al. Identification of a LFA-1 region involved in the HIV-1-induced syncytia formation through phage-display technology. Eur J Immunol 2001; 31 (1):57-63.

Porter JC, Hogg N. Integrins take partners: cross-talk between integrins and other membrane receptors. Trends Cell Biol 1998; 8 (10):390-6.

Preissner KT, Kanse SM, May AE. Urokinase receptor: a molecular organizer in cellular communication. Curr Opin Cell Biol 2000; 12 (5):621-8.

Qu A, Leahy DJ. Crystal structure of the I-domain from the CD11a/CD18 (LFA-1, alpha L beta 2) integrin. Proc Natl Acad Sci U S A 1995; 92 (22):10277-81.

Rabb H, Michishita M, Sharma CP et al. Cytoplasmic tails of human complement receptor type 3 (CR3, CD11b/CD18) regulate ligand avidity and the internalization of occupied receptors. J Immunol 1993; 151 (2):990-1002.

Randi AM, Hogg N. I domain of beta 2 integrin lymphocyte function-associated antigen-1 contains a binding site for ligand intercellular adhesion molecule-1. J Biol Chem 1994; 269 (17):12395-8.

Resnati M, Guttinger M, Valcamonica S et al. Proteolytic cleavage of the urokinase receptor substitutes for the agonist-induced chemotactic effect. Embo J 1996; 15 (7):1572-82.

Rijneveld AW, Levi M, Florquin S et al. Urokinase receptor is necessary for adequate host defense against pneumococcal pneumonia. J Immunol 2002; 168 (7):3507-11.

Rivas GA, Aznarez JA, Usobiaga P et al. Molecular characterization of the human platelet integrin GPIIb/IIIa and its constituent glycoproteins. Eur Biophys J 1991; 19 (6):335-45.

Robinson MK, Andrew D, Rosen H et al. Antibody against the Leu-CAM beta-chain (CD18) promotes both LFA-1- and CR3-dependent adhesion events. J Immunol 1992; 148 (4):1080-5.

Rocco M, Rosano C, Weisel JW et al. Integrin conformational regulation: uncoupling extension/tail separation from changes in the head region by a multiresolution approach. Structure 2008; 16 (6):954-64.

Romer J, Bugge TH, Pyke C et al. Impaired wound healing in mice with a disrupted plasminogen gene. Nat Med 1996; 2 (3):287-92.

Ross GD, Cain JA, Myones BL et al. Specificity of membrane complement receptor type three (CR3) for beta-glucans. Complement 1987; 4 (2):61-74.

Sanchez-Madrid F, del Pozo MA. Leukocyte polarization in cell migration and immune interactions. Embo J 1999; 18 (3):501-11.

Sanchez-Madrid F, Krensky AM, Ware CF et al. Three distinct antigens associated with human T-lymphocyte-mediated cytolysis: LFA-1, LFA-2, and LFA-3. Proc Natl Acad Sci U S A 1982; 79 (23):7489-93.

Shappell SB, Toman C, Anderson DC et al. Mac-1 (CD11b/CD18) mediates adherence-dependent hydrogen peroxide production by human and canine neutrophils. J Immunol 1990; 144 (7):2702-11.

Shattil SJ. Integrins and Src: dynamic duo of adhesion signaling. Trends Cell Biol 2005; 15 (8):399-403.

Shaw JM, Al-Shamkhani A, Boxer LA et al. Characterization of four CD18 mutants in leucocyte adhesion deficient (LAD) patients with differential capacities to support expression and function of the CD11/CD18 integrins LFA-1, Mac-1 and p150,95. Clin Exp Immunol 2001; 126 (2):311-8.

Shi M, Foo SY, Tan SM et al. A structural hypothesis for the transition between bent and extended conformations of the leukocyte beta2 integrins. J Biol Chem 2007; 282 (41):30198-206.

Shi M, Sundramurthy K, Liu B et al. The crystal structure of the plexin-semaphorin-integrin domain/hybrid domain/I-EGF1 segment from the human integrin beta2 subunit at 1.8-A resolution. J Biol Chem 2005; 280 (34):30586-93.

Shimaoka M, Lu C, Palframan RT et al. Reversibly locking a protein fold in an active conformation with a disulfide bond: integrin alphaL I domains with high affinity and antagonist activity in vivo. Proc Natl Acad Sci U S A 2001; 98 (11):6009-14.

Shimaoka M, Shifman JM, Jing H et al. Computational design of an integrin I domain stabilized in the open high affinity conformation. Nat Struct Biol 2000; 7 (8):674-8.

Shimaoka M, Takagi J, Springer TA. Conformational regulation of integrin structure and function. Annu Rev Biophys Biomol Struct 2002; 31:485-516.

Shimaoka M, Xiao T, Liu JH et al. Structures of the alpha L I domain and its complex with ICAM-1 reveal a shape-shifting pathway for integrin regulation. Cell 2003; 112 (1):99-111.

Shimizu Y, Mobley JL. Distinct divalent cation requirements for integrin-mediated CD4+ T lymphocyte adhesion to ICAM-1, fibronectin, VCAM-1, and invasin. J Immunol 1993; 151 (8):4106-15.

Sidenius N, Andolfo A, Fesce R et al. Urokinase regulates vitronectin binding by controlling urokinase receptor oligomerization. J Biol Chem 2002; 277 (31):27982-90.

Simon DI, Ezratty AM, Francis SA et al. Fibrin(ogen) is internalized and degraded by activated human monocytoid cells via Mac-1 (CD11b/CD18): a nonplasmin fibrinolytic pathway. Blood 1993; 82 (8):2414-22.

Simon DI, Rao NK, Xu H et al. Mac-1 (CD11b/CD18) and the urokinase receptor (CD87) form a functional unit on monocytic cells. Blood 1996; 88 (8):3185-94.

Simon DI, Wei Y, Zhang L et al. Identification of a urokinase receptor-integrin interaction site. Promiscuous regulator of integrin function. J Biol Chem 2000; 275 (14):10228-34.

Singer SJ. Intercellular communication and cell-cell adhesion. Science 1992; 255 (5052):1671-7.

Sitrin RG, Pan PM, Harper HA et al. Urokinase receptor (CD87) aggregation triggers phosphoinositide hydrolysis and intracellular calcium mobilization in mononuclear phagocytes. J Immunol 1999; 163 (11):6193-200.

Sitrin RG, Todd RF, 3rd, Albrecht E et al. The urokinase receptor (CD87) facilitates CD11b/CD18-mediated adhesion of human monocytes. J Clin Invest 1996; 97 (8):1942-51.

Spijkers PP, da Costa Martins P, Westein E et al. LDL-receptor-related protein regulates beta2-integrin-mediated leukocyte adhesion. Blood 2005; 105 (1):170-7.

Springer TA. Adhesion receptors of the immune system. Nature 1990; 346 (6283):425-34.

Springer TA. Folding of the N-terminal, ligand-binding region of integrin alpha-subunits into a beta-propeller domain. Proc Natl Acad Sci U S A 1997; 94 (1):65-72.

Springer TA. Traffic signals for lymphocyte recirculation and leukocyte emigration: the multistep paradigm. Cell 1994; 76 (2):301-14.

Staunton DE, Dustin ML, Springer TA. Functional cloning of ICAM-2, a cell adhesion ligand for LFA-1 homologous to ICAM-1. Nature 1989; 339 (6219):61-4.

Stefanidakis M, Bjorklund M, Ihanus E et al. Identification of a negatively charged peptide motif within the catalytic domain of progelatinases that mediates binding to leukocyte beta 2 integrins. J Biol Chem 2003; 278 (36):34674-84.

Stephens P, Romer JT, Spitali M et al. KIM127, an antibody that promotes adhesion, maps to a region of CD18 that includes cysteine-rich repeats. Cell Adhes Commun 1995; 3 (5):375-84.

Stewart M, Hogg N. Regulation of leukocyte integrin function: affinity vs. avidity. J Cell Biochem 1996; 61 (4):554-61.

Sun QH, Liu CY, Wang R et al. Disruption of the long-range GPIIIa Cys(5)-Cys(435) disulfide bond results in the production of constitutively active GPIIb-IIIa (alpha(IIb)beta(3)) integrin complexes. Blood 2002; 100 (6):2094-101.

Suzuki S, Naitoh Y. Amino acid sequence of a novel integrin beta 4 subunit and primary expression of the mRNA in epithelial cells. Embo J 1990; 9 (3):757-63.

Tadokoro S, Shattil SJ, Eto K et al. Talin binding to integrin beta tails: a final common step in integrin activation. Science 2003; 302 (5642):103-6.

Takagi J. Structural basis for ligand recognition by integrins. Curr Opin Cell Biol 2007; 19 (5):557-64.

Takagi J, Petre BM, Walz T et al. Global conformational rearrangements in integrin extracellular domains in outside-in and inside-out signaling. Cell 2002a; 110 (5):599-11.

Takagi J, Springer TA. Integrin activation and structural rearrangement. Immunol Rev 2002b; 186:141-63.

Takagi J, Strokovich K, Springer TA et al. Structure of integrin α5β1 in complex with fibronectin. EMBO J 2003; 22 (18):4607-15.

Talamas-Rohana P, Wright SD, Lennartz MR et al. Lipophosphoglycan from Leishmania mexicana promastigotes binds to members of the CR3, p150,95 and LFA-1 family of leukocyte integrins. J Immunol 1990; 144 (12):4817-24.

Tan SM, Hyland RH, Al-Shamkhani A et al. Effect of integrin beta 2 subunit truncations on LFA-1 (CD11a/CD18) and Mac-1 (CD11b/CD18) assembly, surface expression, and function. J Immunol 2000; 165 (5):2574-81.

Tan SM, Robinson MK, Drbal K et al. The N-terminal region and the mid-region complex of the integrin beta 2 subunit. J Biol Chem 2001; 276 (39):36370-6.

Tang ML, Kong LS, Law SK et al. Down-regulation of integrin alpha M beta 2 ligand-binding function by the urokinase-type plasminogen activator receptor. Biochem Biophys Res Commun 2006; 348 (3):1184-93.

Tang RH, Tng E, Law SK et al. Epitope mapping of monoclonal antibody to integrin alphaL beta2 hybrid domain suggests different requirements of affinity states for intercellular adhesion molecules (ICAM)-1 and ICAM-3 binding. J Biol Chem 2005; 280 (32):29208-16.

Tarui T, Andronicos N, Czekay RP et al. Critical role of integrin alpha 5 beta 1 in urokinase (uPA)/urokinase receptor (uPAR, CD87) signaling. J Biol Chem 2003; 278 (32):29863-72.

Tarui T, Mazar AP, Cines DB et al. Urokinase-type plasminogen activator receptor (CD87) is a ligand for integrins and mediates cell-cell interaction. J Biol Chem 2001; 276 (6):3983-90.

Tian L, Yoshihara Y, Mizuno T et al. The neuronal glycoprotein telencephalin is a cellular ligand for the CD11a/CD18 leukocyte integrin. J Immunol 1997; 158 (2):928-36.

Tng E, Tan SM, Ranganathan S et al. The integrin alpha L beta 2 hybrid domain serves as a link for the propagation of activation signal from its stalk regions to the I-like domain. J Biol Chem 2004; 279 (52):54334-9.

Todd RF, 3rd, Petty HR. Beta 2 (CD11/CD18) integrins can serve as signaling partners for other leukocyte receptors. J Lab Clin Med 1997; 129 (5):492-8.

Trigwell S, Wood L, Jones P. Soluble urokinase receptor promotes cell adhesion and requires tyrosine-92 for activation of p56/59(hck). Biochem Biophys Res Commun 2000; 278 (2):440-6.

Tuckwell DS, Humphries MJ. Molecular and cellular biology of integrins. Crit Rev Oncol Hematol 1993; 15 (2):149-71.

Ugarova TP, Yakubenko VP. Recognition of fibrinogen by leukocyte integrins. Ann N Y Acad Sci 2001; 936:368-85.

Van der Vieren M, Crowe DT, Hoekstra D et al. The leukocyte integrin alpha D beta 2 binds VCAM-1: evidence for a binding interface between I domain and VCAM-1. J Immunol 1999; 163 (4):1984-90.

Van der Vieren M, Le Trong H, Wood CL et al. A novel leukointegrin, alpha d beta 2, binds preferentially to ICAM-3. Immunity 1995; 3 (6):683-90.

van Kooyk Y, van Vliet SJ, Figdor CG. The actin cytoskeleton regulates LFA-1 ligand binding through avidity rather than affinity changes. J Biol Chem 1999; 274 (38):26869-77.

Van Strijp JA, Russell DG, Tuomanen E et al. Ligand specificity of purified complement receptor type three (CD11b/CD18, alpha m beta 2, Mac-1). Indirect effects of an Arg-Gly-Asp (RGD) sequence. J Immunol 1993; 151 (6):3324-36.

Vararattanavech A, Tang ML, Li HY et al. Permissive transmembrane helix heterodimerization is required for the expression of a functional integrin. Biochem J 2008; 410 (3):495-502.

Vidal F, Aberdam D, Miquel C et al. Integrin beta 4 mutations associated with junctional epidermolysis bullosa with pyloric atresia. Nat Genet 1995; 10 (2):229-34.

Vinogradova O, Velyvis A, Velyviene A et al. A structural mechanism of integrin alpha(IIb)beta(3) "inside-out" activation as regulated by its cytoplasmic face. Cell 2002; 110 (5):587-97.

Violette SM, Rusche JR, Purdy SR et al. Differences in the binding of blocking anti-CD11b monoclonal antibodies to the A-domain of CD11b. J Immunol 1995; 155 (6):3092-101.

von Asmuth EJ, van der Linden CJ, Leeuwenberg JF et al. Involvement of the CD11b/CD18 integrin, but not of the endothelial cell adhesion molecules ELAM-1 and ICAM-1 in tumor necrosis factor-alpha-induced neutrophil toxicity. J Immunol 1991; 147 (11):3869-75.

Vorup-Jensen T, Ostermeier C, Shimaoka M et al. Structure and allosteric regulation of the alpha X beta 2 integrin I domain. Proc Natl Acad Sci U S A 2003; 100 (4):1873-8.

Webb DJ, Nguyen DH, Gonias SL. Extracellular signal-regulated kinase functions in the urokinase receptor-dependent pathway by which neutralization of low density lipoprotein receptor-related protein promotes fibrosarcoma cell migration and matrigel invasion. J Cell Sci 2000; 113 (Pt 1):123-34.

Wei Y, Czekay RP, Robillard L et al. Regulation of alpha5beta1 integrin conformation and function by urokinase receptor binding. J Cell Biol 2005; 168 (3):501-11.

Wei Y, Eble JA, Wang Z et al. Urokinase receptors promote beta1 integrin function through interactions with integrin alpha3beta1. Mol Biol Cell 2001; 12 (10):2975-86.

Wei Y, Lukashev M, Simon DI et al. Regulation of integrin function by the urokinase receptor. Science 1996; 273 (5281):1551-5.

Wei Y, Tang CH, Kim Y et al. Urokinase receptors are required for α5β1 integrin-mediated signaling in tumor cells. J Biol Chem 2007; 282 (6):3929-39.

Weisel JW, Nagaswami C, Vilaire G et al. Examination of the platelet membrane glycoprotein IIb-IIIa complex and its interaction with fibrinogen and other ligands by electron microscopy. J Biol Chem 1992; 267 (23):16637-43.

Wilkins JA, Li A, Ni H et al. Control of beta1 integrin function. Localization of stimulatory epitopes. J Biol Chem 1996; 271 (6):3046-51.

Williams MJ, Hughes PE, O'Toole TE et al. The inner world of cell adhesion: integrin cytoplasmic domains. Trends Cell Biol 1994; 4 (4):109-12.

Wright SD, Jong MT. Adhesion-promoting receptors on human macrophages recognize Escherichia coli by binding to lipopolysaccharide. J Exp Med 1986; 164 (6):1876-88.

Wright SD, Rao PE, Van Voorhis WC et al. Identification of the C3bi receptor of human monocytes and macrophages by using monoclonal antibodies. Proc Natl Acad Sci U S A 1983; 80 (18):5699-703.

Xiao T, Takagi J, Coller BS et al. Structural basis for allostery in integrins and binding to fibrinogen-mimetic therapeutics. Nature 2004; 432 (7013):59-67.

Xie C, Shimaoka M, Xiao T et al. The integrin alpha-subunit leg extends at a Ca2+-dependent epitope in the thigh/genu interface upon activation. Proc Natl Acad Sci U S A 2004; 101 (43):15422-7.

Xie J, Li R, Kotovuori P et al. Intercellular adhesion molecule-2 (CD102) binds to the leukocyte integrin CD11b/CD18 through the A domain. J Immunol 1995; 155 (7):3619-28.

Xiong JP, Stehle T, Diefenbach B et al. Crystal structure of the extracellular segment of integrin alpha Vbeta3. Science 2001; 294 (5541):339-45.

Xiong JP, Stehle T, Goodman SL et al. New insights into the structural basis of integrin activation. Blood 2003; 102 (4):1155-9.

Xiong JP, Stehle T, Zhang R et al. Crystal structure of the extracellular segment of integrin alpha Vbeta3 in complex with an Arg-Gly-Asp ligand. Science 2002; 296 (5565):151-5.

Xue W, Kindzelskii AL, Todd RF, 3rd et al. Physical association of complement receptor type 3 and urokinase-type plasminogen activator receptor in neutrophil membranes. J Immunol 1994; 152 (9):4630-40.

Xue W, Mizukami I, Todd RF, 3rd et al. Urokinase-type plasminogen activator receptors associate with beta1 and beta3 integrins of fibrosarcoma cells: dependence on extracellular matrix components. Cancer Res 1997; 57 (9):1682-9.

Yalamanchili P, Lu C, Oxvig C et al. Folding and function of I domain-deleted Mac-1 and lymphocyte function-associated antigen-1. J Biol Chem 2000; 275 (29):21877-82.

Yamamoto K, Loskutoff DJ. Fibrin deposition in tissues from endotoxin-treated mice correlates with decreases in the expression of urokinase-type but not tissue-type plasminogen activator. J Clin Invest 1996; 97 (11):2440-51.

Yang W, Shimaoka M, Salas A et al. Intersubunit signal transmission in integrins by a receptor-like interaction with a pull spring. Proc Natl Acad Sci U S A 2004; 101 (9):2906-11.

Yu W, Kim J, Ossowski L. Reduction in surface urokinase receptor forces malignant cells into a protracted state of dormancy. J Cell Biol 1997; 137 (3):767-77.

Zacharias DA, Violin JD, Newton AC et al. Partitioning of lipid-modified monomeric GFPs into membrane microdomains of live cells. Science 2002; 296 (5569):913-6.

Zang Q, Lu C, Huang C et al. The top of the inserted-like domain of the integrin lymphocyte function-associated antigen-1 beta subunit contacts the alpha subunit beta -propeller domain near beta-sheet 3. J Biol Chem 2000; 275 (29):22202-12.

Zang Q, Springer TA. Amino acid residues in the PSI domain and cysteine-rich repeats of the integrin beta2 subunit that restrain activation of the integrin alpha(X)beta(2). J Biol Chem 2001; 276 (10):6922-9.

Zhang H, Colman RW, Sheng N. Regulation of CD11b/CD18 (Mac-1) adhesion to fibrinogen by urokinase receptor (uPAR). Inflamm Res 2003; 52 (2):86-93.

Zhou M, Todd RF, 3rd, van de Winkel JG et al. Cocapping of the leukoadhesin molecules complement receptor type 3 and lymphocyte function-associated antigen-1 with Fc gamma receptor III on human neutrophils. Possible role of lectin-like interactions. J Immunol 1993; 150 (7):3030-41.

Zhu J, Carman CV, Kim M et al. Requirement of α and β subunit transmembrane helix separation for integrin outside-in signaling. Blood 2007; 110 (7):2475-83.

Zutter MM, Santoro SA. Widespread histologic distribution of the alpha 2 beta 1 integrin cell-surface collagen receptor. Am J Pathol 1990; 137 (1):113-20.